ACKNOWLEDGEMENTS

This thesis is the result of 4 years of work which commenced in November 2000. The main part of the work has been carried out at The Department of Materials Technology at NTNU. One year (2002-2003) was spent at The Department of Chemical & Materials Engineering at The University of Auckland.

I wish to express my gratitude to my supervisor Professor Harald A. Øye for his inspiration, guidance and support throughout this work and to Professor Trygve Foosnæs for his encouragement, good advices and for proofreading my thesis.

I am grateful to Professor Margaret Hyland for introducing me to the field of carbonization chemistry of pitches when I wrote my Master's thesis at The Department of Chemical & Materials Engineering at The University of Auckland in 1999/2000 and for her guidance and support during my second stay in 2002/2003. I was given a warm welcome and have truly enjoyed my time in New Zealand. I would like to acknowledge The Department of Chemical & Materials Engineering at The University of Auckland for allowing me to use their research facilities. Dr. Alec Asadov and Muhammad Shameem are thanked for their assistance during my experimental work.

I would like to thank Elkem Aluminium ANS for giving me the opportunity to do experimental work at their research facilities in Kristiansand and Professor II Morten Sørlie for providing me with pitch samples and analyses. Dr. Lene Solli and Dr. Hogne Linga at Hydro Aluminium PM, Technology and Operational Support in Årdal are thanked for providing me with pitch samples and analyses and for giving me the opportunity to visit the plant in Årdal in 2000.

Professor Jostein Krane is thanked for carrying out the NMR analysis, for teaching me about NMR and for interesting discussions on the interpretation of the results.

I would like to express my gratitude to Dr. María Antonia Díez Díaz-Estébanez for giving me the opportunity to visit Instituto Nacional del Carbón (INCAR) in Oviedo, Spain, in 2001. I learnt a lot during my stay and would also like to thank Dr. Antonio Domínguez Padilla for his help.

Dr. Richard L. Shao at GrafTech International is thanked for an interesting correspondence and for providing me with pitch samples.

I would like to thank Stein Rørvik at SINTEF for teaching me how to use the optical texture analysis equipment and for good advice and guidance on sample preparation. Elin Nilsen is thanked for her instructions on the X-ray diffractometer and accompanying software.

SINTEF Marine Environmental Technology is acknowledged for allowing me to use their GC equipment. Frode Leirvik is thanked for giving me instructions.

I would like to thank my family and friends for their support. A special thanks goes to my father for his interest in my work, good advices and encouragement.

Finally, I would like to acknowledge The Norwegian Research Council (NFR) and The Norwegian Aluminium Industry for financial support through the PROSMAT and CARBOMAT programs.

ABSTRACT

Pitches are used on a large scale in the manufacture of carbon anodes for the production of primary aluminium. The role of the pitch is to act as a binder between the petroleum coke grains. The structure of the carbonized pitch binder (pitch coke) has an important impact on the overall performance of the anode. Even though the binder pitch is the minor constituent in an anode, it is impossible to make a good quality anode without a good quality binder pitch.

Pitch is an extremely complex mixture of numerous, essentially aromatic and heterocyclic compounds derived from pyrolysis of organic material or tar distillation. Upon heat treatment pitches form cokes in relatively high yields. Physical and chemical properties of the anode such as mechanical strength, electrical resistivity, thermal conductivity and resistance towards oxidation by air and CO_2 are dependent on the structure of the aggregate material as well as the carbonized binder pitch. The properties of the pitch coke is in turn mainly dependent on the chemical characteristics of the parent pitch.

Coal-tar pitch is the preferred choice of binder material in anode manufacture today. However, the availability of high quality coal-tar is in decline and at least partial replacement by alternative binder sources will become increasingly important in the future. Due to environmental regulations, petroleum pitches are interesting as they generally have lower PAH emissions than coal-tar pitches during baking. Blends of coal-tar pitches and petroleum pitches are in use today on an industrial scale. The aluminium industry must be prepared to meet the challenges involved in adapting binder pitches from new sources which may be of inferior quality to the pitches available on the market today. An increased understanding of the processes involved in the transformation of a pitch into a coke and the link between raw material composition and properties and the final artifact is thus highly relevant.

Traditionally, the suitability of a binder pitch for use in anodes, has been defined from parameters like softening point, insolubility in toluene (TI) and quinoline (QI), coke yield, H/C atomic ratio, ash content and density. Although these parameters, which are mostly empirical in nature, give an indication of the pitch quality, more information on the chemical characteristics and carbonization behavior of pitches is certainly valuable. The present work aims to describe and explain the link between “classical” pitch properties, hydrogen transfer properties, information derived from NMR spectroscopy and the structure of the carbonized binder pitch.

Coal-tar and petroleum pitches pass through a fluid stage during carbonization. In the early stages of carbonization, free radicals are formed due to thermal rupture of C-C and C-H bonds in reactive components. Polymerization occurs mainly via a free radical mechanism leading to molecular size enlargement (aromatic growth) and the formation of oligomeric systems (mesogens). If the intermolecular reactivity of the pitch constituents is too high, extensive cross-linking and a rapid transformation of pitch molecules through polymerization will occur at a relatively low temperature. In this case, either mesophase will not be formed or the growth and coalescence of mesophase will take place under low fluidity/high viscosity conditions leading to a premature solidification of the pyrolysis system. An isotropic coke or a pitch coke of small optical domains will then be formed. On the other hand, if the pitch has a low

thermal reactivity, aromatic growth is constrained and the mesogens will have sufficient mobility to stack parallel to each other and establish a liquid crystal system (mesophase). The growth and coalescence of mesophase take place at a higher temperature where the viscosity of the pyrolysis system is at a low level. Eventually, the system will solidify and an anisotropic coke of large well-developed optical domains is formed.

In particular, the presence of alkyl side chains and oxygenated functional groups are considered to lead to an increased thermal reactivity. If free radicals formed by thermal rupture of bonds in reactive pitch species can be stabilized by hydrogen transfer from within the system, extensive cross-linking at a too early stage is prevented. The initiation, growth and coalescence of mesophase are facilitated and consequently a coke of large well-developed optical domains is formed. Hydroaromatic rings and naphthenic rings in hydroaromatic species are considered to be principal hydrogen donor groups. Oxygen acceptor sites are believed to deplete the supply of donatable hydrogen and leave radicals free to recombine. The thermal reactivity of a pitch is thus dependent on both the amount of reactive species and the ability of the pitch to stabilize free radicals by hydrogen transfer.

In the present work, the subject of study was five coal-tar pitches and four petroleum pitches. In addition, a QI-free coal-tar pitch supplied by GrafTech International was studied. The pitches were characterized by ^{1}H NMR and ^{13}C NMR spectroscopy, hydrogen transfer properties, elemental analysis and the release of volatiles during carbonization. In addition, the pitches were characterized by more “traditional” pitch parameters like insolubility in quinoline (QI), insolubility in toluene (TI), softening point and coking value. The structure of the carbonized pitches was examined by optical microscopy and X-ray diffraction.

The hydrogen transfer properties of the pitches were evaluated from their ability to donate hydrogen to an acceptor compound, anthracene, or abstract hydrogen from a donor compound, 1,2,3,4-tetrahydronaphthalene (tetralin). A mixture of pitch and anthracene or tetralin was heat treated in sealed glass tubes filled with argon gas at 400 ºC. Two different heat treatment procedures were tested. In the first, the sample was kept at 400 ºC for 8 hours while in the second, the sample was heated at a rate of 5 ºC/min to 400 ºC with no soaking time. The major hydrogenated products from the reaction between anthracene and pitch were 9,10-dihydroanthracene (DHA) and 1,2,3,4-tetrahydroanthracene (THA). After the reaction, the semi-coke residue was dissolved in carbon disulphide and analyzed by gas chromatography. The hydrogen donor ability (HDa) was calculated from the amounts of DHA and THA formed and expressed as milligrams of hydrogen transferred to anthracene per gram of pitch. For the hydrogen donor ability test, the less severe heat treatment (5 ºC/min to 400 ºC, no soaking time) was found to be the most appropriate. The reaction between tetralin and pitch gave one major dehydrogenated product, naphthalene. The hydrogen acceptor ability (HAa) was calculated from the ratio of naphthalene to tetralin as determined by gas chromatography and expressed as milligrams of hydrogen transferred per gram of pitch. For the acceptor ability test, the heat treatment at 400 ºC with 8 hours soaking time was found to be the most appropriate.

The release of volatiles during carbonization was studied by thermogravimetric analysis. The amount of volatiles released between 300 and 500 ºC (VM300-500)

relative to the total amount of volatiles released at 1000 ºC was selected as a parameter reflecting the thermal behavior of pitches during the critical stages of carbonization.

Carbonization of pitches was performed under inert gas pressure (15 bar) and the green cokes obtained at 550 ºC were studied by optical microscopy. Computerized image analysis was performed to quantify the optical texture. The output parameters from the image analysis were the mosaic index, which is a measure of the optical domain size, and the fiber index, which is a measure of the parallel alignment of optical domains. The green cokes were further heat treated to 1150 ºC and the microstructure of the resulting calcined pitch cokes was characterized by X-ray diffraction.

The carbon disulphide soluble part of the pitches was investigated by ^{1}H NMR and ^{13}C NMR spectroscopy. Results from elemental analysis of the pitches were used in conjunction with the results obtained from the NMR spectroscopy. The main objective of the NMR analysis was to identify and quantify structures in the pitch which are considered either to increase or decrease the thermal reactivity. The coal-tar pitches were as expected found to be more aromatic than the pitches of petroleum origin. A relationship was found between the aromaticity of the pitches and the H/C atomic ratio as determined from elemental analysis. Elemental analysis is a rapid and convenient method to estimate the aromaticity of pitches. Due to a more hydroaromatic structure, the petroleum pitches were in general found to have a higher estimated concentration of donatable hydrogen which will suppress intermolecular reactivity. However, the petroleum pitches also had a high concentration of alkyl side chains which are generally believed to give increased thermal reactivity. Carbon connected to oxygen could not be distinguished in the NMR spectra. Pitch constituents containing heteroatoms are generally concentrated in the heavier pitch fractions which may not be soluble in carbon disulphide. This could be an explanation for the failure in the detection of aromatic carbon connected to heteroatoms. However, the oxygen content was determined by elemental analysis.

The pitches could be distinguished due to their ability to donate hydrogen to anthracene or abstract hydrogen from tetralin. The hydrogen donor ability was not found to correlate with the concentration of donatable hydrogen (NMR) which might have been expected. A likely explanation for this apparent inconsistency is that potential donatable hydrogen in reactive pitches will be preferentially consumed by free radicals and oxygenated acceptor sites instead of being transferred to anthracene. A correlation between the hydrogen donor (HDa) and acceptor ability (HAa) was not found. This indicates that the two parameters represent two separate properties where both are linked to the thermal reactivity of the pitch. The ratio between the hydrogen donor and acceptor ability, HDa/HAa, was used as a parameter reflecting the thermal reactivity of pitches. Pitches which exhibit a high HDa/HAa ratio (low thermal reactivity) are expected to form an anisotropic coke of large optical domains. On the other hand, pitches with a relatively low HDa/HAa ratio are expected to have a high thermal reactivity and form a more isotropic (small optical domains) coke. Despite the higher concentration of donatable hydrogen, the petroleum pitches were not generally considered to have a lower thermal reactivity than the coal-tar pitches expressed by the HDa/HAa ratio.

The processes taking place during thermal treatment of pitches are reflected in the release of volatiles. A correlation was observed between the HDa/HAa ratio and the relative amount of volatiles released between 300 and 500 ºC (VM300-500). Thermally reactive pitches exhibiting a low HDa/HAa ratio will have a high activity at low temperatures and release low boiling point molecules and fragmentation species. If on the other hand the pitch has a low thermal reactivity, fragmentation species will be stabilized by hydrogen transfer and retained in the pyrolysis system. The resulting thermally stable molecules of relatively low molecular weight may then act as solvating vehicles maintaining a low viscosity in the system and may also be important as hydrogen shuttling agents. When the system has reached a critical stage for mesophase growth and coalescence, these smaller thermally stable molecules (non-mesogens) are eventually released at higher temperatures.

The petroleum pitches developed cokes of relatively large optical domains (coarse mosaic). A correlation was observed between the HDa/HAa ratio and the mosaic index (size of optical texture) for the petroleum pitches. As expected, a high thermal reactivity (low HDa/HAa ratio) resulted in a pitch coke of small optical domains (high mosaic index). The HDa/HAa ratio was, however, not successful in predicting the size of optical texture in the cokes obtained from the coal-tar pitches. This was mainly due to the influence of QI material on the pitch coke structure. It is recognized that particulate matter (primary QI material) hinders the growth and coalescence of mesophase. This was found for the coal-tar pitches. Scanning electron (SEM) and polarized light microscopy images taken at a high magnification revealed how the QI particles were arranged and clustered around smaller anisotropic domains. The detrimental effect of QI material on the development of anisotropic texture in the resulting coke was demonstrated by comparing the structure of the coke obtained from a QI-free coal-tar pitch and a coal-tar pitch containing QI. The QI-free pitch developed a coke of large optical domains whereas the coke obtained from the pitch containing QI material had mainly a fine mosaic texture (small optical domains). However, some large anisotropic domains were present in between the QI clusters. It is also not to be excluded that the QI fraction not only acts physically by obstructing the growth and coalescence of mesophase but may also be chemically active. Findings indicate that the oxygen is concentrated in the QI fraction. Solid QI particles with oxygenated functional groups or heteroatomic structures containing oxygen, which due to their large size are insoluble in quinoline, may act as acceptor sites for hydrogen thus increasing the thermal reactivity.

The average coherent stacks of the calcined (1150 ºC) pitch cokes was found to consist of between 7 and 8 graphene layers (L_c divided by d_{002}). The average crystallite size (L_c) was fairly similar for all the calcined pitch cokes but significant differences were found. The coal-tar pitches generally developed cokes of slightly higher average crystallite sizes than the pitches of petroleum origin. The microstructure of the coal-tar pitch cokes is probably influenced by the amount and nature of the QI fraction. For the petroleum pitches there was a tendency that a high average crystallite size was connected to a more well-developed structure (larger domains) at the green coke stage.

The evaluation of hydrogen donor and acceptor abilities provides a rapid and relatively simple method to differentiate pitches which can be linked to the development of structure during carbonization. These properties thus reflect the

thermal reactivity of pitches and can be connected to the release of volatiles during pyrolysis. However, for coal-tar pitches the QI content was found to be the most influential factor on the development of optical texture and must be considered in addition to the hydrogen transfer properties. Considerations on thermal reactivity from NMR spectroscopy and elemental analysis were found to generally support the results from the hydrogen donor and acceptor ability tests.

TABLE OF CONTENTS

1 INTRODUCTION 13
1.1 Carbon Electrodes in the Production of Primary Aluminium 13
1.2 The Role of Pitch as a Binder in Carbon Electrodes 15
1.3 Scope of the Present Work 16

2 BACKGROUND 18
2.1 Production and Applications of Pitches 18
2.1.1 Coal-tar Pitch 18
2.1.2 Petroleum Pitch 19
2.1.3 Pitch from Hydrogenation of Anthracite 21
2.2 Composition and Physical Properties of Pitches 21
2.3 Characterization of Pitches 23
2.3.1 Material Properties 23
2.3.2 Structural Features and Individual Compounds 24
2.4 Carbonization Chemistry of Pitches 27
2.4.1 Mechanism of Aromatic Growth 27
2.4.2 Mesophase Formation and Development 28
2.4.3 Free Radical Stabilization by Hydrogen Transfer 29

3 EXPERIMENTAL 33
3.1 Materials 33
3.2 Nuclear Magnetic Resonance (NMR) 35
3.3 Evaluation of Hydrogen Transfer Properties 40
3.3.1 Hydrogen Donor Ability 40
3.3.2 Hydrogen Acceptor Ability 42
3.4 Thermogravimetric Analysis 45
3.5 Carbonization 45
3.6 Optical Texture Analysis 46
3.7 X-ray Diffraction 47
3.8 Scanning Electron Microscopy 50
3.9 Statistical Analysis 50

4 RESULTS 51
4.1 Nuclear Magnetic Resonance 51
4.2 Hydrogen Donor and Acceptor Abilities 58
4.2.1 Hydrogen Donor Ability 58
4.2.2 Hydrogen Acceptor Ability 64
4.3 Thermogravimetric Analysis 70
4.4 Optical Texture Analysis 73
4.5 X-ray Diffraction 83

5 DISCUSSION 88
5.1 Nuclear Magnetic Resonance 88
5.1.1 Concentration of Donatable Hydrogen 89
5.1.2 Alkyl Side Chains 94
5.1.3 Aromatic Hydrogen and Carbon 96
5.2 Hydrogen Donor and Acceptor Abilities 102
5.2.1 Hydrogen Donor Ability 102

5.2.2 Hydrogen Acceptor Ability....103
5.2.3 Hydrogen Donor and Acceptor Ability and Thermal Reactivity....104
5.3 Thermogravimetric Analysis....107
5.4 Optical Texture of Green Pitch Cokes....110
5.5 X-ray Diffraction....113
5.6 Comparison of Pitch and Pitch Coke Properties....115

CONCLUDING REMARKS....119

REFERENCES....120

APPENDIX....125

1 INTRODUCTION

1.1 Carbon Electrodes in the Production of Primary Aluminium

The Hall-Héroult process, which is named after its inventors Charles Hall and Paul Héroult, is the only method by which aluminium is industrially produced today. In 1886, they independently discovered and patented this process in which liquid aluminium is produced by electrolytic reduction of alumina (Al_2O_3). The alumina is dissolved in a liquid salt bath mainly consisting of cryolite (Na_3AlF_6) kept at a temperature around 960 ºC. The overall reaction is represented by Equation 1-1 while a schematic drawing of a modern electrolysis cell is shown in Figure 1.1.

$$\frac{1}{2}Al_2O_3(dissolved)+\frac{3}{4}C(s)=Al(l)+\frac{3}{4}CO_2(g) \qquad \textbf{(1-1)}$$

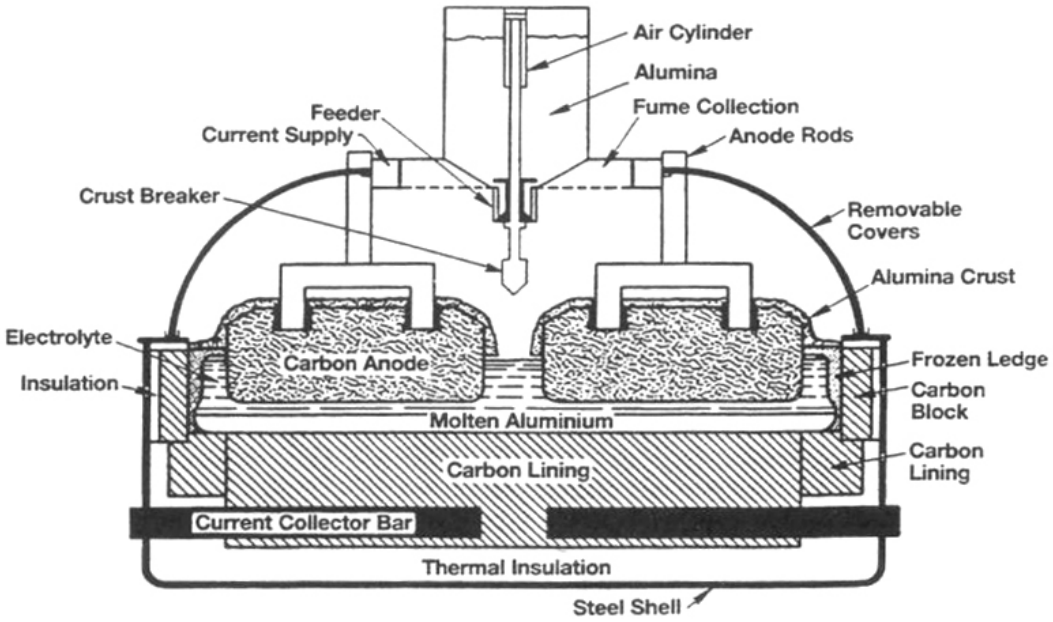

Figure 1.1. Schematic drawing of an electrolysis cell with prebaked anodes [1].

Although the interface between the electrolyte and the liquid metal pad is the actual cathode in the process, the whole container of the cell is often referred to as the "cathode". The main part of the cathode consists of carbon blocks joined by a carbonaceous seam mix. Calcined anthracite, petroleum coke or graphite are common aggregates in carbon cathode blocks. The aggregate is mixed with a binder pitch and vibrated or extruded into a rectangularly shaped body and heat treated at a temperature between 1000 and 3000 ºC. The quality of the cathode carbon is important as it strongly affects the life time of the cell. A long cell life time is crucial to reduce costs related to relining and loss of production time. New trends towards increasingly higher current densities mean that there is a constant demand for improvement of the carbon cathode block material.

The anode is made of carbon and is gradually consumed as it reacts with aluminium-oxygen-fluorine anions in the melt to form carbon dioxide. The depolarization of carbon reduces the reaction voltage from - 2.21 V (without carbon) to -1.18 V.

There are two fundamental anode designs currently in use, the prebaked anode and the Söderberg anode. The principle difference lies in the way the so-called green anode is baked to give the final product. Prebaked anodes are, as the name implies, prepared prior to installation in the cell. A mixture of petroleum coke (50 - 65 %), recycled anode butts (15 – 30 %) and binder pitch (14 – 17 %) is formed into blocks which are baked in a separate furnace at a low heating rate. The final baking temperature is around 1250 ºC. As carbon is consumed during electrolysis, the prebaked anode blocks have to be replaced at regular intervals, typically when they are reduced to one third or one forth of their original size. This is usually after 20 to 30 days in operation. One electrolysis cell contains several blocks, typically between 20 and 30. Introduction of a new anode block causes unfavorable disturbances to the cell operation. The main virtues of the Söderberg design are that the anodes are continuous and self-baking. Briquettes made from petroleum coke and binder pitch are added to the top of the Söderberg anode block. Typically, the binder pitch content is around 25 weight percent. The briquettes soften into a paste which slides slowly downwards through a rectangular steel casing. Eventually, the paste is baked into a solid carbon body as the pitch is carbonized by heat generated in the cell.

Despite the principal advantages of the Söderberg design, all new aluminium electrolysis cells use prebaked technology. Prebaked anodes are more quality consistent than Söderberg anodes. Due to lower baking temperatures, Söderberg anodes are in general more susceptible to unfavorable reactions with air and carbon dioxide leading to excess anode consumption. However, the most important aspect that makes Söderberg technology less attractive than prebaked technology is the environmental one. Almost double the amount of binder pitch is used in the preparation of Söderberg anodes compared to prebaked anodes. Most of the volatiles released during carbonization of prebaked anodes are simply burnt off to provide additional heat in the baking process. The release of potentially hazardous polycyclic aromatic compounds (PAC) is a much more serious problem for Söderberg technology.

From the overall electrochemical reaction given in Equation 1-1, the theoretical anode consumption is 0.334 kg C/kg Al produced. However, the real carbon consumption will always be considerably higher. Reactions with air at the hot anode top and CO_2 that enters pores in the anode body are the most important factors that contribute to an additional anode consumption. Due to selective oxidation of the more reactive binder matrix, small coke particles are dislodged from the anode. This is referred to as “dusting”. Carbon loss due to unfavorable oxidation and dusting is termed excess carbon consumption. Depending on the anode quality and technology used, the excess carbon consumption is normally in the range 0.02 – 0.15 kg C/kg Al. The current efficiency (CE) is always less than 100 % due to the back reaction or re-oxidation of metal by CO_2. The electrochemical consumption (0.334/CE) is usually in the range 0.35 – 0.41 kg C/kg Al produced. The net carbon consumption, which is the sum of the excess and the electrochemical consumption, may be close to 0.4 kg C/kg Al for modern smelters with prebaked anodes. Discarded anode butts material, mainly in the form of fines containing an unacceptably high level of bath contaminations, also

contributes to an increased carbon consumption. The gross consumption may amount to 0.5 – 0.55 kg C/kg Al.

1.2 The Role of Pitch as a Binder in Carbon Electrodes

Pitch is an extremely complex mixture of numerous, essentially aromatic and heterocyclic compounds derived from pyrolysis of organic material or tar distillation. Due to their high carbon content and polycyclic aromatic nature, pitches form isotropic or anisotropic cokes in relatively high yields upon thermal treatment. Almost all applications of pitches rest on this characteristic chemical property. In the present work, the pitch and its behavior during carbonization will be discussed from an aluminium smelting anode perspective. However, the results and discussion presented herein will also be relevant to the use of pitches in graphite electrodes in electric arc production of steel, in cathode blocks for the Hall-Héroult process or for instance in a pitch-based carbon fiber composite. Common for these application examples is the role of the pitch which is to act as a binder for some kind of aggregate. At a temperature above the softening point, the pitch and the aggregate are mixed into a paste which can be formed into a green body of desired shape. Pyrolysis in an inert atmosphere transforms the viscous binder pitch into a solid coke which acts as a bridge between the aggregate particles.

The microscopy image of a green anode shown in Figure 1.2 illustrates the distribution of the pitch between the coke grains. After mixing and compaction, the binder pitch should fill the space between the coke grains to provide a green body of a high density. A binder pitch should ideally give a high carbon yield after carbonization to keep the porosity at a lowest possible level.

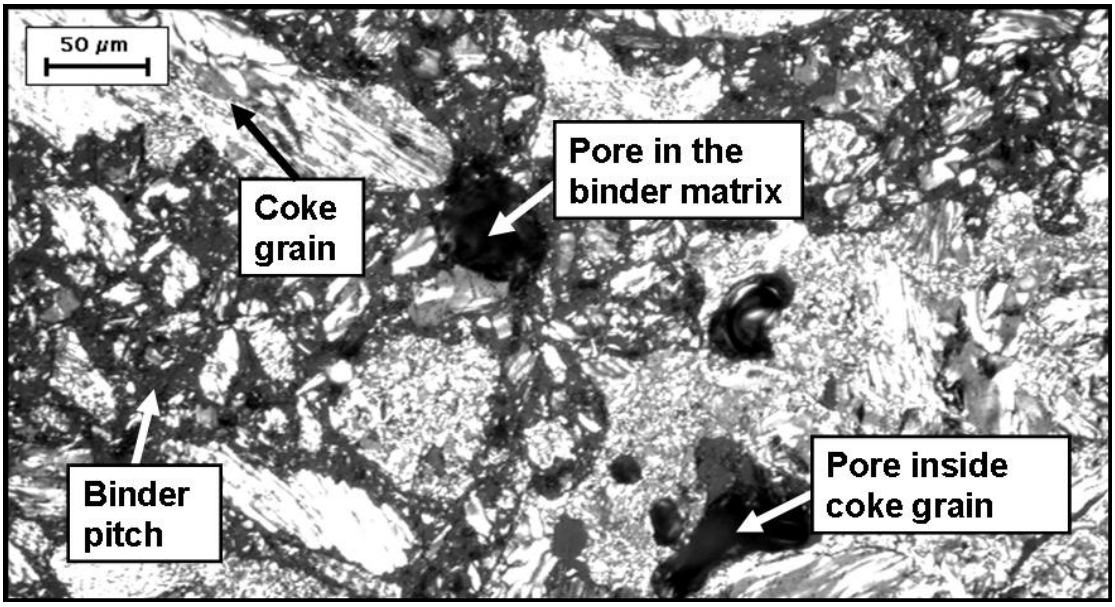

Figure 1.2. Cross-polarized reflected light microscopy image of a green (before baking) anode. The anisotropic petroleum coke grains appear white or light grey. The dark grey filler between the coke grains is the isotropic binder pitch. Also shown is a pore in the binder matrix due to poor mixing and a pore inside a coke grain.

Low porosity usually means higher strength and also that the anode is less susceptible to air-burn and oxidation by carbon dioxide. Inorganic impurities in the pitch like sodium and vanadium should be kept at a minimum level as they catalyze the excess oxidation of the anode.

Even though the binder pitch is the minor constituent in an anode, it is impossible to make a good quality anode without a good quality binder pitch. In addition to the above-mentioned factors like porosity and the inorganic impurity level, the structure of the pitch coke itself has an important influence on the chemical and physical properties of the anode which in turn affects the overall performance. The strength of the anode must be sufficient to prevent its breakage during handling and operation. A high mechanical strength is favored by an isotropic (fine mosaic) pitch coke structure. The ohmic loss over the anode should be minimized. In other words, the anode should have a low electrical resistivity and this is favored by an anisotropic (coarse mosaic) structure. The air-burn on the anode top is, among other factors, dependent on the temperature. This is in turn determined by the thermal conductivity. To decrease the temperature on the anode top, the thermal conductivity should be low which means an isotropic coke structure. However, and maybe more importantly, an ordered anisotropic structure will be more resistant towards oxidation by air and carbon dioxide. Thus, there is a conflict as different properties are favored by different coke structures. A pitch coke of high overall performance should have a structure carefully balanced between isotropic and anisotropic.

1.3 Scope of the Present Work

Coal-tar pitch is the preferred choice of binder material in anode manufacture today. However, the availability of high quality coal-tar is in decline and at least partial replacement by alternative binder sources will become increasingly important in the future. Due to environmental regulations, petroleum pitches are interesting as they generally have lower PAH emissions than coal-tar pitches during baking. Blends of coal-tar pitches and petroleum pitches are in use today on an industrial scale. The aluminium industry must be prepared to meet the challenges involved in adapting binder pitches from new sources which may be of inferior quality to the pitches available on the market today. An increased understanding of the processes involved in the transformation of a pitch into a coke and the link between raw material composition and properties and the final artifact is thus highly relevant.

Traditionally, the suitability of a binder pitch for use in anodes, has been defined from parameters like softening point, insolubility in toluene (TI) and quinoline (QI), coke yield, ash content and density. Although these parameters, which are mostly empirical in nature, give an indication of the pitch quality, more information on the chemical characteristics and carbonization behavior of pitches is certainly valuable. The present work aims to describe and explain the link between the pitch composition and the resulting coke structure based on the concept of hydrogen transfer during carbonization.

Coal-tar and petroleum pitches are graphitizable carbons that pass through a fluid stage during carbonization. Hydrogen transfer is recognized as one of the main reactions involved in the formation of large sheet-like aromatic molecules (mesogens)

from thermally induced polymerization of pitch constituents. The mesogens rearrange and stack parallel to each other forming a liquid crystalline system, mesophase, in the isotropic fluid pitch matrix. Mesophase growth and coalescence will in turn determine the anisotropy of the resulting semi-coke. In the present work, the hydrogen transfer properties of a range of coal-tar and petroleum pitches are evaluated from their ability to donate hydrogen to anthracene or accept hydrogen from tetralin during thermal treatment. Their carbonization behavior is discussed on the basis of the hydrogen transfer abilities and in relation with the pitch composition. Proton and carbon nuclear magnetic resonance (NMR) spectroscopy and elemental analysis are used in the characterization of the pitches. Also, the pitches are characterized by more "traditional" parameters like insolubility in quinoline and toluene, softening point and coking value. The rate of volatiles release during carbonization is studied by thermogravimetric analysis. Carbonization of pitches under controlled conditions is performed and the resulting pitch coke structure is characterized by cross-polarized reflected light microscopy and by X-ray diffraction. Computerized image analysis is used to quantify the optical texture.

2 BACKGROUND

2.1 Production and Applications of Pitches

2.1.1 Coal-tar Pitch

Coal is carbonized on a large scale to produce metallurgical coke. Coal-tar pitch is derived from coal-tar, which is a by-product in this process. The coking chamber is operated at temperatures between 1000 ºC and 1200 ºC with residence times from 14 to 20 hours. Coke is the main product from the process with a yield of about 75 wt% relative to feed coal. In addition, coke oven gas, benzene, ammonia, water and crude coal-tar are obtained. The tar yield is approximately 3.5 wt% relative to feed coal [2]. The hot gaseous products are collected and quenched with an ammonia flushing liquor. At this stage, the tar contains water and inorganic chlorides which cause corrosion of steel tubing in the processing plant. The refining process involves removal of water and neutralization of chlorides by NaOH or Na_2CO_3. This is the main source of sodium in the tar. The light fractions are removed from the dewatered and neutralized tar by vacuum distillation, leaving a residue of high boiling point compounds. This residue, which amounts to 50-55 wt% of the crude tar, is the coal-tar pitch. A schematic drawing of the steps involved from the coal coking chamber to the pitch by-product is shown in Figure 2.1.

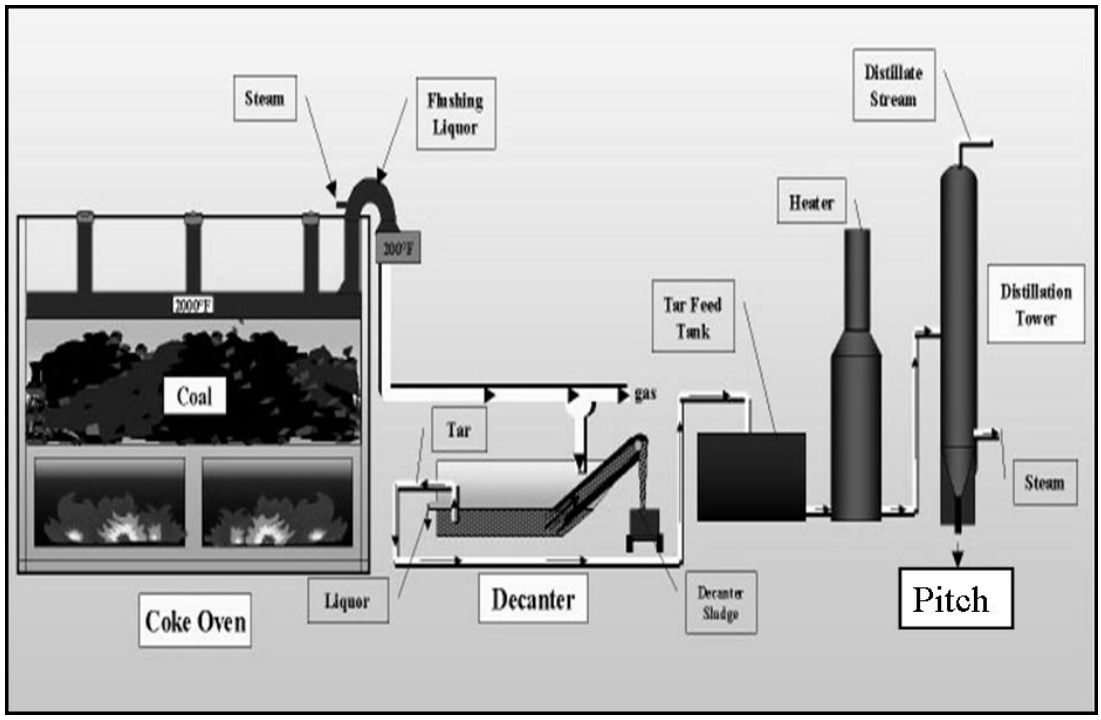

Figure 2.1. Steps involved in the production of coal-tar pitch.

The pitch from the tar distillation plant typically has a softening point of around 90 ºC (Mettler). Depending on the application, a higher softening point may be required. The softening point can be increased by heat treatment of the pitch under pressure or by air-blowing. In these processes, low boiling compounds are removed and thermally induced polycondensation reactions of aromatic molecules lead to larger aromatics.

Coal-tar pitches play a crucial role as binders in carbon electrodes, mainly in anodes for aluminium smelting and graphite electrodes for steel making. However, the unique properties of coal-tar pitches have also resulted in numerous other applications which include production of carbon-carbon composites, carburizer for iron and steel production, precursors for mesocarbon microbeads for the production of high-density isotropic graphites [3], precursors for isotropic and mesophase carbon fibers and as additives for coking coal to improve coking properties [4].

The production of coal-tar and pitch is inevitably linked to the production of metallurgical coke. Blast furnace operations have improved and the amount of coke required to produce a ton of iron has steadily decreased. The amount of iron produced is being reduced due to the use of continuous casting which increases the yield of steel and the recycling of steel via the electric furnace. Also, the use of pulverized coal injection into the blast furnace is increasing and may reduce the coke requirement by up to 40 % [5]. The coke industry, at least in the United States, may return to a similar version of the beehive oven which incinerates the tar as it is produced [6]. All of these factors have a negative impact on coal-tar production volume. Consequently, the availability of coal-tar pitch will be in steady decline. There is already an unbalance between tar supply and demand in South and North America [7]. Europe is not yet a net importer of coal-tar [8]. The world-wide demand for coal-tar pitch as a binder in the aluminium industry, which accounts for about 70 – 75 % of the total consumption, is expected to grow around 3 % annually, especially due to an expected change in demand from the Chinese prebaked anode marked which make China an importer instead of exporter. By 2008, a shortfall of coal-tar binder pitch of about 640,000 tons is expected worldwide [9].

2.1.2 Petroleum Pitch

The raw material for the production of petroleum pitch is crude oil. The currently most important feedstocks for petroleum pitches are decant oil from the fluid catalytic cracking unit and pyrolysis tar from the steam cracking of naphtha and gas oil for the production of ethylene. In Figure 2.2 a production process for petroleum pitch is schematically depicted. Petroleum pitches with a wide range of properties can in principle be produced by using different feedstocks and by adjustment of the production process.

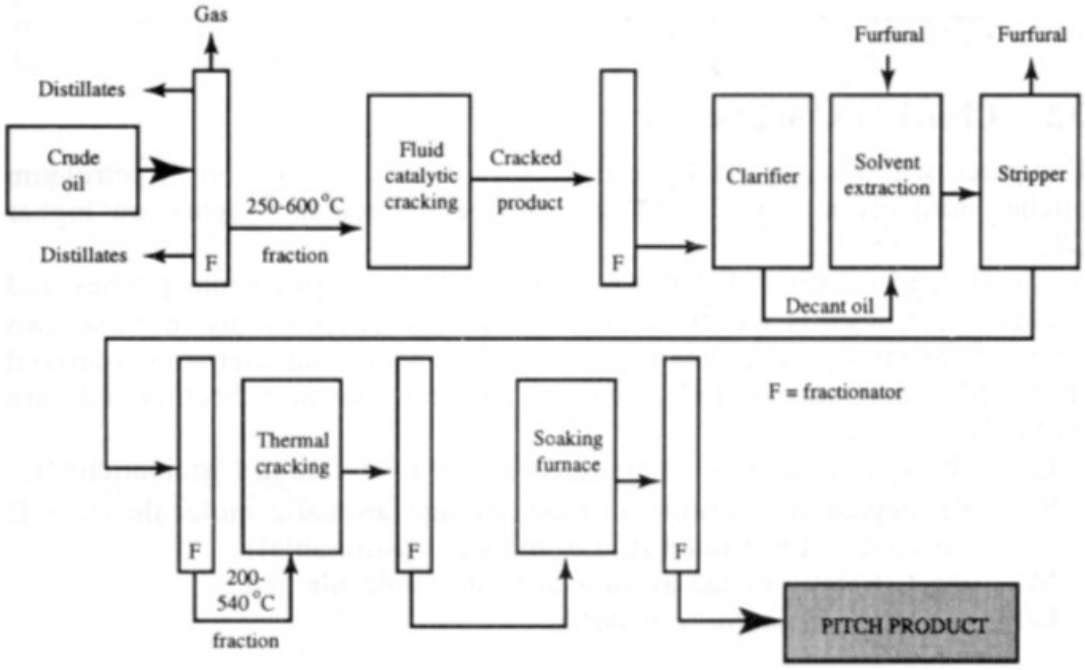

Figure 2.2. Schematic representation of a process for the production of petroleum pitch [10].

Petroleum pitches are generally less aromatic and give a lower coke yield upon carbonization compared to pitches of coal-tar origin and their use is therefore more limited. However, important applications for petroleum pitches include the use as precursor for isotropic carbon fibers and as precursor for mesophase pitch for the manufacture of graphitizable fibers of very high modulus and tensile strength. Another use of petroleum pitch is as an impregnation agent in the production of graphite electrodes for the electric arc production of steel. Traditionally, petroleum derived pitches have found only a limited use as binders in the production of anodes for aluminium smelting but this is likely to change in the near future. Blends of coal-tar and petroleum pitches are promising. Turner *et al*. [8] report a positive synergistic effect between the two binder fractions on the properties of bench scale anodes and claim that a blend with up to 50 wt% petroleum fraction is as good as or even better than the reference prepared using either coal-tar pitch or petroleum pitch. Acuña *et al.* [7] have investigated the suitability of a petroleum pitch produced at a commercial scale from a highly aromatic refinery stream. After optimization, full scale anodes with 100 wt% petroleum pitch binder were prepared and tested in a smelter. The performance was equivalent to anodes produced on a regular basis in the anode plant using coal-tar pitch as binder. An important advantage of the petroleum pitch based anodes over the reference coal-tar pitch based anodes was the low PAH emmision level during baking. The reduced PAH emmisions associated with the use of petroleum pitches would be even more attractive for Söderberg anode design where these emmisions are of a greater concern than for prebaked technology.

2.1.3 Pitch from Hydrogenation of Anthracite

The interest for the conversion of coal into distillable liquid fuels peaked during the 1920's, the Second World War and the oil crisis of the 1970's. In the future, when fossil fuel shortages are inevitable, liquefaction of coal through hydrotreatment is likely to be a major source of liquid fuel for combustion [11]. However, another interesting product from hydrogenation of coal is pitch or pitch-like materials. Andrésen *et al.* [12] consider a significant potential in the conversion of anthracite into a pitch through treatment with a hydrogen donor compound. Anthracites contain more than 90 % carbon which is mostly located in large polycyclic aromatic sheets, making it an interesting precursor for pitches that would form cokes of high carbon yield and an ordered structure. Experiments show that it is possible to convert anthracite into a material with similar softening behavior to that of a high softening point coal-tar pitch [13].

2.2 Composition and Physical Properties of Pitches

Coal-tar pitches are known to have an extremely complex composition consisting of more than 10,000 different compounds [14]. As determined by size exclusion chromatography (SEC), the molecular weight distribution of the pyridine soluble part of a typical coal-tar pitch covers a range from ~200 to more than 2500 amu (atomic mass unit) [15]. About 95 wt% of the pitch was soluble in pyridine. The vast compositional complexity of coal-tar pitches is to some degree compensated by the similarity of the constituents as they belong to relatively few classes of compounds. The types of compounds found in coal-tar pitches are: Polycyclic aromatic hydrocarbons (PAH), alkylated PAH, PAH with cyclopenteno moieties ("acenaphthylenes"), partially hydrogenated PAH, hetero-substituted PAH, *e.g.* amino and hydroxy derivates, carbonyl derivates of PAH, polycyclic heteroaromatic compounds (predominantly benzologues of furan, thiophene and pyridine) and oligomeric/polymeric systems [16]. A typical coal-tar pitch may contain around 93 wt% carbon, 4.5 wt% hydrogen, 1 wt% nitrogen, 1 wt% oxygen and 0.5 wt% sulphur as determined from elemental analysis.

The proportion of aromatic carbon in coal-tar pitches is typically around 97 %. In addition to monomeric aromatic compounds, systems consisting of several aromatic units joined by C-C single bond bridges or bridging structures are also present in pitches. According to Parker *et al.* [17] the bridging structures often include furan, thiophene or pyrrole. Using laser desorption mass spectroscopy (LD-MS), structures with molecular masses up to 12,000 amu in coal-tars and extracts have been detected. The high molecular weight portion of coal-tar pitches is probably predominantly a mixture of polycyclic heteroaromatic compounds instead of polycyclic aromatic hydrocarbons [18].

Coal-tar pitch contains dispersed solid matter and is thus not a single phase system. Basically, there are two types of particulate matter, primary and secondary. The primary particles are present in the crude coal-tar and is partly inorganic (ash) but predominantly of organic nature. The carbonaceous solid matter arises from the gas phase pyrolysis of vapors. It forms sphere-like particles having diameters typically

below 1 μm. Both discrete spheres and agglomerates are present. The primary particles have an atomic C/H ratio of about 3.5. The secondary type of particles are anisotropic spheres (mesophase) with diameters between 1 and 60 μm and form during thermal treatment of pitches [19]. These particles have a lower atomic C/H ratio of about 2.1. The particulate matter is often referred to as primary QI (quinoline insoluble matter) and secondary QI. The mesophase may be partly soluble in quinoline while some isotropic pitch matrix may be insoluble. Primary QI absorbs microwave radiation while secondary QI does not and this finding has been used to distinguish the two types [20].

Petroleum pitches differ significantly in composition depending on the feedstock used and the process applied. The chemical composition of petroleum pitches is no less complex than for coal-tar pitches. There are, however, some important differences. Petroleum pitches have a higher degree of alkyl-substituted and partially hydrogenated PAH. Accordingly, the fraction of aromatic carbon is usually 10 to 20 % lower than for a typical coal-tar pitch. Another difference is that particularly heterocyclic compounds containing nitrogen are present in lower concentrations in petroleum pitches than in coal-tar pitches. Petroleum pitches contain almost no particulate matter and the QI content is close to nil. However, there may be a small amount of secondary QI formed during thermal treatment.

Pitches are solid at room temperature. Upon heating, they have no defined melting point, but behave like a glass forming material and pass through a glass transition region before forming a viscous liquid [21]. The rheology of pitches depends strongly on the molecular weight distribution. Another factor which has a significant influence on the rheological properties of coal-tar pitches is the primary QI content. The presence of dispersed material raises the viscosity at all rates of shear. This will to some degree determine the wetting behavior against coke grains, which is of great importance for the use of coal-tar pitch as a binder in carbon anodes.

2.3 Characterization of Pitches

2.3.1 Material Properties

Pitches are commonly characterized by material properties such as softening point, coking value, ash content and solubility in organic solvents. These properties are measured on a routine basis as a measure of the suitability of binder pitches for the use in aluminium smelting anodes. Some commonly measured properties of coal-tar pitches used for prebaked anodes and their typical ranges are shown in Table 2.1.

Table 2.1. Typical range of the properties of coal-tar pitch used for prebaked anodes [22].

Properties		Method	Unit	Typical range
Water content		ISO 5939	%	0.0 – 0.2
Distillation	0 – 270 ºC	ISO N647	%	0.1 – 0.5
	0 – 360 ºC	As above	%	3.0 – 6.0
Softening point		ISO 5940	ºC	110 – 115
Viscosity at	140 ºC	ISO 8003	cP	8000 – 14000
	160 ºC	As above	cP	1200 – 2000
	180 ºC	As above	cP	300 – 500
Density in water		ISO 6999	kg/dm^3	1.310 – 1.330
Coking value		ISO 6998	%	56 – 60
Insoluble in quinoline (QI)		ISO 6791	%	6 – 16
Insoluble in toluene (TI)		ISO 6376	%	26 – 34
Ash content		ISO 8006	%	0.1 – 0.3
Sulphur content		ISO 10238	%	0.4 – 0.6
Trace elements, XRF	Na	ISO 12980	ppm	50 – 250
	K	As above	ppm	10 – 50
	Mg	As above	ppm	5 – 30
	Ca	As above	ppm	20 – 100
	Cl	As above	ppm	50 – 150

It is common practice to characterize the rheology of pitch materials by the determination of a softening point instead of determining the glass transition temperature. The softening point is essentially an isoviscous temperature. There are several different standardized methods for softening point determination which include the Kraemer-Sarnow method, the Ring and Ball method, the Mettler method and the Cube in Air method. In the Mettler method, the softening point is defined as the temperature where a pitch sample placed in a cylindrical nipple with a 6.35 mm diameter hole in the bottom flows a vertical distance of 19 mm due to its own weight. The softening temperature is registered automatically as the pitch droplet interrupts a light beam. In addition to softening point determination, it is also quite common to measure the viscosity at certain temperatures relevant to the mixing of liquid pitch and coke grains.

The coking value is a bulk pitch characteristic. Several standardized methods also exist for determination of the coking value. A small pitch sample is heated at 550 ºC for 2.5 hours in a ceramic crucible. The crucible is covered by petroleum coke to

prevent oxidation by air. The coking value is reported as weight percent of residue after carbonization relative to the weight of the pitch sample.

Many of the elements present in the ash derived from pitches act as catalysts for oxidation by air and/or CO_2. In particular, the sodium content is of importance. X-ray fluorescence spectroscopy is the most widely used technique for trace analysis of pitch ash.

Routine characterization of binder pitches by solvent fractionation is usually based on the percentage of pitch material insoluble in toluene (TI) and quinoline (QI). A weighed amount of pitch is dissolved and the amount of insolubles is determined by weighing the washed and dried residue after filtration. The insoluble content is given as weight percent relative to the weighed amount of pitch. The difference between TI and QI is commonly referred to as β-resin (wt%).

According to Zander [23], the characterization of pitches in terms of insolubles has disadvantages from a scientific point of view as these properties are purely empirical in nature. Solvent fractionation is, however, extensively used for practical applications in the industry. In many cases the determination of QI and TI contents is well suited to distinguish pitches albeit on an empirical basis.

2.3.2 Structural Features and Individual Compounds

Rheological properties of pitches but also the behavior and chemistry during carbonization are dependent on the average molecular weight and the molecular weight distribution.

The most common method to determine the average molecular weight (M_n) of pitches is by vapor pressure osmometry (VPO). Readings are normally taken at four or five different concentrations of material dissolved in dry pyridine at 60 ºC and extrapolated to zero-concentration [15]. Haenel and Zander have reported that fluorescence spectroscopy of high molecular weight fractions of coal-tar pitch in pyridine can be a rapid and convenient method to determine the average molecular weight [24, 25]. This method was found to agree quite well with vapor pressure osmometry.

Size exclusion chromatography (SEC) is frequently used in the investigation of molecular weight distribution of pitches [15, 24, 26, 27]. The aim is to separate and fractionate a pitch exclusively according to molecular size and not due to chemical constitution and functionality. The method is based on the selective retardation of solute molecules due to their relative degree of penetration into solvent filled pores in a gel matrix. The gels used are typically a three-dimensional network of cross-linked polymeric chains of controlled porosity. Due to its high solvent power for pitch, a sufficient degree of polarity and a sufficiently low viscosity at the column temperature applied (60 ºC), pyridine is commonly the eluent of choice for SEC. Elution occurs in order of decreasing molecular size. UV absorption or refractive index are commonly used physical properties to detect eluted compounds in routine SEC.

Different mass spectroscopic methods based on laser desorption have been found to be particularly useful in the estimation of molecular mass distributions in pitches [17, 26-28]. John *et al.* [29] have detected structures of molecular masses ranging from over 200,000 amu in coal-tar pitches by matrix assisted laser desorption mass spectroscopy (MALDI-MS).

Extrography is used to fractionate pitches mainly due to polarity or functionality. The separation is, however, to a certain extent also dependent on the molecular weight of the constituents. This method is essentially a combination of extraction and chromatography. The pitch sample is suspended or dissolved in a suitable solvent. An adsorbent, often silica gel, is then added to the solution. After mixing, the solvent is removed by distillation and the residue is dried and packed into a glass column. Eluents of increasing polarity are passed through the column and the fraction is collected and the solvent is removed by evaporation. A great advantage of extrography is that rather large samples can be separated in a short time. This means that the fraction sizes are sufficiently large for further physical and chemical examinations. The study of the structural composition and the carbonization of fractions obtained by extrography has provided significant information on the chemical characteristics and insight into the thermal behavior of pitches [30-33]. According to Bermejo *et al.* extrography provides a way to separate apparently very similar pitches due their different distribution of fractions [34].

Nuclear magnetic resonance (NMR) is a powerful and widely used tool in the characterization of pitches. Proton NMR gives detailed structural information about the periphery of the molecules. The spectra give a direct measurement of the distribution of the protons in differing chemical environments such as hydrogen attached to an aromatic carbon, hydrogen in an alkyl group or hydrogen attached to a carbon atom in a bridging position between two aromatic rings. Structural information gained from ^{1}H NMR analysis is useful to distinguish pitches or pitch fractions and may provide valuable insight into the thermal behavior of pitches [33, 35]. The functionality of the external framework has an important influence on the carbonization chemistry of pitches. It is common to perform measurements on pitch solutions. The disadvantage of this is that pitches are not completely soluble in solvents suitable for NMR spectroscopy. To overcome this difficulty, ^{1}H NMR spectra can be measured in the fused state at a temperature above the softening temperature of the pitch. Fused state or high-temperature ^{1}H NMR spectroscopy has proven to be a powerful technique for *in-situ* investigation of processes taking place during carbonization of pitches, coals or co-carbonization systems [36-38].

Whereas ^{1}H NMR measurements only give direct information about the periphery of the pitch constituents, ^{13}C NMR analysis also gives detailed information about the internal framework. With regard to quantitative measurements, the basic drawback of ^{13}C NMR compared to ^{1}H NMR spectroscopy, is the significantly lower sensitivity. However, the development of techniques such as inverse gated proton decoupling has made quantitative measurements in solution state possible. Carbon NMR spectroscopy is well suited for determination of aromaticity for pitches. Due to the limited solubility of pitches in suitable solvents, much attention has been given to solid state ^{13}C NMR. The main objectives of solid state ^{13}C NMR are to obtain reliable information about aromaticity and the fraction of quaternary (non-protonated) carbon for the entire pitch. The fraction of quaternary carbon is a measure of the

degree of condensation. Techniques involving magic-angle spinning (MAS) and cross-polarization (CP) allow spectra of high resolution to be obtained. Even though these spectra provide reliable values for the aromaticity of pitches, the quaternary carbon concentration are underestimated. Snape *et al.* [39] have proposed an indirect method based on elemental composition and hydrogen and carbon aromaticities to gauge the degree of condensation in coal-tar pitch. More recently, the Bloch decay or single pulse excitation (SPE) technique has been recognized as the best approach to obtain reliable quantitative information about aromaticity and non-protonated carbon concentrations. Maroto-Valer *et al.* [40] have found that H/C ratios derived from SPE measurements were in good agreement with those found by elemental analysis. This is a good indication of the quantitative reliability of the SPE method. Fused state (melt) ^{13}C NMR spectroscopy generally suffer from inferior resolution compared to that achieved in the solid state. Azami and co-workers have, however, employed high-temperature ^{13}C NMR successfully in an *in-situ* monitoring of mesophase formation in pitches [41].

Fourier transformed infrared spectroscopy (FTIR) can be used as a semi-quantitative analysis tool in the detection and determination of functional groups in pitches [42]. Compounds containing carbonyl functional groups are often present in very low concentrations in pitches and can not be detected by most analytical techniques. Due to the very high sensitivity to FTIR spectroscopy, carbonyl compounds can detected by this method.

Although the composition of pitches is far too complex to allow for a determination of all the compounds, the qualitative and quantitative analysis with regard to individual compounds is important. Due to environmental legislation and from an occupational hazard perspective, the quantitative determination of carcinogeneous compounds like benzo[a]pyrene in pitches and pitch fumes is of great importance. However, the determination of individual compounds may also be important to achieve a greater understanding of pitch structure and behavior. The most frequently used technique is gas chromatography (GC). A wide range of columns and detectors allow for efficient separation of compounds with molecular masses less than 350 amu. For the separation of compounds with molecular masses of up to 600 amu, high-pressure liquid chromatography can be used (HPLC). The separation is, however, rather modest due to the enormous compositional complexity of the higher molecular weight proportion of pitches.

2.4 Carbonization Chemistry of Pitches

Coal-tar and petroleum pitches pass through a fluid stage during carbonization. As the temperature is increased the viscosity of the isotropic pitch decreases. In the early stages of carbonization, thermal rupture of C-C bonds and C-H bonds in reactive compounds leads to defragmentation and the formation of free radicals. Cleavage of reactive aliphatic C-C bonds leads primarily to gasification. Smaller thermally stable molecules are distilled out as the heat treatment temperature is increased. Dehydrogenative polymerization proceeds mainly via a free radical mechanism leading to molecular size enlargement (aromatic growth) and the formation of oligomeric systems. Larger aromatic sheet-like molecules (mesogens) rearrange to form an anisotropic liquid crystal phase, mesophase, in the isotropic fluid matrix at temperatures between 350 and 500 ºC. Having reached a minimum, the viscosity of the reaction system increases and cross-linking and mesophase growth take place until eventually a solid semi-coke (green coke) is irreversibly formed.

2.4.1 Mechanism of Aromatic Growth

The thermally reacting pitch is an extremely complex system. An insight into the main mechanisms involved during carbonization can be achieved through the study of pure aromatic precursors. In Figure 2.3, the main reaction pathway occurring during heat treatment of naphthalene at temperatures between 400 and 500 ºC is depicted.

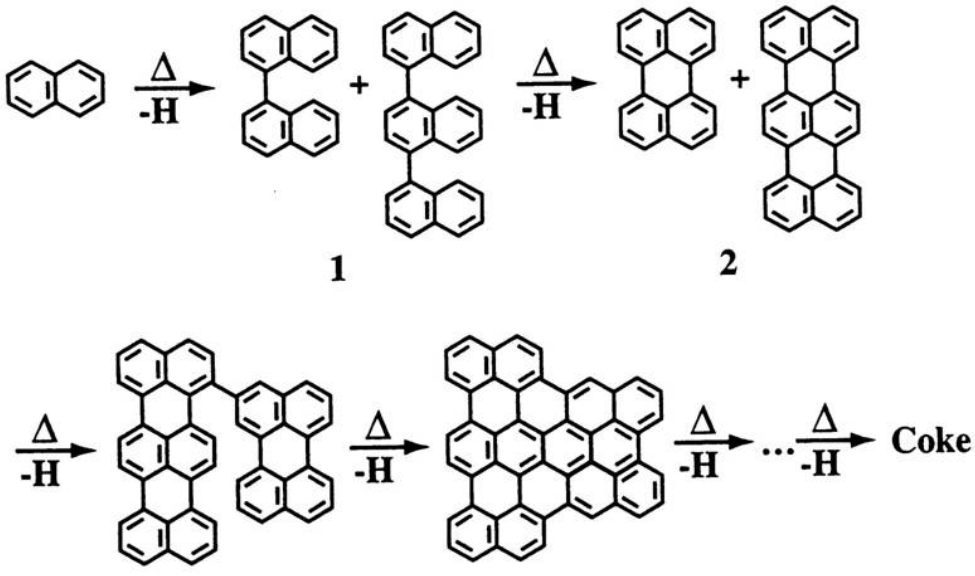

Figure 2.3. Mechanism of aromatic growth of naphthalene [43].

In the first step of aromatic growth, bi-aryls and oligo-aryls are formed from a monomeric PAH or a structurally related heteroaromatic system. In the next step, bi- and oligo-aryls undergo intramolecular dehydrocyclization reactions to form pericondensed aromatic systems. This sequence of reactions occur repetitively until eventually cross-linking between large aromatic systems leads to an abrupt increase in

viscosity and the formation of a green coke. The first step, formation of bi-aryls, is very likely rate determining [43].

In addition to dehydrogenative polymerization, other chemical mechanisms are also involved in the transformation of pitches to cokes. The step of thermal rearrangements is very important during the early stages of carbonization [44]. Due to these reactions, it is often very difficult to relate the starting material to the subsequent course of carbonization. Fragmentation and alkylation reactions also play an important role. This is particularly true for petroleum pitches which are rich in side chains. Through quantitative studies of cracking and gas formation of alkyl (methyl through butyl) groups on large aromatic molecules, Greinke has found that the side chain tend to fracture at the alpha position to the aromatic ring [45]. This leads predominantly to the formation of aryl-aryl bridges in pitch dimers.

2.4.2 Mesophase Formation and Development

In 1968 Brooks and Taylor first recognized and advanced the relevance of mesophase as an essential intermediate in the formation of anisotropic cokes from the liquid stage during carbonization [46]. They found that optically anisotropic spheres (mesophase) formed in the isotropic pitch matrix during thermal treatment of coal-tar pitch. Mesophase exhibits properties that resemble those of nematic liquid crystals. The liquid crystals formed during carbonization are generated from the isotropic pitch itself and never reach an equilibrium position. As such, they differ from other liquid crystal systems which are reversibly thermotropic.

Upon heat treatment pitches first melt and then starts to flow as a liquid. At around 200 ºC translational energy exceeds cohesion energy and the isotropic pitch exhibits flow properties approaching those of a Newtonian fluid. Upon further heat treatment to around 400 ºC, the molecular weight of the pitch constituents reach 600 – 900 amu due to dominantly dehydrogenative polymerization and the cohesion energy exceeds the translational energy [47]. At this stage, the aromatic sheet-like molecules often termed mesogens remain attached to each other following a collision. Further mesogens of similar size and shape are collected until, eventually, the anisotropic clusters can be observed by optical microscope. During the initial growth stages of mesophase formation, the discotic mesogen molecules are stacked parallel and vertical to each other. The growing mesophase takes on a spherical shape to minimize the surface energy [48].

As the mesophase spheres continue to grow, they will come into contact and coalesce. If this process can take place unhindered, the resulting coke will be anisotropic with large optical domains. However, if the viscosity of the pyrolysis system is high, the growth and coalescence may be obstructed and a fine mosaic coke (small optical domains) will be formed. Particulate matter with diameters less than 1 μm such as primary QI tend to adhere to the surface of the mesophase spheres. This prevents coalescence and a coke of smaller optical texture is formed. The size of optical texture is therefore smaller in cokes derived from QI containing coal-tar pitches compared to petroleum pitches.

The formation, growth and coalescence of mesophase determine the size of the optical texture of the green coke and consequently the physical and chemical properties of final carbon product.

2.4.3 Free Radical Stabilization by Hydrogen Transfer

The generation of mesophase within a pyrolyzing pitch system is almost exclusively determined by the chemical properties of the parent pitch. If the intermolecular reactivity of the pitch constituents is too high, cross-linking will occur at a temperature lower than mesophase formation and the system solidifies prematurely to form an isotropic coke. According to Greinke and Singer, the intermolecular reactivity of constituents in the pyrolysis system should be constrained so that the molecules resulting from aromatic growth do not exceed molecular weights exceeding ~ 900 amu [49]. The pyrolysis system must also have a sufficiently low viscosity/high fluidity to allow enough mobility for the mesogens to stack parallel to each other and establish a liquid crystal system. Cross-linking reduces the fluidity. The intermolecular reactivity of the constituent molecules of the mesophase must be constrained to facilitate growth, coalescence and mobility of the liquid crystal system. Several factors that are crucial for mesophase initiation and development are therefore dependent on the stability of the parent pitch upon heat treatment. In particular, the presence of alkyl side chains, reactive functional groups such as hydroxyl and carboxyl and heteroatoms within the molecules leads to an increased reactivity of the pitch [47].

Marsh and Neavel advanced the concept and relevance of hydrogen transfer first in co-carbonization systems of coal and pitch [50]. If free radicals formed by thermal rupture of bonds in reactive species can be stabilized by hydrogen transfer from within the system, extensive cross-linking at a too early stage is prevented thus allowing initiation, growth and coalescence of mesophase and formation of an anisotropic coke structure. The molecular growth is thus delayed and the zone of temperature of maximum fluidity is extended. This process is illustrated in Figure 2.4.

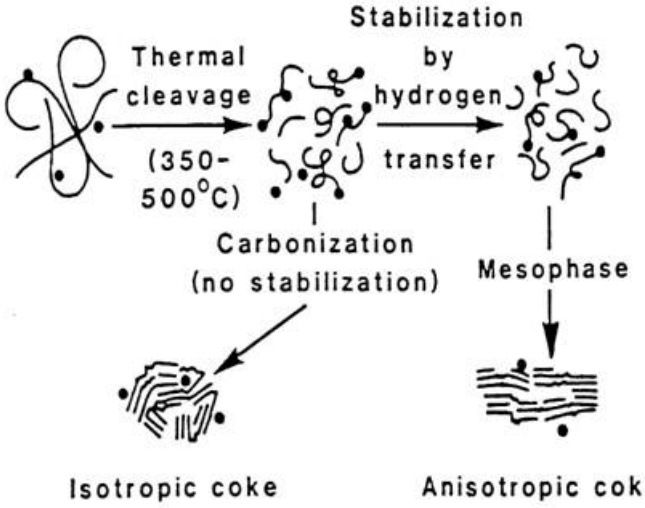

Figure 2.4. Free radical stabilization by hydrogen transfer during carbonization [51].

A proposed mechanism for hydrogen transfer from a hydroaromatic molecule (9,10-dihydroanthracene) to stabilize free radicals formed from cleavage of an ethylene bridge is shown in Figure 2.5. Smaller molecules stabilized by hydrogen transfer during the early stages of carbonization may serve as solvating vehicles maintaining a low viscosity in the system and may also be important as hydrogen shuttling agents [52].

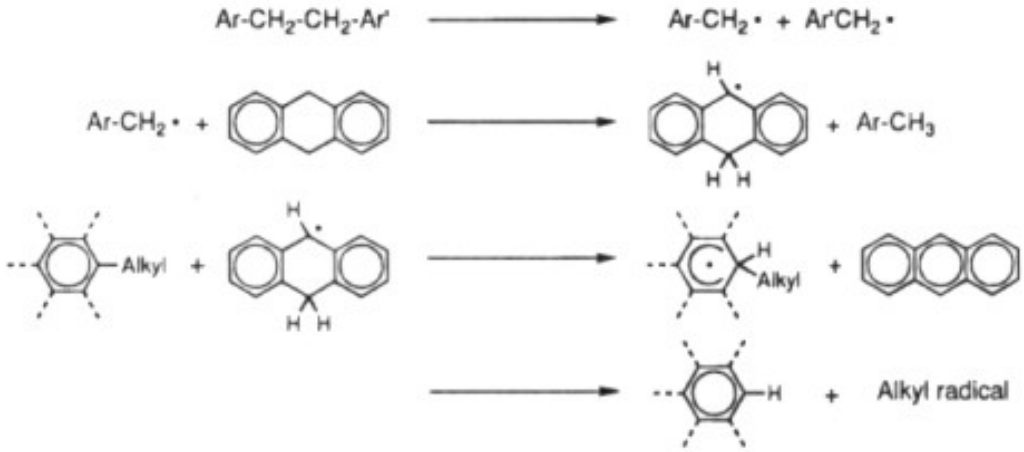

Figure 2.5. Hydrogen transfer from a hydroaromatic molecule to stabilize radicals formed from the thermal rupture of an ethylene bridge connecting two aromatic structures [53]**.**

Yokono, Marsh and Yokono [54] assessed if pitches which form cokes of larger optical domains or have a greater ability to modify the carbonization behavior of coals act as hydrogen shuttling agents in the carbonization system. Co-carbonization of pitch and a hydrogen acceptor agent, anthracene, was carried out at 400 ºC at a heating rate of 5 ºC/min with no soaking time in sealed pyrex tubes. The reaction product was extracted with chloroform and studied by ^{1}H NMR spectroscopy. They found that 9,10-dihydroanthracene (DHA) was the major hydrogenated product formed from anthracene. The results indicated that pitches forming the largest amounts of DHA also produced semi-cokes of larger optical domains. Such pitches had a greater facility to 'shuttle' hydrogen atoms from donating molecules to accepting radicals thus stabilizing the carbonization system. Obara *et al.* [55] used a similar procedure in the study of carbonization behavior of hydrogenated ethylene tar pitch. They also concluded that the ability of the pitch to donate hydrogen is an important factor governing the development of optical texture of the resultant coke.

The formation of free radicals during carbonization of pitches can be monitored by high temperature electron spin resonance spectroscopy (ESR). This technique is therefore a useful means of studying the thermal reactivity. Yokono *et al.* [51] have found a relationship between hydrogen donor ability and spin concentration during heat treatment of petroleum residues. The residues that had a higher ability to donate hydrogen to anthracene measured by the formation 9,10-dihydroanthracene as determined by ^{1}H NMR spectroscopy showed a lower spin concentration at high temperatures. Carbonization of petroleum residues with a relatively high donor ability led to the formation of cokes with extended optical texture.

In a later study, Yokono, Takahashi and Sanada [56] investigated the hydrogen donor and acceptor abilities of three coal-tar pitches fractionated into hexane solubles, a

hexane soluble fraction free of polar material and pyridine insolubles. The hydrogen donor ability (HDa) was measured as described above while the acceptor ability (HAa) was measured from the amount of anthracene formed in the co-carbonization of pitch and 9,10-dihydroanthracene which acts as a hydrogen donor compound. They found that the hexane soluble fraction showed a higher HDa and a lower HAa compared to the unfractionated pitch. This was attributed to the higher proportion of naphthenic structures as determined by ^{1}H NMR spectroscopy in this fraction. Clarke, Rantell and Snape [57] have found that the principal hydrogen donor groups are hydroaromatic and naphthenic rings in hydroaromatic species. When the polar material was removed from the hexane soluble fraction, an increase in HDa and a decrease in HAa was observed. Oxygenated functional groups are considered as a primary acceptor site in addition to free radicals. Sulphur-containing species might also act as acceptor sites for hydrogen. The pyridine insoluble fraction showed a very limited donor ability probably due to the highly condensed structure with few active sites. The acceptor ability was also lower than for the unfractionated pitch but in the same range as for the polar material free hexane soluble fraction. This indicates that also the heavier pitch fractions influence the total hydrogen acceptor ability.

Uemasu and Kushiyama [58] have investigated the suitability of capillary gas chromatograpy in the evaluation of transferable hydrogen in heavy oils. They found that this technique has advantages over the use of ^{1}H NMR spectroscopy for the determination of the amount of 9,10-dihydroanthracene formed in the co-carbonization with anthracene. The capillary gas chromatography method was superior in precision and accuracy, especially in the detection and quanfification of trace amounts of DHA.

The products arising from thermal reactions with anthracene or 9,10-dihydroanthracene at 400 ºC have been investigated using both gas chromatography and ^{1}H NMR spectroscopy by Bermejo *et al.* [59]. Both methods were found to give similar results but gas chromatography was viewed as both simpler and faster. Importantly, gas chromatography revealed the presence of 1,2,3,4-tetrahydroanthracene (THA) in the product from the thermal reaction of both anthracene and DHA with pitch. The signal of THA in the ^{1}H NMR spectrum overlaps with signals from pitch constituents and has probably for this reason been overlooked in previous studies. Heat treatment of pitch and anthracene yielded significant amounts of THA in addition to DHA. The amount of THA formed should therefore be included in the hydrogen donor ability (milligrams of hydrogen transferred per gram of pitch). Bermejo and co-workers also found significant amounts of THA in addition to anthracene in the product from the heat treament of pitch and 9,10-dihydroanthracene. This suggested that DHA displays a dual role as both a hydrogen acceptor and hydrogen donor. Heating of DHA alone showed a partial disproportionation into anthracene and THA. However, when heated in the presence of pitch much larger amounts of THA were formed. The THA formation was thus sample promoted. It was also found that the formation of THA was dependent on the heat treatment temperature. The formation mechanism of THA is not clearly understood. The authors suggested that the amount of hydrogen attributed to the formation of THA should be subtracted from the amount of hydrogen involved in the formation anthracene when calculating the hydrogen acceptor ability (mg H/g pitch).

Díez *et al.* [60] have measured the hydrogen donor and acceptor abilities of a range of pitches of different origin at 400 ºC with a heating rate of 5 ºC/min and no soaking time. Gas chromatography with fluorene as internal standard was used for quantification of reaction products. Petroleum pitches exhibited significantly higher hydrogen donor abilities than coal-tar pitches. The hydrogen acceptor ability was fairly similar for the two groups of pitches. The formation of THA was found to be sample promoted as pitches with a greater source of donatable hydrogen also produced larger amounts of THA. Moreover, there appears to be a link between the ability of pitches to donate hydrogen to anthracene and accept hydrogen from 9,10-dihydroanthracene. However, no direct correlation between HDa and HAa was found. Díez and co-workers also studied the carbonization behavior of the range of pitches by thermogravimetric analysis. The hydrogen donor and acceptor abilities were found to be related to the percentage of volatile matter released between 400 and 500 ºC. However, pitches of different origin fell into separate groups in the correlation.

Tetralin (1,2,3,4-tetrahydronaphthalene) has been used as a hydrogen donor compound in the study of hydrogen transfer to coal by Pajak [61]. This compound has advantages over 9,10-dihydroanthracene as a hydrogen donor due to its higher thermal stability. It does not self-disproportionate when heated to 400 ºC alone and only one major dehydrogenated product, naphthalene, is formed in the thermal reaction with pitch. Machnikowski *et al.* [62] have used tetralin as a hydrogen acceptor compound in the study of a coal-tar pitch and its extrographic fractions. The hydrogen acceptor ability was calculated from the ratio of naphthalene to tetralin. Anthracene was used as a hydrogen acceptor compound. The soaking time at the reaction temperature of 360 ºC was varied from 15 minutes to 8 hours. Both hydrogen donor and acceptor abilities remained practically unchanged after about 6 hours heat treatment. The extrographic fractions could be clearly separated from their hydrogen transfer characteristics. The hydrogen acceptor ability was found to increase markedly with the elution depth of the extrographic fractions. A good correlation between HAa and the total oxygen content in the fractions was found. In general, the ability of the fractions to develop cokes of large optical textures decreased with elution depth.

3 EXPERIMENTAL

3.1 Materials

The series of pitches used in this study includes five coal-tar pitches labeled CTP1-5 and four petroleum pitches labeled PP1-4. In addition, a QI-free coal-tar pitch labeled CTPN supplied by GrafTech International has been studied. Coal-tar pitch N is prepared by removing the QI particles from the parent coal-tar in a continuous method using cross-flow ceramic membranes with a pore size of 0.05 μm. More details about this process are given by Shao, Lewis and Chang [63]. A QI-free pitch has also been prepared by GrafTech International from CTP1 through a small unit batch operation probably involving filtration through a porous metal disk under pressure and elevated temperature. Details about the process are business confidential and has not been revealed to the author. This pitch is labeled CTP1N. Both the softening point and the β-fraction have increased after QI-removal (Table 3.1). The pitch analyses for CTP2, CTP3, CTPN and CTP1N have been provided for this study by Hydro Aluminium's Research Laboratory in Årdal while the analyses for the remaining pitches have been obtained from Elkem's Research Center in Kristiansand. The two laboratories have used the same standardized methods for measuring the pitch properties.

Table 3.1. Pitch properties.

Pitch	Softening Point (°C)[1]	Coking Value (wt%)[2]	TI (wt%)[3]	QI (wt%)[4]	β-fraction (wt%)†
CTP1	110.7	61.0	32.6	12.9	19.7
CTP2	119.7	60.1	30.1	9.6	20.5
CTP3	187.2	78.1	53.0	25.0	28.0
CTP4	118.4	59.7	33.1	6.6	26.5
CTP5	116.5	60.4	32.0	4.7	27.9
CTPN	120.0	60.4	22.6	0.6	22.0
CTP1N	114.2	NA	23.6	0.6	23.0
PP1	123.1	54.4	7.4	0.1	7.3
PP2	112.3	48.1	13.7	0.3	13.4
PP3	120.3	50.4	12.0	0.2	11.8
PP4	109.2	46.9	10.2	0.0	10.2

1. Mettler softening point, ASTM D 3104, 2. ISO 6998, 3. Toluene Insolubles (TI), ISO 6376, 4. Quinoline Insolubles (QI), ISO 6791, † Difference between TI and QI.

The elemental analysis (Table 3.2) was performed for this study by Instituto Nacional del Carbón (INCAR) in Oviedo, Spain. The carbon, hydrogen and nitrogen contents were determined with a LECO-CHN-2000 unit while the sulphur content was determined with a LECO S-144-DR unit.

The chemicals used in this study are listed in Table 3.3.

Table 3.2. Elemental analysis of pitches.

Pitch	C (wt%)	H (wt%)	N (wt%)	O (wt%)*	S (wt%)	H/C†
CTP1	93.57	4.24	0.98	0.63	0.58	0.54
CTP2	93.77	4.35	1.03	0.25	0.60	0.55
CTP3	94.25	3.85	0.94	0.44	0.52	0.49
CTP4	93.10	4.36	1.02	0.86	0.66	0.56
CTP5	92.63	4.69	0.87	1.24	0.57	0.60
CTPN	93.79	4.49	0.95	0.23	0.54	0.57
CTP1N	93.63	4.53	1.03	0.22	0.59	0.58
PP1	93.64	5.27	0.16	NA	1.20	0.67
PP2	93.02	6.09	0.33	NA	1.10	0.78
PP3	93.51	6.02	0.31	NA	0.68	0.77
PP4	92.09	6.11	0.02	1.67	0.11	0.79

* By difference. The sum of C, H, N and S exceeded 100 wt% for PP1, PP2 and PP3, † Atomic ratio.

Table 3.3. Chemicals.

Chemical	Producer	Quality
Carbon disulphide, CS_2	ACROS Organics	Pro Analysis
Fluorene, $C_{13}H_{10}$	ACROS Organics	Purity > 98 %
Anthracene, $C_{14}H_{10}$	Aldrich Chemical Company Inc.	Purity > 99 %
9,10-dihydroanthracene, $C_{14}H_{12}$	Aldrich Chemical Company Inc.	Purity > 97 %
Naphthalene $C_{10}H_8$	Merck	Purity > 99 %
1,2,3,4-tetrahydronaphthalene (tetralin)	Fluka	Purity > 99.5 %

3.2 Nuclear Magnetic Resonance (NMR)

Carbon disulphide was chosen as the solvent for pitches in the preparation of samples for NMR analysis. The reason for this was twofold. Firstly, it does not have any resonance in the proton spectrum and the resonance in the carbon spectrum does not overlap with any of the regions of interest. Deuterated chloroform, which is a common solvent for pitch in NMR studies, will always contain amounts of non-deuterated chloroform which cause a signal overlap in the proton spectrum. Secondly, carbon disulphide is an even stronger solvent for pitch than chloroform [64].

An exact volume of carbon disulphide was added to a weighed amount of ground pitch in a small glass flask closed with a lid. It was found that a pitch concentration of approximately 15 wt% was adequate for ^{13}C NMR spectra of high resolution and a relatively good signal to noise ratio. A concentration of 3 wt% pitch was chosen for the ^{1}H NMR experiments, as this concentration was found to be optimum by Guillén, Díaz and Blanco [35]. Guillén *et al.* [64] have investigated the solubility of six coal-tar pitches and found that the extraction yield in CS_2 varied between ~ 67 wt% and ~ 80 wt%. The glass flask was placed in an ultrasonic bath for a period of 2 hours ensuring a high degree of extraction. The CS_2 extract was filtered through a membrane syringe filter with a pore size of 0.2 μm. 500 μL of the filtered extract was then added to a 5 mm NMR tube. Deuterated dioxane (1,4-dioxane-8d), with a chemical shift of 3.53 ppm in proton spectra and 66.6 ppm in carbon spectra [65] relative to TMS (tetramethylsilane), was chosen as the lock substance as it is soluble in the CS_2 extract.

All spectra were recorded on a Bruker Avance DRX 600 spectrometer using the XWINNMR 3.5 software. The spectrometer was equipped with a cryogenic probe. Operating frequencies were 600.18 MHz for ^{1}H and 150.93 MHz for ^{13}C and the temperature was 293 K. Proton spectra were recorded with a ^{1}H-pulse angle of 30º, an acquisition of 8k data points and 8 scans each. The relaxation delay was 5 s and the pulse width was 3.9 μs (90º). After zero filling to 16k the free induction decay (FID) was Fourier transformed to spectra with a spectral range of 7861.64 Hz (~13.1 ppm). Carbon spectra were obtained by using an inverse gated pulse program sequence (zgig30), a 30º read pulse, an acquisition of 16k data points and 5120 scans each. After zero filling to 32k data points the FID was Fourier transformed to spectra with a width of 25641 Hz (~170 ppm). Zero filling was performed to increase the spectral resolution. The line broadening was 5 Hz and the pulse delay 5 s while the pulse width was 14.8 μs (90º). Proton decoupling was performed using the Waltz 16 routine. The DEPT (Distortionless Enhancement by Polarization Transfer) sequence was used with a proton pulse of 135º [66]. Subspectra obtained show CH and CH_3 groups in phase while CH_2 is 180º out of phase. Quaternary (non-protonated) carbons are not recorded in the subspectrum (see Figure 3.4). The working conditions for the NMR measurements are summarized in Table 3.4. Fourier transformation of the FIDs, baseline and phase corrections and integration of spectra were performed using the MestReC version 4.3.6 software.

Table 3.4. Working conditions for NMR measurements.

	^{1}H	^{13}C
Frequency (MHz)	600.18	150.93
Spectral range (Hz/ppm)	7861.64/~13.1	25641/~170
Number of data points	16k	32k
Pulse width at 90º (μs)	3.9	14.8
Pulse delay (s)	5	5
Acquisition time (s)	0.24	0.78
Number of scans	8	5120

Guillén, Díaz and Blanco [35] have investigated CS_2 extracts of coal-tar pitches by ^{1}H NMR and assigned proton chemical shifts. The chemical shift classification reported in their article, which is shown in Table 3.5, has been used in the present work as the sample preparation and experimental conditions are similar. The chemical shift regions are also illustrated as an example in the proton spectrum of PP1 shown in Figure 3.2.

Table 3.5. Proton NMR chemical shifts (ppm) relative to tetramethylsilane (TMS) [35].

Symbol	Description	Chemical shift (ppm)
H_{ar2}	Aromatic hydrogens in sterically hindered positions, highly pericondensed PACs, next to heteroatoms and some hydrogens joined to nitrogen.	9.5 – 8.36
H_{ar1}	All other aromatic hydrocarbons.	8.36 – 6.3
H_F	Aliphatic hydrogens in methylene groups α to two aromatic rings.	4.5 – 3.69
H_A	Aliphatic hydrogens in methylene groups α to an aromatic ring and β to another.	3.69 – 3.0
$H_{\alpha 1}$	Aliphatic hydrogens in methyl or methylene groups α to an aromatic ring which can also be attached in γ position or further to another or the same aromatic ring.	3.0 – 2.0
$H_{\beta 2}$	Alicyclic hydrogens in β position to an aromatic rings	2.0 – 1.6
$H_{\beta 1}$	Aliphatic hydrogens in methyl or methylene groups β to an aromatic ring.	1.6 – 1.0
Hγ	Aliphatic hydrogens in methyl or methylene groups γ to an aromatic ring	1.0 – 0.5

An illustration of the types of hydrogen is displayed in Figure 3.1 below.

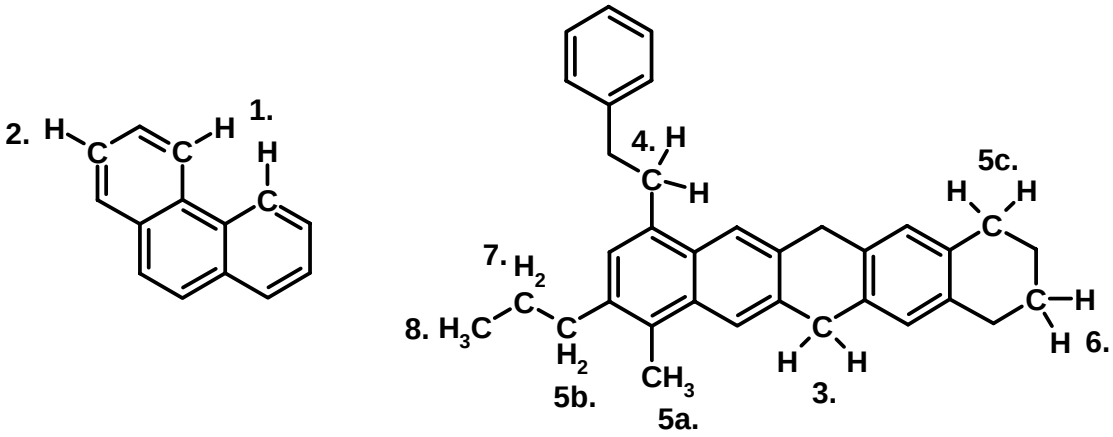

Figure 3.1. Illustration of types of hydrogen. Description and chemical shift ranges in ^{1}H NMR is given above (Table 3.5).
H_{ar2}: 1, H_{ar1}: 2, H_F: 3, H_A: 4, $H_{\alpha1}$: 5a,b,c, $H_{\beta2}$: 6, $H_{\beta1}$: 7 and H_γ: 8.
Hydrogen in α-methyl group: 5a, Hydrogen in α-methylene in alkyl side chain: 5b and Hydrogen in α-methylene in hydroaromatic ring (5c).

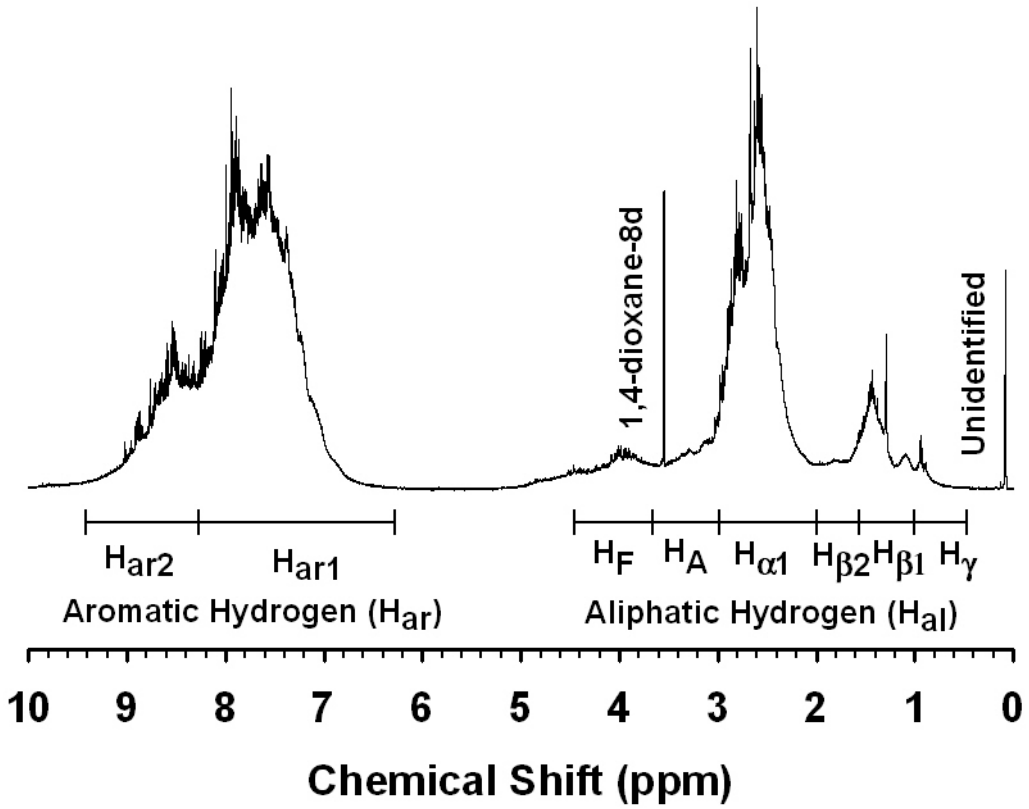

Figure 3.2. Assignment of chemical shifts in the ^{1}H NMR spectrum of a petroleum pitch (PP1) dissolved in CS_2 (~3 wt% pitch). 1,4-dioxane-8d has been added as the lock substance. Shift assignment described in detail in Table 3.5.

The 1,4-dioxane-8d peak overlaps with the H_A region. For quantification of this region, the area under the dioxane peak was subtracted. The unidentified peak is probably due to minor amounts of a silicon containing species arising from

dissolution of the plastic film which was used to keep the lid tight during extraction. It does, however, not overlap with any of the spectral regions of interest and consequently the nature and source of this impurity has not been investigated any further.

Díaz and Blanco [67] have characterized coal-tar pitches using a combination of ^{13}C and ^{1}H NMR analyses. Samples were prepared by extraction in CS_2. The samples were slightly more concentrated, about 20 wt% pitch, compared to the concentration used in the present work. This concentration difference is not considered to influence the cut-off points for the chemical shift regions to a significant extent. The carbon chemical shifts reported by Díaz and Blanco [67] are shown in Table 3.6. In addition, the methyl carbon region has been divided into two sub-regions as CH_3 groups in an α position to an aromatic carbon (23-17 ppm) can be distinguished from a carbon atom in a terminal position at an alkyl side chain (17-11 ppm). Clarke, Rantell and Snape [57] have defined the resonance region due to non-α-CH_3 carbons from 16.5 to 11 ppm. Also, aliphatic carbon connected to one hydrogen (CH_{al}) was found to give rise to a signal in the region from approximately 45 ppm to 65 ppm in the DEPT spectra of PP2, PP3 and PP4. This region therefore overlaps slightly with the $C_{\alpha 2}$ region defined by Díaz and Blanco [67]. Both the conventional ^{13}C NMR spectrum and the DEPT spectrum for a petroleum pitch (PP1) are shown in Figure 3.4. The resolution of the DEPT spectrum is better than the conventional carbon spectrum. It has therefore been used for a more accurate quantification of the aliphatic region. For quantification of the DEPT spectra the integral under the CH_2 region has been multiplied by -1 and divided by the square root of 2 [66].

Table 3.6. Carbon NMR chemical shifts (ppm) relative to tetramethylsilane (TMS) [67].

Symbol	Description	Chemical shift (ppm)
$C_{ar1,2}$	Catacondensed aromatic carbon, aromatic carbon with heteroatomic or aromatic substituents and aromatic carbon joined to aliphatic chain.	160 – 129.5
$C_{ar1,3}$	Pericondensed aromatic carbon and protonated aromatic carbon.	129.5 – 108
CH_{al}	Aliphatic carbon connected to one hydrogen.	~ 65 - 45
$C_{\alpha 2}$	Methylene carbon in α position to two aromatic rings (bridge/hydroaromatic structures).	49.3 – 34
CH_2	Other methylene carbon	34 – 23
α-CH_3	Methyl carbon in α position to an aromatic carbon	23 – 17
t-CH_3	Methyl carbon at terminal position of an alkyl chain	17 – 11

An illustration of the types of carbon is displayed in Figure 3.3 below.

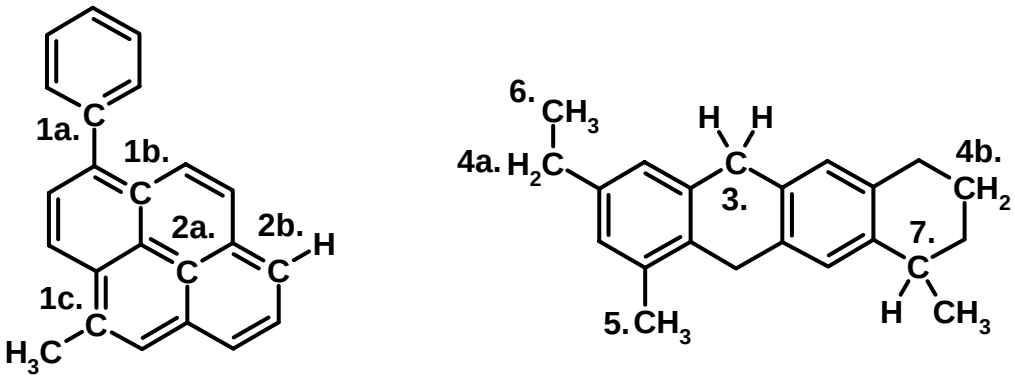

Figure 3.3. Illustration of types of carbon. Description and chemical shift ranges in ^{13}C NMR is given above (Table 3.6). $C_{ar1,2}$: 1, $C_{ar1,3}$: 2, $C_{\alpha 2}$: 3, CH_2: 4, α-CH_3: 5, t-CH_3: 6 and CH_{al}: 7. Aliphatic carbon with one hydrogen attached (CH_{al}) could only be distinguished in the DEPT sequence.
Aromatic carbon with aromatic substituent: 1a, Catacondensed aromatic carbon: 1b, Aromatic carbon joined to aliphatic chain: 1c, Pericondensed aromatic carbon: 2a, Protonated aromatic carbon: 2b, Methylene carbon in alkyl side chain: 4a and Methylene carbon in hydroaromatic ring: 4b. Only protonated carbons are revealed in the DEPT sequence (Figure 3.4).

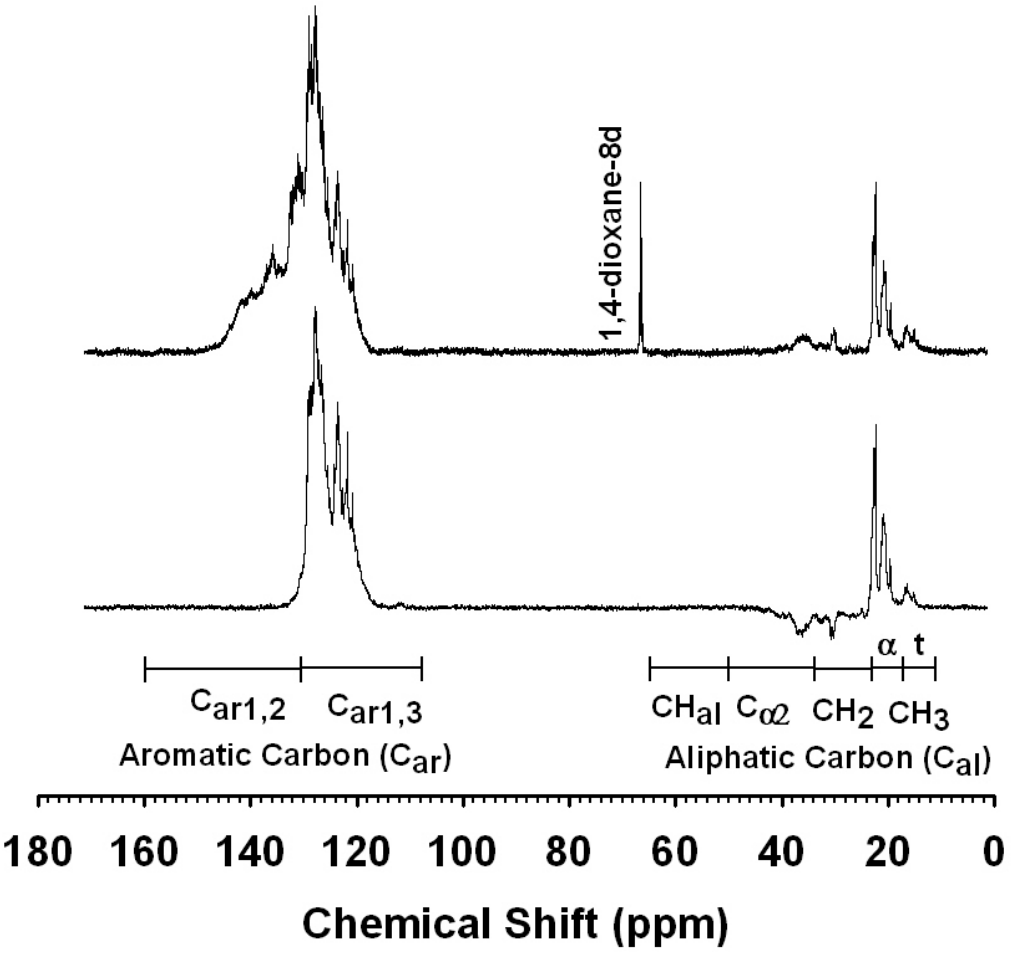

Figure 3.4. Assignment of chemical shifts in the ^{13}C NMR spectrum (top) of a petroleum pitch (PP1) dissolved in CS_2 (~15 wt% pitch). DEPT spectrum also shown (bottom). The CH_3 region is divided into two sub-regions, one for α-CH_3 (23-17 ppm) and one for t-CH_3 (17-11 ppm). Shift assignment explained in detail in Table 3.6.

3.3 Evaluation of Hydrogen Transfer Properties

3.3.1 Hydrogen Donor Ability

Anthracene (ANT) was used as a hydrogen acceptor compound to evaluate the hydrogen donor ability (HDa) [54, 59, 60, 62]. A mixture of 0.2 g anthracene and 0.2 g pitch was added to a pyrex glass tube. The tube with inner diameter 12 mm was filled with argon gas and sealed to avoid reaction with air. After sealing, the tubes had a length of approximately 6.5 cm. For experiments performed in The Chemical & Materials Department at The University of Auckland (the author had a one year research stay here in 2002/2003) heat treatment was carried out by immersing the glass tubes in a salt bath consisting of a mixture of potassium nitrate and sodium nitrite at 400 °C. This temperature was used for all the experiments. The standard heat treatment time was 8 hours. However, for two of the pitches, CTP1 and CTP2, the kinetics of the hydrogen transfer from pitch to anthracene was investigated for soaking times in the range from 10 minutes to 13 hours. After heat treatment, the sealed tubes were quenched, first with pressurized air, then in water to stop the reactions.

For reasons discussed in Chapter 4.2, the hydrogen donor ability was also measured after a less severe heat treatment. The sealed glass tubes were in this case heated in a muffle furnace at a rate of 5 °C/min to 400 °C with no soaking time. They were left to cool at room temperature. These experiments were performed in The Institute of Materials Technology at NTNU. In these experiments, the new pitch labeled CTPN was added to the range of pitches studied.

After heat treatment and cooling the samples were stored in the refrigerator at 5 °C until the subsequent GC-analysis was carried out. The reaction tubes were opened and the residue dissolved in approximately 25 mL CS_2. Fluorene, which was used as an internal standard, was added at this stage [60]. The opened tubes were left in an ultrasonic bath for 15 minutes to dissolve the coke residue. Undissolved material present in the CS_2 extract was removed using a 0.2 μm membrane syringe filter. For the experiments performed at The University of Auckland, separations were achieved with an HP-5MS column with a length of 30 meters and inner diameter of 0.32 mm. The film thickness was 0.25 μm. GC-analysis was performed on a Shimadzu GC-MS QP5000. The accompanying software was used for quantification and qualitative analysis. The temperature was programmed from 100 to 190 ºC with a heating rate of 4 ºC/min while the injector temperature was 300 ºC and the detector temperature was 290 ºC. Helium was used as carrier gas (flow-rate, 2 mL/min). The split ratio was 1:50 with an injection volume of approximately 1 μL. For the experiments carried out at NTNU analyses were achieved on an Agilent 6890N gas chromatograph equipped with a flame ionization detector (FID). Separations were performed using a HP-5 column with a length of 30 meters and 0.25 mm inner diameter. The film thickness was 0.25 μm. The temperature program was the same as described above but both injector and detector temperatures were set to 300 °C. Split ratio and injection volume were the same as above but the helium carrier gas flow was 3 mL/min.

The GC-MS analysis showed that the reaction between anthracene and pitch gave two major hydrogenated products, 9,10-dihydroanthracene (DHA) and 1,2,3,4-tetrahydroanthracene (THA) as shown in Figure 3.5. The presence of methyl-

substituted anthracenes is observed in the chromatogram. Anthracene heated alone to 400 °C for 8 hours showed no sign of disproportionation. The hydrogen donor ability (HDa) was calculated from the amount of DHA and THA formed from anthracene and expressed as milligrams of hydrogen per gram of pitch as shown in Equation 3-1. Two moles of hydrogen have been transferred from the pitch to anthracene for every mole of DHA formed and likewise four moles for every mole of THA formed. The total HDa is the sum of the HDa attributed to the formation of DHA (HDa(DHA)) and the HDa attributed to the formation of THA (HDa(THA)). The reaction between pitch and anthracene is illustrated in Figure 3.6.

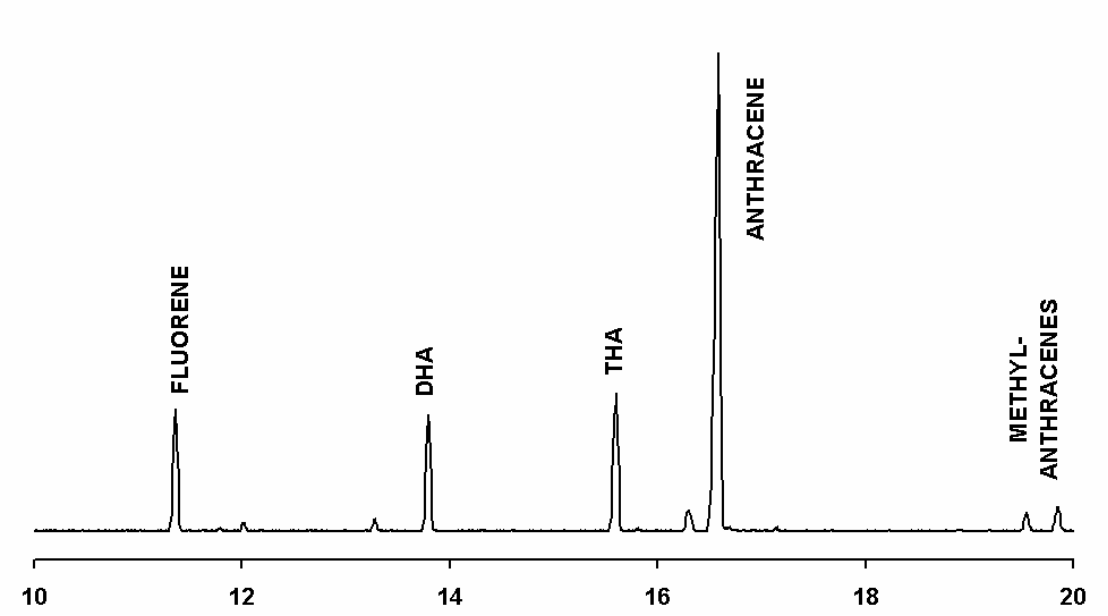

Figure 3.5. Chromatogram of the CS_2 extract of the product from the reaction between petroleum pitch (PP4) and anthracene at 400 °C, 8 hours soaking time. Fluorene has been added as internal standard.

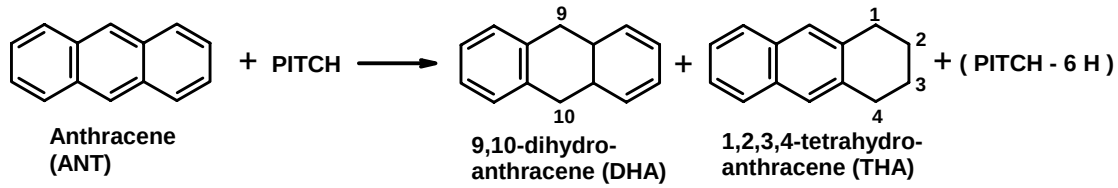

Figure 3.6. Schematic representation of the reaction between pitch and anthracene.

$$HDa(total) = HDa(DHA) + HDa(THA) = \frac{2 \cdot 1000 \cdot m_{DHA}}{m_{pitch} \cdot M_{DHA}} + \frac{4 \cdot 1000 \cdot m_{THA}}{m_{pitch} \cdot M_{THA}} \quad \textbf{(3-1)}$$

M_{DHA} and M_{THA} are the molecular weights of DHA (180.2 g/mol) and THA (182.3 g/mol), repectively, while m_{pitch} is the mass of pitch sample added to the reaction tube. The mass of DHA (m_{DHA}) was calculated from the amount of internal fluorene standard added multiplied by the ratio between the DHA peak area and the fluorene peak area taking the relative response factor into account.

$$m_{DHA} = m_{fluorene} \cdot \frac{A_{DHA}}{A_{fluorene}} \cdot RRF_{DHA} \quad \textbf{(3-2)}$$

where $m_{fluorene}$ is the amount of fluorene internal standard added and RRF_{DHA} is the relative response factor of DHA to fluorene. A_{DHA} and $A_{fluorene}$ are the peak areas of DHA and fluorene, respectively.

The mass of THA (m_{THA}) and anthracene were calculated in the same way. For the analyses performed on the GC-MS unit at The University of Auckland, the relative response factors of DHA and anthracene to fluorene were found to deviate from unity. Carbon disulphide extracts containing known amounts of fluorene, DHA and anthracene were analyzed and the relative response factor was calculated from Equation 3-3 [68]. The concentration of the compounds was similar to that found after heat treatment of the pitch/anthracene mix.

$$RRF_{DHA} = \frac{m_{DHA}}{m_{fluorene}} \cdot \frac{A_{fluorene}}{A_{DHA}} \quad \textbf{(3-3)}$$

The relative response factor for DHA was found to be 0.979 while the relative response factor for anthracene was 0.768. THA was not available from any of the suppliers contacted and this response factor has therefore not been determined. The relative response factor for THA has been set equal to one.

For the GC equipped with a Flame Ionization Detector (FID), which was used in the analysis performed at NTNU, the relative response factor of DHA to fluorene was not found to differ significantly from one. The relative response factor of anthracene to fluorene was found to be 0.930.

The recovery rate for anthracene was calculated from the fraction of anthracene found after reaction compared to the amount of anthracene initially added to the reaction tube taking into account that some of the anthracene had been transformed to DHA and THA.

3.3.2 Hydrogen Acceptor Ability

Tetralin (1,2,3,4-tetrahydronaphthalene) was selected as a hydrogen donor compound due to its high thermal stability [61, 62]. The experimental conditions and equipment were the same as described above under the hydrogen donor ability except for the temperature of the GC column which was programmed from 60 °C to 110 °C. The only major product from the reaction between pitch and tetralin was naphthalene as determined by GC-MS analysis. In addition, two minor peaks identified as arising from the presence of butylbenzene and 1-methylindan were also observed in the chromatogram (Figure 3.7).

Fluorene has a longer retention time than tetralin and naphthalene. This would influence the relative response factor. Also, the relative response factor is dependent on the number of carbon atoms in a compound [69], which is 13 for fluorene and 10 for both naphthalene and tetralin. Fluorene was therefore not considered to be a

suitable internal standard. Quantification was performed from relative peak areas instead of using an internal standard.

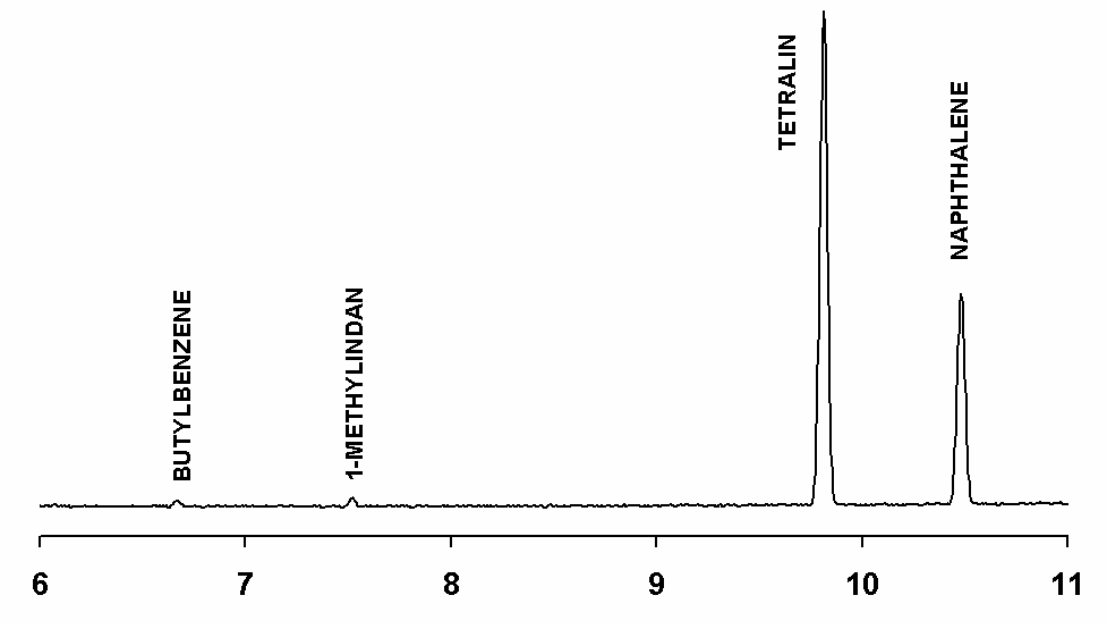

Figure 3.7. Chromatogram of the CS_2 extract of the product from the reaction between petroleum pitch (PP4) and tetralin at 400 °C, 8 hours soaking time.

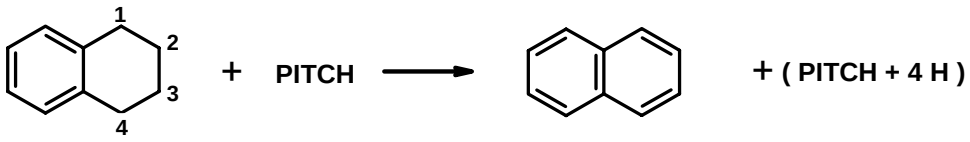

1,2,3,4-tetrahydro-naphthalene (tetralin) **Naphthalene**

Figure 3.8. Schematic representation of the reaction between pitch and tetralin.

The acceptor ability (HAa) was calculated from the molar ratio of naphthalene to tetralin ($x_{naphthalene}$) as found from the respective peak areas and is expressed as milligrams of hydrogen per gram of pitch (Equation 3-4).

$$HAa = \frac{4 \cdot 1000 \cdot m_{tetralin}}{m_{pitch} \cdot M_{tetralin}} \cdot x_{naphthalene} \qquad \textbf{(3-4)}$$

where $M_{tetralin}$ is the molecular weight of tetralin (132.2 g/mol) while m_{pitch} and $m_{tetralin}$ are the amounts of pitch and tetralin added to the reaction tube, respectively. The molar ratio of naphthalene to tetralin after reaction, $x_{naphthalene,}$ was caculated from the respective peak areas of tetralin ($A_{tetralin}$) and naphthalene ($A_{naphthalene}$) (Equation 3-5).

$$x_{naphthalene} = \frac{M_{tetralin}}{M_{naphthalene}} \cdot \frac{A_{naphthalene}}{A_{tetralin}} \cdot RRF_{naphthalene} \qquad \textbf{(3-5)}$$

Carbon disulphide extracts containing known amounts of naphthalene and tetralin where the concentration of the compounds was similar to that found after heat treatment of the pitch/tetralin mix were analyzed and the relative response factor was calculated from Equation 3-6.

$$RRF_{naphthalene} = \frac{m_{naphthalene}}{m_{tetralin}} \cdot \frac{A_{tetralin}}{A_{naphthalene}} \quad \textbf{(3-6)}$$

The relative response factor of naphthalene to tetralin ($RRF_{naphthalene}$) was found to be 0.795.

The relative response factor of naphthalene to tetralin was not found to differ significantly from one for the GC equipped with FID used in the analyses performed at NTNU.

3.4 Thermogravimetric Analysis

The thermogravimetric analysis was performed on a Mettler/Toledo TGA/SDTA851[e] with a sample size of approximately 5 mg. The samples were heated to 1000 °C at a rate of 10 °C/min [34] under a nitrogen gas flow of 50 mL/min. Derivation of the weight loss curves (DTG) was performed using the accompanying STAR[e] software.

3.5 Carbonization

Each of the 11 pitches was heat treated separately in a pressurized carbonization chamber. The pressure was maintained at 15 bar with a small amount of argon flowing through the system. The sample size was 70 g for all of the pitches except CTP1N. Due to a limited amount of this pitch, only 20 g was carbonized. Aluminium crucibles with a diameter of 6.5 cm and height of 9 cm were used inside the stainless steel reactor chamber to facilitate easy removal of the pitch coke. The reaction chamber was heated at a rate of 5 °C/ min up to 300 °C, then at a rate of 2 °C/min up to 400 °C and finally at a rate of 0.5 °C/min up to the maximum temperature of 550 °C. The temperature was held at 550 °C for one hour before the furnace was left to cool. Removal of the sample was done when the furnace had reached 150 °C. The laboratory coker is described in detail by Eidet [70].

About 15 g of each of the 11 pitch cokes obtained after carbonization under pressure was heat treated in a second step to 1150 °C in a furnace purged with argon gas. The heating rate was 5 °C/min and the samples were kept at the maximum temperature for 4 hours before the furnace was left to cool at its natural rate.

3.6 Optical Texture Analysis

The semi-cokes resulting from carbonization of the pitches to 550 °C under pressure (Section 3.5) were investigated by optical microscopy. The pitch coke was ground using pestle and mortar and screened to a narrow fraction of 0.5 – 0.6 mm grain size. A few grams of this fraction was embedded in epoxy in 30 mm diameter cylindrical molds. The grinding and polishing were performed on a RotoForce-4 unit attached to a RotoPol-31 unit supplied by Struers. Three samples at the same time were mounted in a holder and ground and polished using silicon carbide paper. A force of 10 N per sample was applied and the rotation speed was 300 RPM. The grinding paper was continuously wetted by water and the grinding time was 30 seconds. Fine grinding was performed using a fine grinding disc supplied by Struers. The disc was coated with a 9 µm diamond spray and continuously wetted by ethanol during the two minutes grinding time. The samples were then polished in three consecutive steps using 6 µm, 3 µm and 1 µm diamond spray on a polishing cloth wetted continuously by ethanol. For these steps, the grinding time was 5 minutes, rotation speed 300 RPM and the force applied per sample was 20 N. The final polishing step was performed using a cloth soaked with a colloidal silica suspension. The force per sample was lowered to 10 N and opposite rotation direction for sample and polishing disc was used. During the last 30 seconds of a total polishing time of one minute, the disc was wetted by water.

Optical texture analysis was performed on a Leica MeF3A metallurgical inverted reflecting light microscope with polarizing modules. The microscope is equipped with a Sony DXC 930P digital video camera and connected to a computer. The software used is an image analysis program, a modified version of NIH Image version 1.62. A total of 144 grains is selected automatically from a low magnification overview image. One image per grain is then acquired at 250x magnification. From this color image, a high contrast greyscale image is obtained which is used to extract the texture gradient lines. Each image is divided into 24 (6x4) sub-frames. The program automatically extracts gradient lines between the optical domains in the coke grains and calculates a mosaic index and a fiber index for each of the sub-frames. The mosaic index is a measure of the length of the boundaries and hence the average optical domain size. It is a relative number smaller than 1 where a fine texture will give a high value. The fiber index is a measure of the optical domain anisotropy and is also a relative number smaller than 1. An anisotropic structure will give a high value. A detailed description of the procedure and equipment is given by Rørvik, Aanvik, Sørlie and Øye [71].

3.7 X-ray Diffraction

Each of the 11 pitch cokes heat treated to 1150 °C (Section 3.5)was ground to a fine powder and sieved to a fraction size less than 106 µm. Ultra-pure (purity > 99.9999 %) silicon was ground and screened to a fraction –63+32 µm and mixed with the coke powder (10 wt% Si) using pestle and mortar. The powder mix was then transferred to a sample holder with a diameter of 25 mm. The sample thickness was 1.5 mm.

Powder X-ray diffraction profiles were collected for each of the 11 samples on a Siemens D5005 X-ray diffractometer. Nickel-filtered CuKα X-ray was used. The accelerating voltage was 40 kV with a current of 50 mA. Step-scanning was performed from 15° to 35° (2θ) with a step width of 0.02° and acquisition time of 6 s per step. The width of the divergence slit was 2° and the radius of the goniometer was 20.05 cm.

Due to the low absorption coefficient of carbon materials for X-rays, a shift to the lower angle side and also a broadening of the diffraction profile is observed. The use of an internal standard like high purity silicon is therefore essential when analyzing carbon materials by powder X-ray diffraction [72]. Also the broad peaks observed for disordered carbons like cokes need to be intensity corrected. This is especially true when calculating the interlayer spacing, d_{002}, from a (002) peak exceeding several degrees [73]. Instrument and sample dependent factors like Lorentz (L), polarization (P), absorption (A) and carbon atom scattering (f_c) are functions of 2θ and will cause a shift of the observed diffraction profile to the lower angle side [72]. These factors were taken into account when processing the X-ray diffraction data.

The diffraction profile was corrected by dividing each reflection, one at each step of 0.02°, by the intensity correction factor $L{\cdot}P{\cdot}A{\cdot}f_c^2$.

$$L = \frac{1}{\sin^2\theta \cdot \cos\theta} \qquad \textbf{(3-7)}$$

$$P = \frac{1}{2}\left(1 + \cos^2 2\theta\right) \qquad \textbf{(3-8)}$$

$$A = \left(1 - \frac{\sin(2\theta)}{\mu' \cdot b_r}\right) \cdot \left(1 - \exp\left(\frac{-2 \cdot \mu' \cdot t}{\sin\theta}\right)\right) + \frac{2 \cdot t \cdot \cos\theta}{b_r} \cdot \exp\left(\frac{-2 \cdot \mu' \cdot t}{\sin\theta}\right) \qquad \textbf{(3-9)}$$

Here, µ' is the apparent absorption coefficient of the sample. µ' is equal to 10 cm^{-1} when 10 wt% silicon has been added to the sample [72]. The specimen thickness, t, is 0.15 cm and b_r is the breadth of the X-ray beam at the sample position and is expressed as:

$$b_r = R \cdot \sin\beta \qquad \textbf{(3-10)}$$

where R and β are the radius of the goniometer (20.05 cm) and the width of the divergence slit (2°), respectively.

$$f_c = 2.26069 \cdot \exp\left(-22.6907 \cdot s^2\right) + 1.56165 \cdot \exp\left(-0.656665 \cdot s^2\right) + 1.05075 \cdot \exp\left(-9.75618 \cdot s^2\right) + 0.839259 \cdot \exp\left(-55.5949 \cdot s^2\right) + 0.286977 \quad \textbf{(3-11)}$$

where $s = \frac{\sin\theta}{\lambda}$ [72]. The wavelength of the X-ray, λ, is 1.54056 Å for Kα1.

The effect of the intensity correction on the observed diffractogram for a petroleum pitch coke (PP1) is demonstrated in Figure 3.9, shifting the position of the (002) reflection for carbon to a higher angle from 25.74º to 25.84º.

A Pseudo-Voigt function was fitted to the intensity corrected diffraction profile for the (002) reflection of carbon and the (111) reflection of silicon using the Profile software. A linear background was subtracted. The goodness of fit was examined with an R-factor defined as:

$$R = \frac{\sum_{2\theta} \left| \left(I(2\theta) - P_r(2\theta) \right) \right|}{\sum_{2\theta} I(2\theta)} \cdot 100 \quad \textbf{(3-12)}$$

where I and P are the experimental and fitted intensities as a function of 2θ, respectively.

According to Iwashita et al. [72] the R-factor should preferably be below 10. The R-factor was always lower than 5 for all the curve fittings performed in this work.

The angle displacement was found from the difference in diffraction angle between the silicon standard ($2\theta_{Si}$ = 28.467°) [72] and the peak position of the curve fitted to the experimentally observed silicon reflection. The (002) reflection for carbon found from the fitted curve was corrected by adding the angle displacement. This corrected 2θ-position was then used to calculate the d_{002} interlayer spacing of the pitch coke from the Bragg equation:

$$2 \cdot d_{002} \cdot \sin\theta = \lambda \quad \textbf{(3-13)}$$

where λ is the wavelength of the X-ray (1.54056 Å for Kα1).

The average crystallite size, L_c, was calculated using the Scherrer equation with a shape factor K equal to 0.89 [74].

$$L_c = \frac{K \cdot \lambda}{\beta \cdot \cos\theta} \quad \textbf{(3-14)}$$

Here, β is the full width at half maximum (FWHM) corrected for broadening and is calculated in the following way:

$$\beta = \sqrt{B^2 - b^2} \quad \textbf{(3-15)}$$

where B is the FWHM of the carbon (002) reflection and b is the FWHM of the silicon (111) reflection.

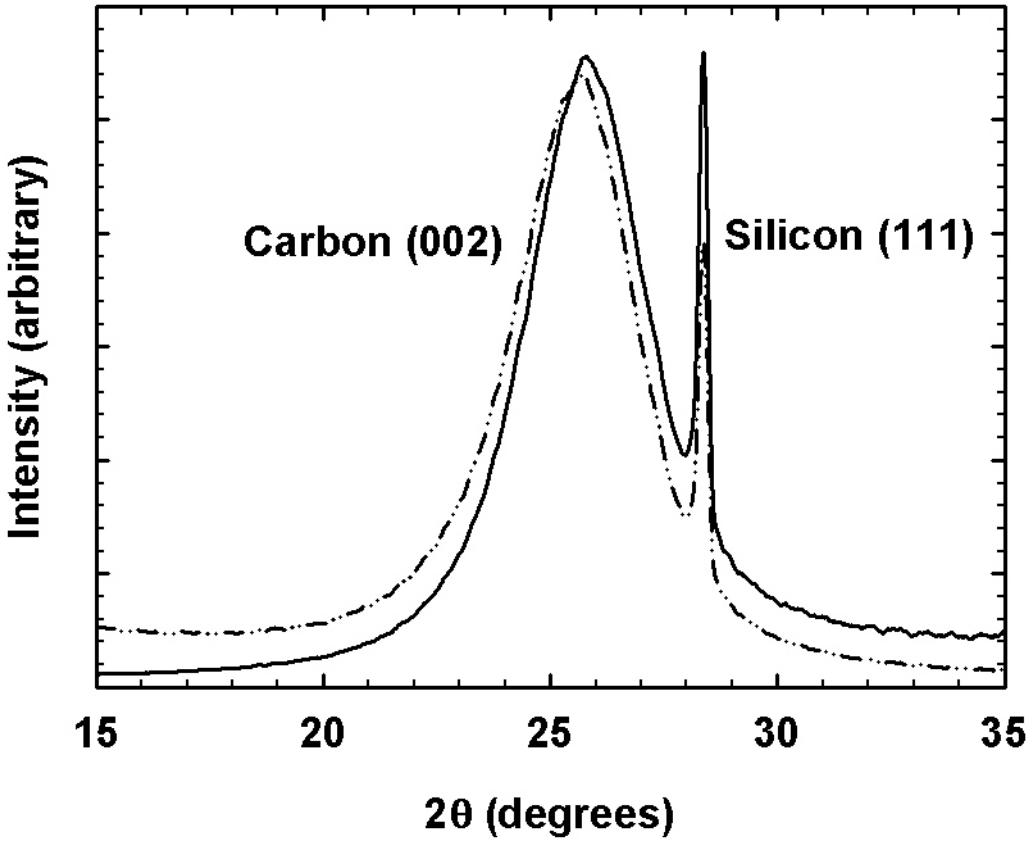

Figure 3.9. Diffraction profile corrected for Lorentz, polarization, absorption and carbon atom scattering factors (solid line) and observed diffraction profile (dashed line) for a petroleum pitch coke (PP1) heat treated to 1150 °C.

3.8 Scanning Electron Microscopy

Scanning electron microscopy was used to study the polished surface of coke grains. The idea was to investigate whether it was possible to distinguish the QI particles from the pitch coke matrix and thereby study their clustering and orientation. Due to the difference in hardness between the QI particles and the pitch coke matrix, a relief effect after polishing was expected to be observed. The samples were sputtered with gold. Images were acquired in secondary electron modus using a Hitachi S-3500N SEM.

3.9 Statistical Analysis

The MINITAB 14 software was used in the statistical analysis. Tukey's pairwise comparisons were used to test the significance of difference between mean values [75].

4 RESULTS

4.1 Nuclear Magnetic Resonance

As examples, the proton spectra of CTP1, CTP5, PP1 and PP4 are shown in Figure 4.1. The other spectra are given in the Appendix section. The normalized integration data under the shift regions (Table 3.5) are shown in Figure 4.2.

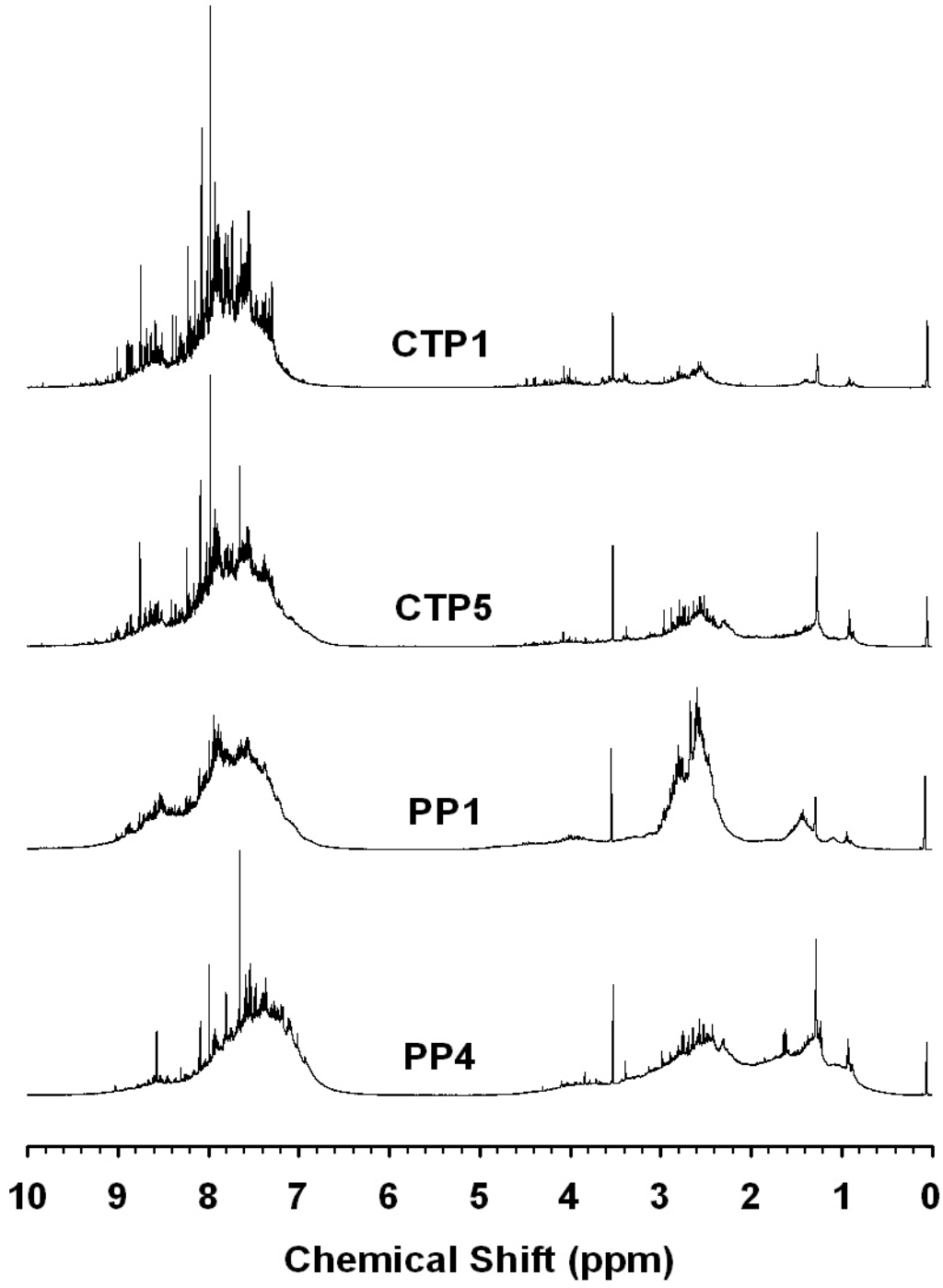

Figure 4.1. ^{1}H NMR spectra of CS_2 extracts of pitches. Aromatic hydrogen region to the left and aliphatic hydrogen region to the right. The sharp peak at 3.53 ppm is the lock substance (1,4-dioxane-8d).

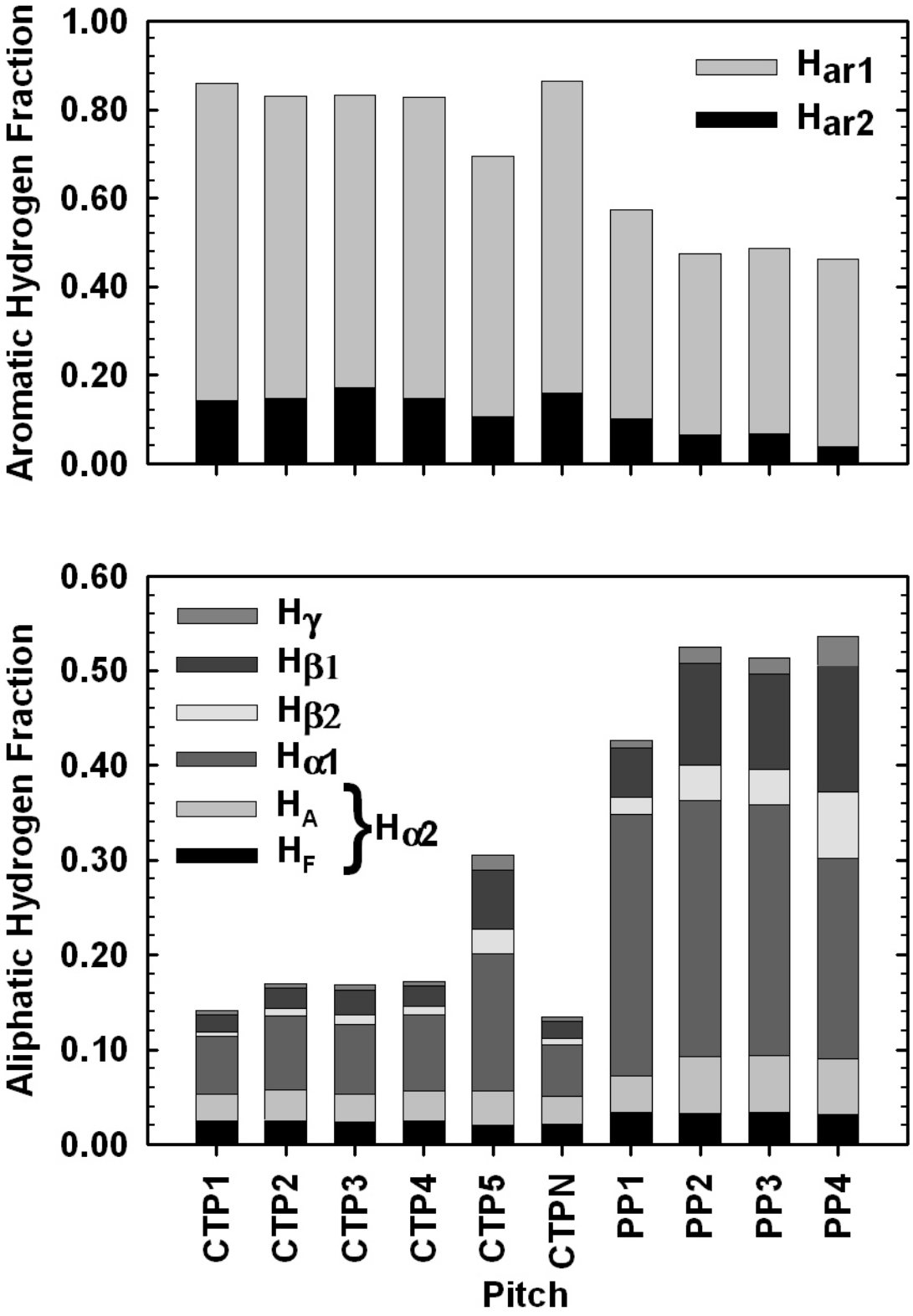

Figure 4.2. Normalized integration data of the chemical shift regions for ^{1}H NMR spectra of pitch extracts in CS_2. Aromatic hydrogen fraction (top) and aliphatic hydrogen fraction (bottom). The chemical shift classification is given in Table 3.5.

As examples, the ^{13}C NMR spectra of CTP1, CTP5, PP1 and PP4 are shown in Figure 4.3. The other spectra are given in the Appendix section. The normalized integration data under the shift regions (Table 3.6) from all the ^{13}C NMR pitch spectra are shown in Figure 4.4.

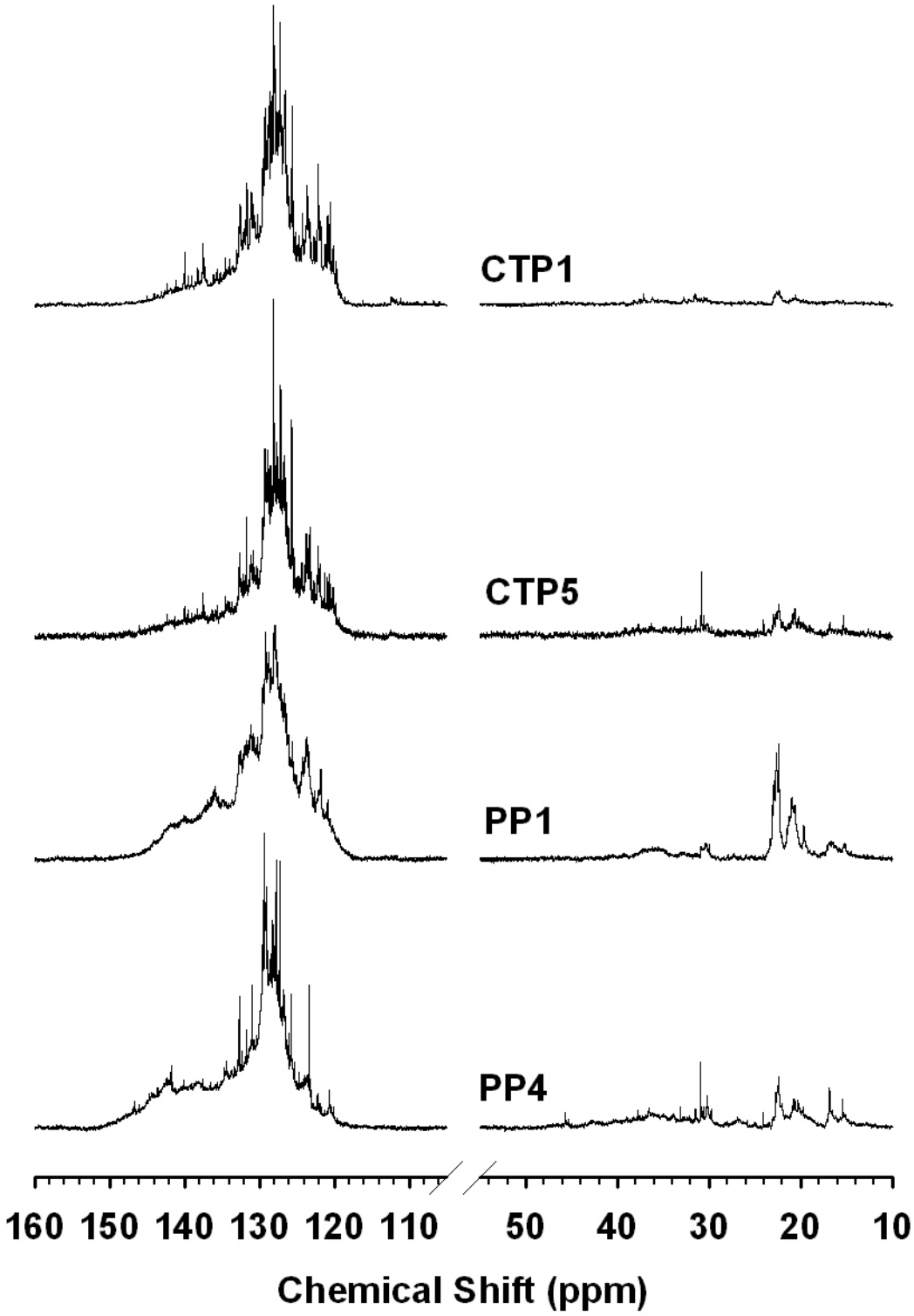

Figure 4.3. ^{13}C NMR spectra of pitch extracts in CS_2. Aromatic region to the left and aliphatic region to the right.

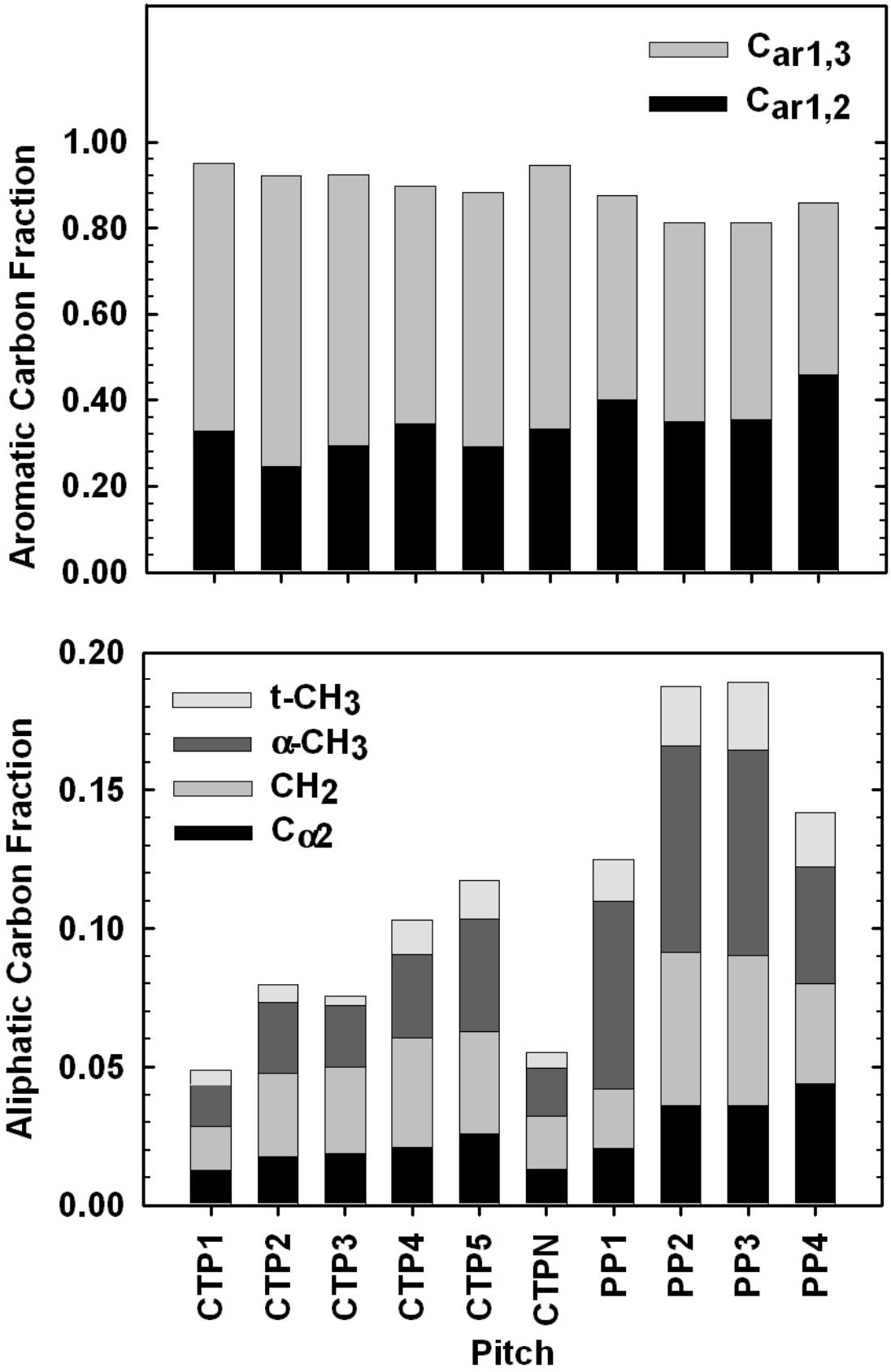

Figure 4.4. Normalized integration data of the chemical shift regions for ^{13}C NMR spectra of pitch CS_2 extracts. Aliphatic carbon fraction (bottom) and aromatic carbon fraction (top). Chemical shift classification given in Table 3.6.

An advantage of a DEPT spectrum compared to a conventional ^{13}C NMR spectrum is the improved signal to noise ratio. The intensity in the aliphatic region of coal-tar pitch ^{13}C NMR spectra is usually quite low and the DEPT spectrum can therefore be very useful for the detection of minor differences between pitches. As examples, the DEPT spectra of CTP1, CTP5, PP1 and PP4 are shown in Figure 4.5. The other spectra are shown in the Appendix section. The normalized integration data for the aliphatic region (see Table 3.6) in the DEPT spectra are shown in Figure 4.6.

The fraction of CH_3 in a terminal position of an alkyl chain seems to be over-estimated in the conventional ^{13}C NMR spectra compared to the DEPT spectra. This is especially true for the coal-tar pitches. The DEPT spectra of PP4 (Figure 4.5), PP2 and PP3 (Appendix section, Figure A.3.3) show a wide region of low intensity at higher chemical shifts than the CH_2 region. This region was not detected in the conventional carbon spectra but can be observed in the DEPT spectrum because of higher sensitivity and the ability to distinguish between CH or CH_3 and CH_2 due to the 180º phase difference. The region in the spectral range of ~ 45 - 65 ppm is probably due to aliphatic CH groups which could be connected to heteroatoms, aliphatic carbons in branched side chains or alkyl groups attached to a naphthenic or hydroaromatic ring (Figure 3.3). According to Kidena, Murata and Nomura [53], aliphatic carbon connected to oxygen (-O-CH_3) has a chemical shift around 56 ppm. The aliphatic carbon fractions of the DEPT spectra (Figure 4.6) can not be directly compared with the aliphatic carbon fraction of the conventional ^{13}C NMR spectra (Figure 4.4). The reason for this is that the aromatic carbon fraction will be relatively smaller for the DEPT spectra as the quaternary carbons are excluded.

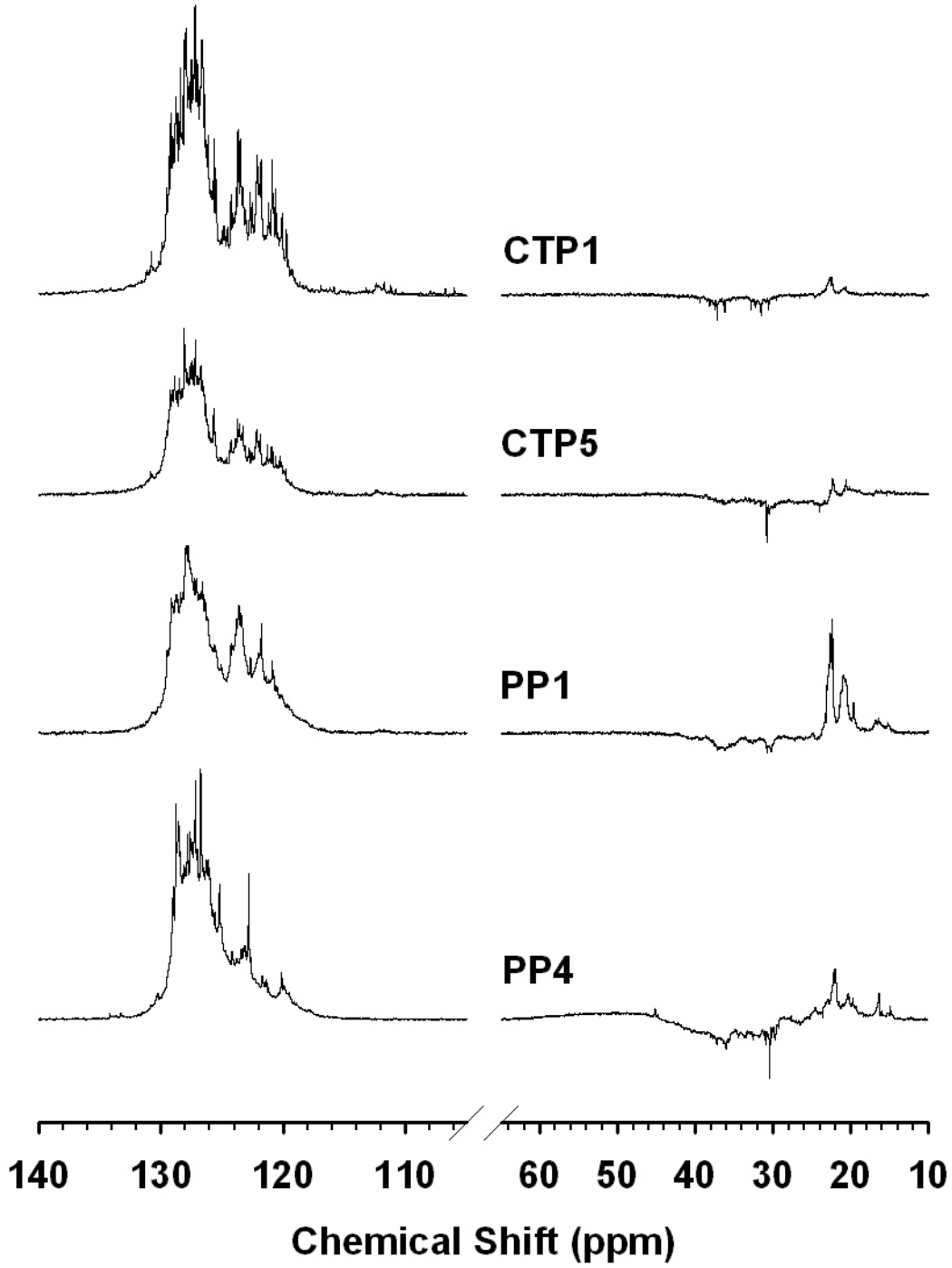

Figure 4.5. DEPT spectra of the CS_2 extracts of pitches. Aromatic non-quaternary carbons to the left and aliphatic carbons to the right. CH and CH_3 are in phase while CH_2 is 180º out of phase.

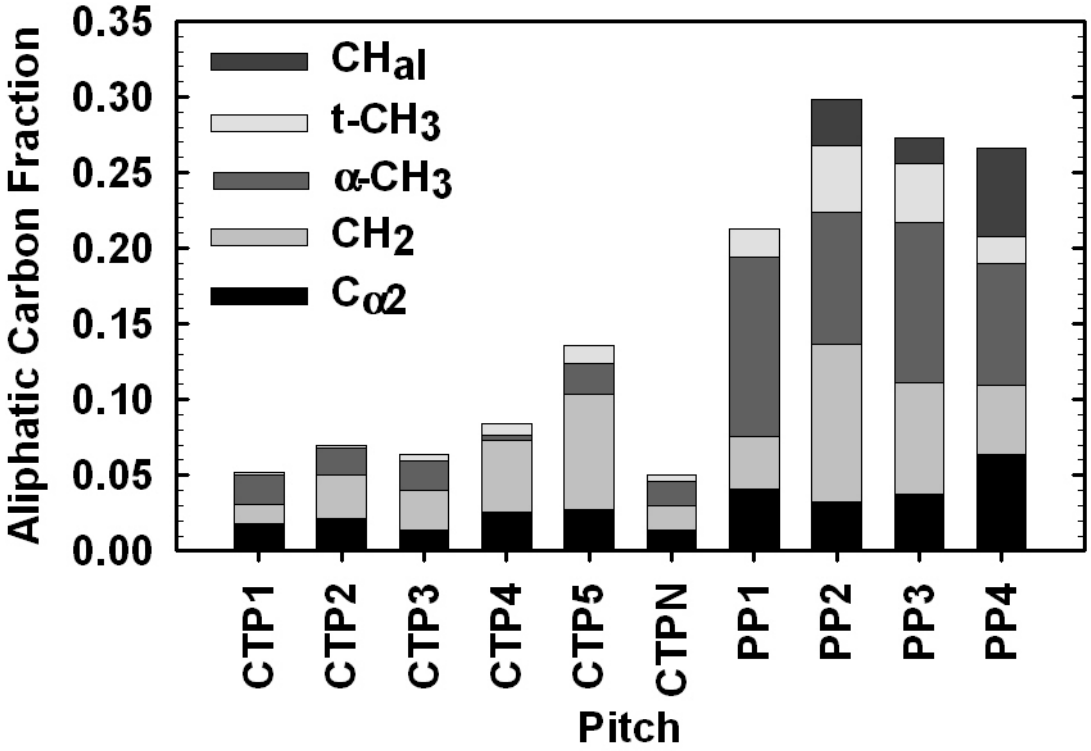

Figure 4.6. Distribution of the aliphatic carbon fraction in CS_2 extracts of pitches as determined from the DEPT spectrum. The integration data are normalized over the whole spectral region. CH_{al} is aliphatic carbon connected to one H and further to an alkyl carbon.

4.2 Hydrogen Donor and Acceptor Abilities

4.2.1 Hydrogen Donor Ability

Hydrogen donor abilities (HDa) for two of the coal-tar pitches, CTP1 and CTP2, were measured at 400 °C for soaking times ranging from 10 minutes to 13 hours. The results are shown in Figure 4.7.

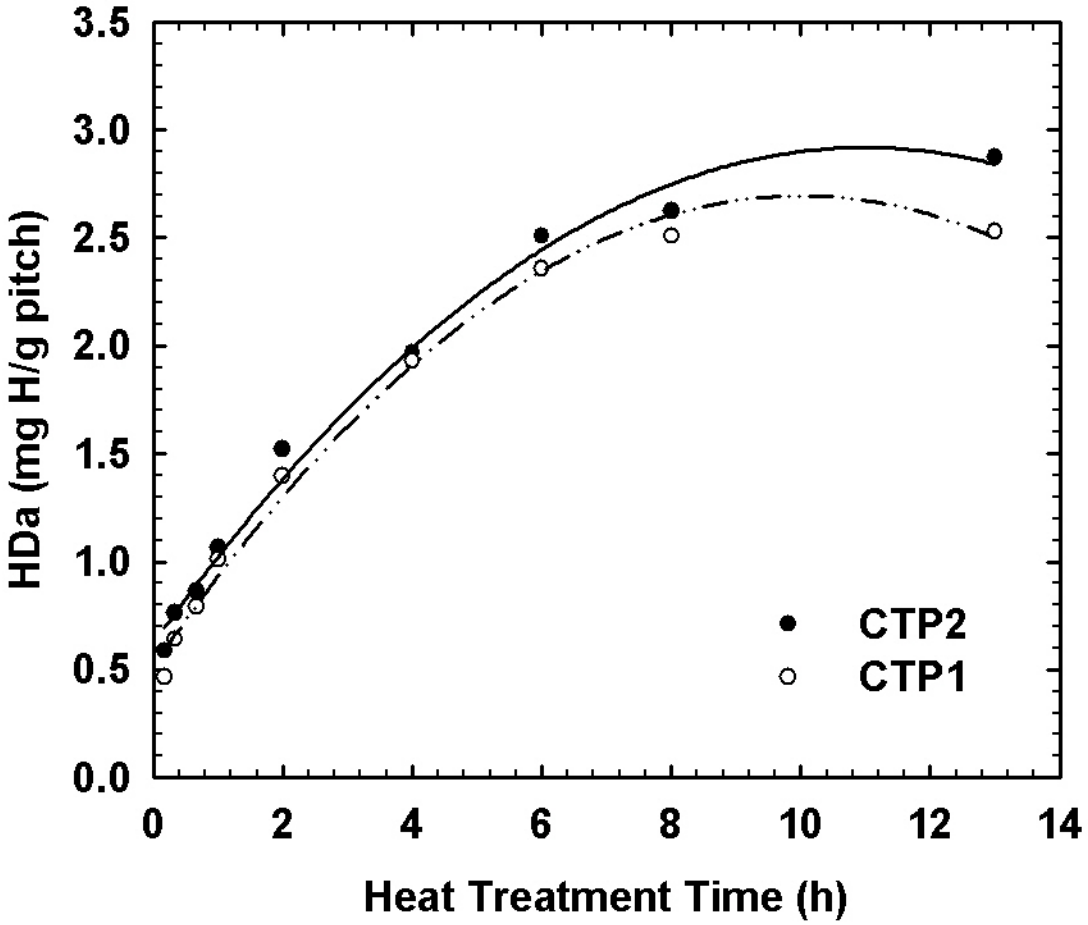

Figure 4.7. Hydrogen donor ability (HDa) for coal-tar pitches CTP1 and CTP2 at 400 °C for different soaking times.

Both pitches show a similar trend but CTP2 exhibits a slightly higher HDa for all of the investigated heat treatment times. The transfer of hydrogen from the pitch to the acceptor compound (anthracene) occurs continuously. More than half of the hydrogen is transferred within the first two hours of heat treatment. The rate of hydrogen transfer seems to decrease with increasing heat treatment time for both of the pitches. A decrease in reaction rate can be expected because the supply of donor hydrogen will be consumed by the reaction system and free radicals formed during thermal rupture of bonds are ”stabilized” by re-polymerization. However, between 10 minutes and one hour there is a linear relationship between the amount of hydrogen transferred from CTP1 to anthracene and the heat treatment time. This relationship is also seen for

CTP2 and is shown in Figure 4.8. The reaction rate must be higher initially as the linear trend line can not be extrapolated to origin.

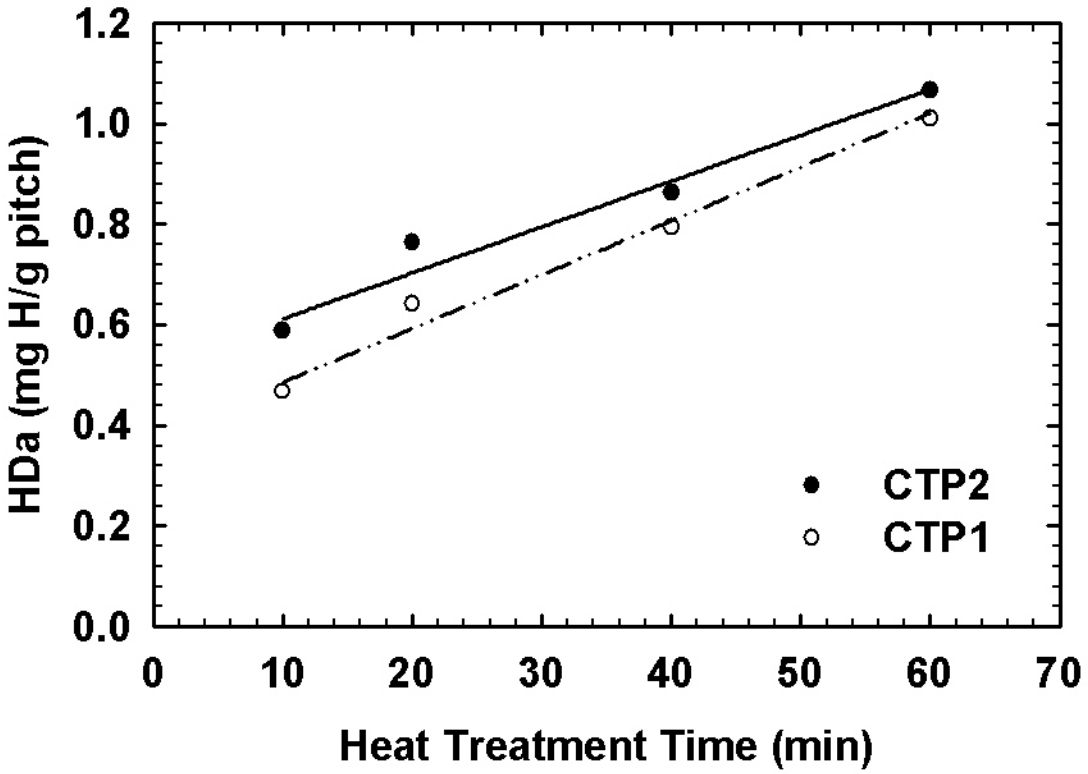

Figure 4.8. Hydrogen donor ability (HDa) for coal-tar pitches CTP1 and CTP2 at 400 °C for different soaking times within the first hour.

The HDa attributed to the formation of DHA, the HDa attributed to the formation of THA and the total HDa, which is the sum of the two, are shown in Figure 4.9 and Figure 4.10 for CTP1 and CTP2, respectively. For both pitches, the proportion of THA in the reaction product increases more rapidly than that of DHA. After a heat treatment time of about 3.5 hours, THA is the compound which contributes the most to the total hydrogen donor ability. The amount of DHA actually decreases for the prolonged heat treatment time of 13 hours.

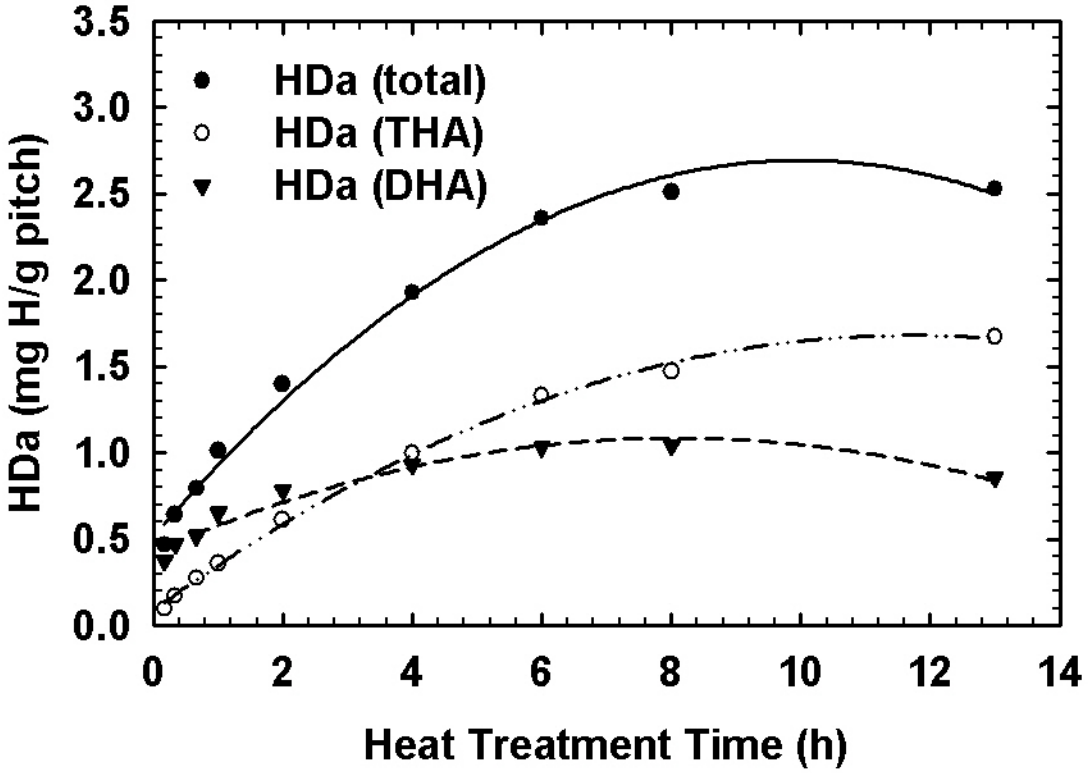

Figure 4.9. Partial and total hydrogen donor abilities (HDa) for coal-tar pitch CTP1 at 400 °C for different soaking times.

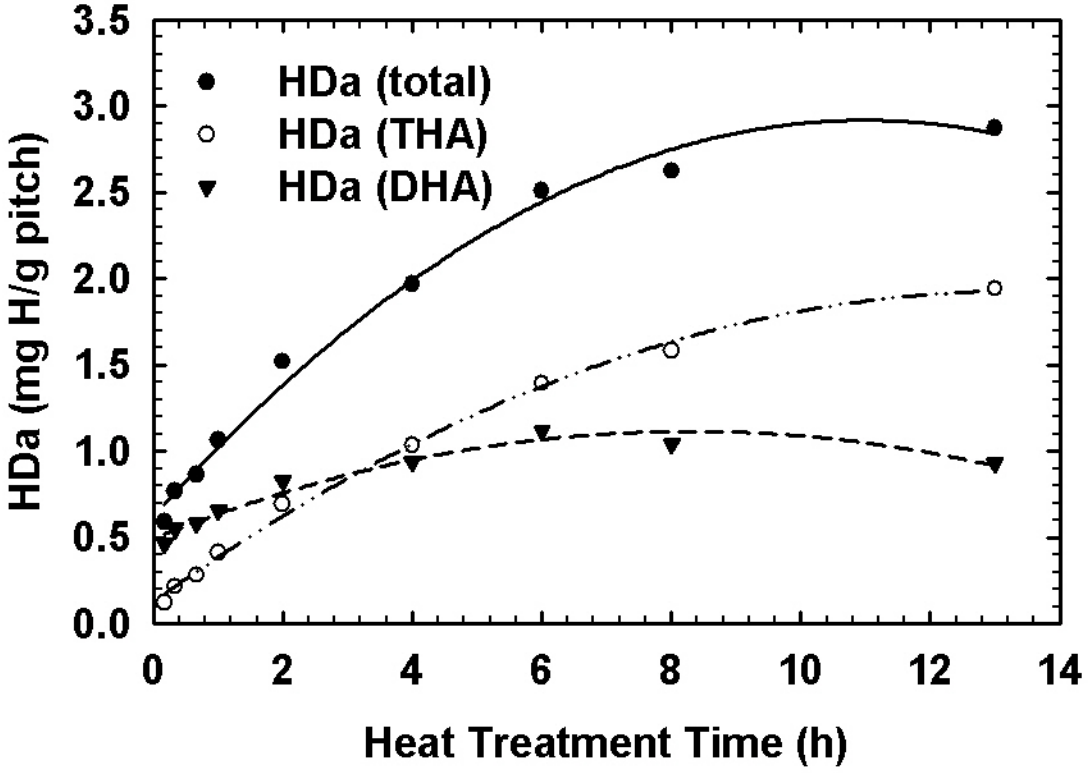

Figure 4.10. Partial and total hydrogen donor abilities (HDa) for coal-tar pitch CTP2 at 400 °C for different soaking times.

The results from the donor ability test performed at 8 hours heat treatment time and a temperature of 400 °C are represented graphically for all tested pitches in Figure 4.11. Two parallels were measured for each of the pitches.

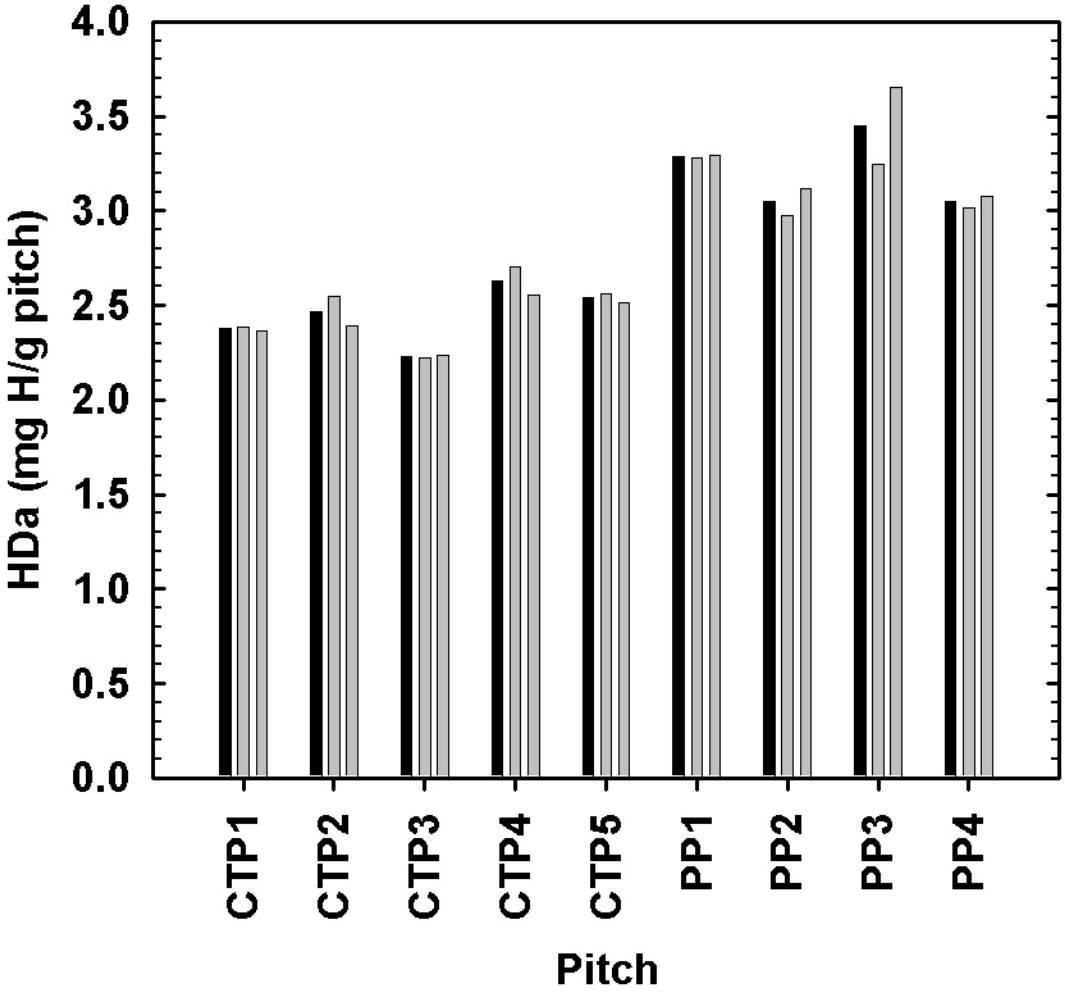

Figure 4.11. Hydrogen donor ability (HDa) measured after heat treatment at 400 °C and 8 hours soaking time. Black bars are averages of the parallels (grey bars).

All of the four petroleum pitches exhibit higher hydrogen donor abilities than the coal-tar pitches. Tukey's pairwise comparisons were used to test if there were significant differences in HDa values among pitches. There was found a significant difference between the two groups of pitches but not among the individual pitches within one group.

The partial and total hydrogen donor abilities are given in Table 4.1. In addition, the recovery of unreacted anthracene and 9,10-dihydroanthracene and 1,2,3,4-tetrahydroanthracene which are formed during the reaction is shown. There is not a large variation in the HDa attributed to the formation of DHA among the pitches, not even between the two groups. The amount of DHA formed seems to have reached a maximum. This agrees well with the observations done on the kinetics for CTP1 and CTP2 which are shown in Figure 4.9 and Figure 4.10, respectively. It is the amount of THA formed that really differentiates the pitches. The petroleum pitches exhibit higher hydrogen donor abilities but also lower recovery rates than the coal-tar pitches.

The low recovery rates indicate that anthracene itself or more likely DHA or THA undergo further reactions to form other products. This would probably lead to an underestimation of the hydrogen donor ability and might be part of the explanation for the decreasing kinetic trend seen in Figure 4.7, Figure 4.9 and Figure 4.10. A more thorough discussion is given in Chapter 5.

Table 4.1. Partial and total hydrogen donor abilities (HDa) measured after heat treatment at 400 °C and 8 hours soaking time.

Pitch	HDa (DHA) (mg H/g pitch)	HDa (THA) (mg H/g pitch)	HDa (total) (mg H/g pitch)	Recovery of anthracene (%)†
CTP1	0.937	1.440	2.377	63.9
CTP2	0.956	1.513	2.469	64.0
CTP3	0.931	1.299	2.230	64.7
CTP4	0.972	1.658	2.629	61.0
CTP5	0.938	1.602	2.539	59.3
PP1	0.962	2.324	3.286	52.4
PP2	0.915	2.134	3.049	48.1
PP3	0.989	2.455	3.443	47.5
PP4	0.884	2.165	3.049	46.4

† Recovery of unreacted anthracene and 9,10-dihydroanthracene (DHA) and 1,2,3,4-tetrahydroanthracene (THA) which are formed in the pitch/anthracene system.

Due to the relatively low recovery rates after heat treatment at 400 °C and 8 hours soaking time, it was decided to also perform the hydrogen donor ability test under a less severe heat treatment. The pitch/anthracene mix was heated at a rate of 5 °C/min to 400 °C with no soaking time. The results are shown in Figure 4.12.

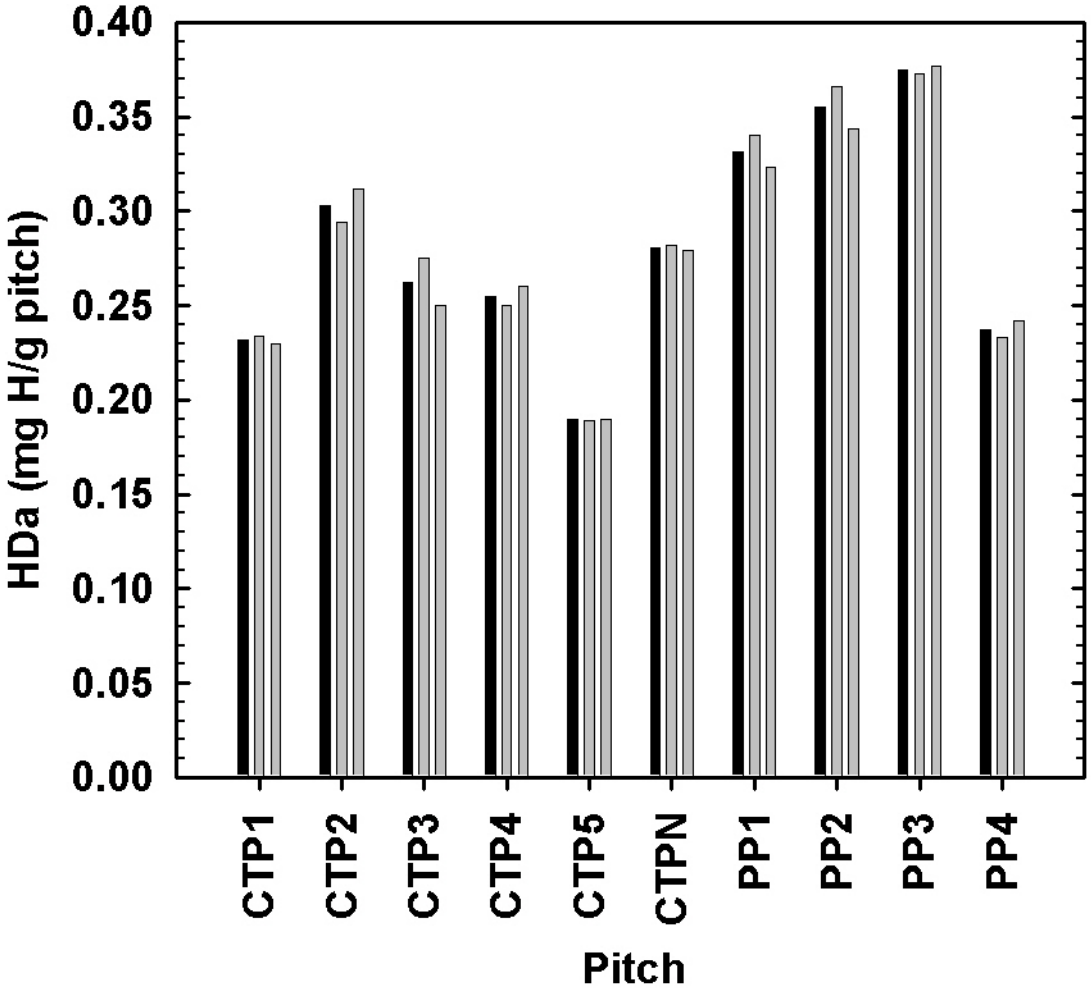

Figure 4.12. Hydrogen donor ability (HDa) at 400 °C with heating rate of 5 °C/min and no soaking time. The black bars are averages of the parallels (grey bars).

Tukey's pairwise comparisons were used to test if there were significant differences in HDa values for the pitches (Table 4.2).

Table 4.2. Tukey's Pairwise Comparisons for the hydrogen donor ability (HDa) of pitches (400 °C, no soaking time). Family Error rate of 5 %. Significant difference marked "+", non-significant difference marked "-".

	CTP1	CTP2	CTP3	CTP4	CTP5	CTPN	PP1	PP2	PP3
CTP2	+								
CTP3	-	+							
CTP4	-	+	-						
CTP5	+	+	+	+					
CTPN	+	-	-	-	+				
PP1	+	-	+	+	+	+			
PP2	+	+	+	+	+	+	-		
PP3	+	+	+	+	+	+	+	-	
PP4	-	+	-	-	+	+	+	+	+

The hydrogen donor ability test performed at a less severe heat treatment is more successful in differentiating the pitches. There are significant differences also among

the individual pitches within one group. Petroleum pitch 4 is distinguished due to its low HDa compared to the other petroleum pitches. Petroleum pitch 3 exhibits the highest HDa of all the pitches but is not significantly different from PP2. The lowest HDa of all is exhibited by CTP5.

The formation of DHA is by far the most important for the hydrogen donor ability test performed at the less severe heat treatment (Table 4.3). The recovery rate is high for all of the pitches investigated indicating that ring-opening and other reactions than hydrogen transfer to anthracene to form DHA and THA do not occur to a significant extent. However, two of the pitches, CTP5 and PP4, are distinguished due to their lower recovery rates of 94.4 % and 93.6 %, respectively.

Table 4.3. Partial and total hydrogen donor abilities (HDa) at 400 °C with a heating rate of 5 °C/min and no soaking time.

Pitch	HDa (DHA) (mg H/g pitch)	HDa (THA) (mg H/g pitch)	HDa (total) (mg H/g pitch)	Recovery of anthracene (%)†
CTP1	0.221	0.011	0.232	97.4
CTP2	0.296	0.007	0.303	99.2
CTP3	0.254	0.008	0.262	99.4
CTP4	0.251	0.004	0.255	99.0
CTP5	0.187	0.003	0.190	94.4
CTPN	0.272	0.009	0.281	97.2
PP1	0.315	0.017	0.331	96.8
PP2	0.342	0.013	0.355	97.6
PP3	0.359	0.016	0.375	98.0
PP4	0.224	0.013	0.238	93.6

† Recovery of unreacted anthracene and 9,10-dihydroanthracene (DHA) and 1,2,3,4-tetrahydroanthracene (THA) which are formed in the pitch/anthracene system.

Due to the low recovery rates and low resolution of the hydrogen donor ability test performed with 8 hours soaking time, it was believed that the donor test with no soaking time at 400 °C better reflected the true hydrogen donor power of the pitches. The results obtained at the less severe heat treatment will therefore be the focus of the following discussion given in Chapter 5.

4.2.2 Hydrogen Acceptor Ability

Hydrogen acceptor abilities (HAa) for two of the coal-tar pitches, CTP1 and CTP2, were measured at 400 °C for soaking times ranging from 10 minutes to 12 hours. The results are shown in Figure 4.13.

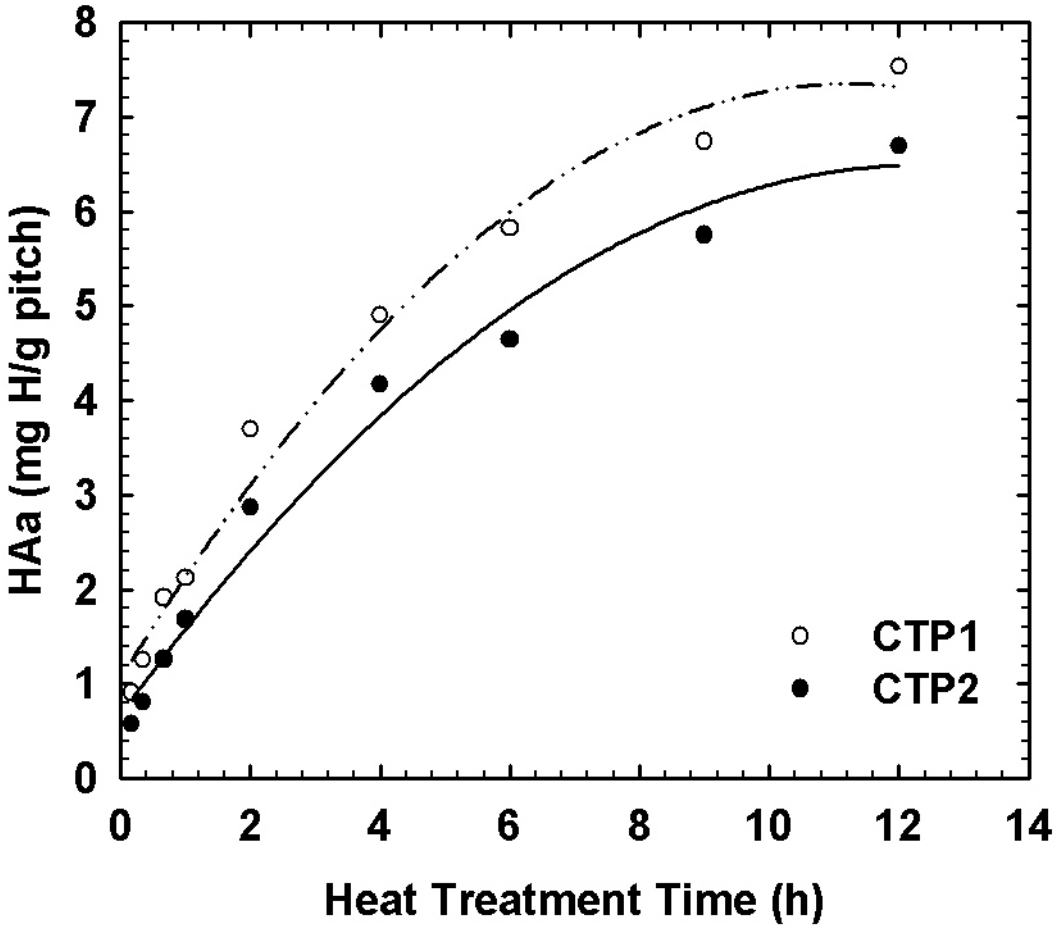

Figure 4.13. Hydrogen acceptor ability (HAa) for coal-tar pitches CTP1 and CTP2 at 400 °C for different soaking times.

The transfer of hydrogen from tetralin to CTP1 and CTP2 occurs continuously but with decreasing kinetics over the entire soaking time period and both pitches show a similar trend. The hydrogen acceptor ability of CTP1 is always higher than for CTP2. Compared to the donor ability reaction (Figure 4.7), the acceptor ability reaction shows a slightly lower decrease in reaction rate. This might be explained by the higher thermal stability of tetralin and the product naphthalene compared to the reactants and products in the donor ability test. Between 10 minutes and one hour a linear relationship between the soaking time and the acceptor ability is observed (Figure 4.14). The reaction rate must also here be higher initially as the linear trend line can not be extrapolated to origin.

The chromatogram from the analysis of the CS_2 extract of the residue from the reaction between pitch and tetralin (Figure 3.7) shows that also minor amounts of butylbenzene and 1-metylindan are formed in addition to naphthalene. As shown in Figure 4.15, the amount of these additional products seems to increase linearly with increasing heat treatment time for CTP1. The same trend was observed for CTP2. When calculating the amounts of these compounds, the relative response factors were not taken into account. The weight percentages shown in Figure 4.15 must therefore be taken as estimates and not as accurate values. However, the amounts of butylbenzene and 1-methylindan formed after 8 hours soaking time are quite small

and not considered to influence the hydrogen acceptor abilities significantly. The formation mechanism of these compounds and the influence on the HAa are discussed in more detail in Chapter 5.

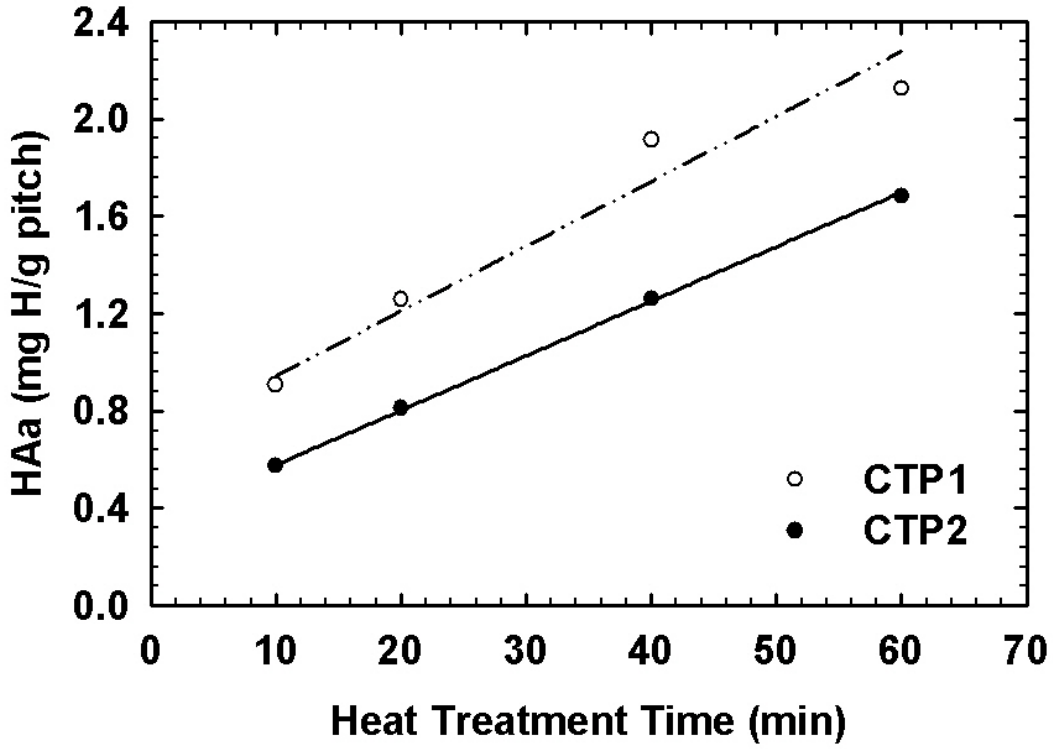

Figure 4.14. Hydrogen acceptor abilities (HAa) for coal-tar pitches CTP1 and CTP2 for different soaking times within the first hour.

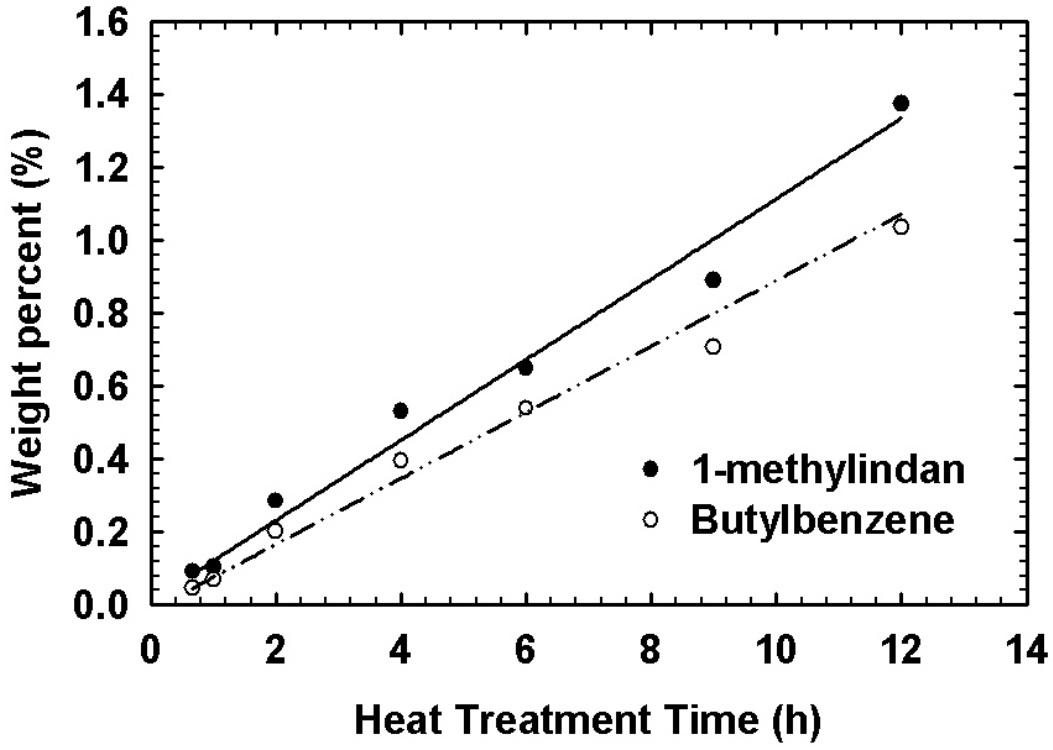

Figure 4.15. Amounts of 1-methylindan and butylbenzene formed in the reaction between CTP1 and tetralin at 400 °C for different soaking times.

The results from the hydrogen acceptor ability test performed after 8 hours heat treatment at 400 °C are shown in Figure 4.16. Two or three parallels were studied for each of the pitches. Tukey's pairwise comparisons were used to test if differences in the mean HAa were significant (Table 4.4).

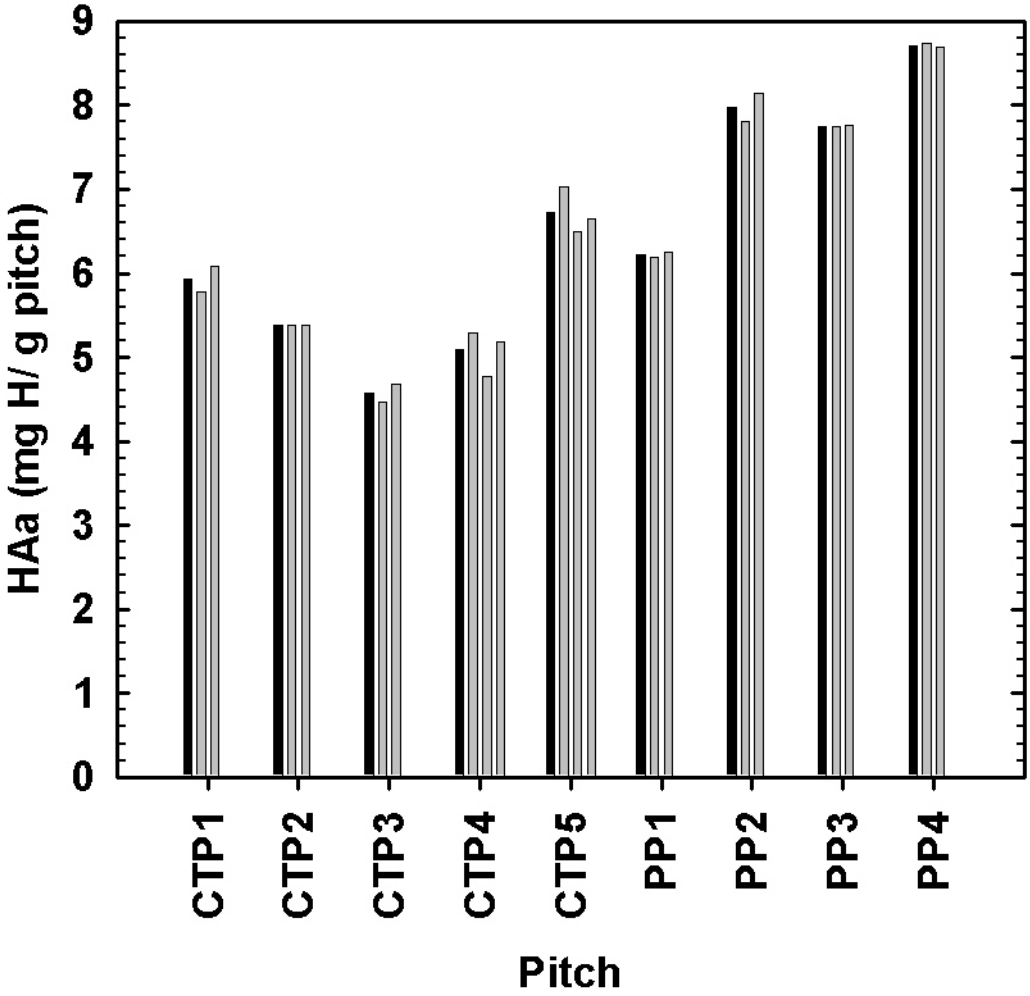

Figure 4.16. Hydrogen acceptor ability (HAa) measured after heat treatment at 400 °C and 8 hours soaking time. The black bars are averages of the parallels (grey bars).

Table 4.4. Tukey's pairwise comparisons for the hydrogen acceptor ability (HAa) of pitches (400 °C, 8 hours soaking time). Family error rate of 5 %. Significant difference marked "+", non-significant difference marked "-".

	CTP1	CTP2	CTP3	CTP4	CTP5	PP1	PP2	PP3
CTP2	-							
CTP3	+	+						
CTP4	+	-	-					
CTP5	+	+	+	+				
PP1	-	+	+	+	-			
PP2	+	+	+	+	+	+		
PP3	+	+	+	+	+	+	-	
PP4	+	+	+	+	+	+	-	+

Except for PP1, the petroleum pitches exhibit higher hydrogen acceptor abilities than the coal-tar pitches. Petroleum pitch 4 shows the highest HAa, although the difference between the HAa for this pitch and PP2 was not significant. Coal-tar pitch 5 is distinguished due to its significantly higher hydrogen acceptor ability compared to the other coal-tar pitches. Although there is not a straight relationship between the HDa shown in Figure 4.12 and the HAa, it is interesting that the two pitches exhibiting the lowest hydrogen donor ability within their group, show the highest acceptor abilities. The relationship between the hydrogen donor and acceptor abilities is discussed in detail in Chapter 5.

The hydrogen acceptor ability was also measured following a less severe heat treatment. This heat treatment was the same as the one used for the donor ability test, 5 °C/min to 400 °C with no soaking time. The results are shown in Figure 4.17. The variation between the parallels (grey bars) is quite pronounced, but is not arbitrary. There seems to be a systematic difference between the parallels. In particular, parallel three is distinguished due to much higher HAa values than the other two parallels. Unknown to the author at the time of experiments, there had been done some changes to the equipment between the parallels. Between parallel 1 and 2 the carrier gas had been changed from hydrogen to helium, while the column length had been cut between parallel 2 and 3. These changes might influence the response factors and probably explain the systematic variation between parallels. The naphthalene peak was minute compared to the tetralin peak which meant that the uncertainty in the calculated HAa might be quite high. Due to these factors, the hydrogen acceptor ability test performed with 8 hours soaking time probably gave a better representation of the true hydrogen acceptor behavior of the pitches. These results are therefore used in the following discussion given in Chapter 5. It is, however, interesting that the HAa for both of the heat treatments shows common features. Petroleum pitch 4 is differentiated from the other petroleum pitches and CTP5 is differentiated from the other coal-tar pitches due to their significantly higher hydrogen acceptor abilities. Also, CTP2, CTP3 and CTP4 exhibit similar but low acceptor abilities while CTP1 is somewhat higher. There are no results for the HAa of CTPN measured after 8 hours soaking time. However, if the trend for the other pitches from the acceptor ability test performed under the less severe heat treatment conditions is followed, it would probably fall in the same range as CTP2, CTP3 and CTP4.

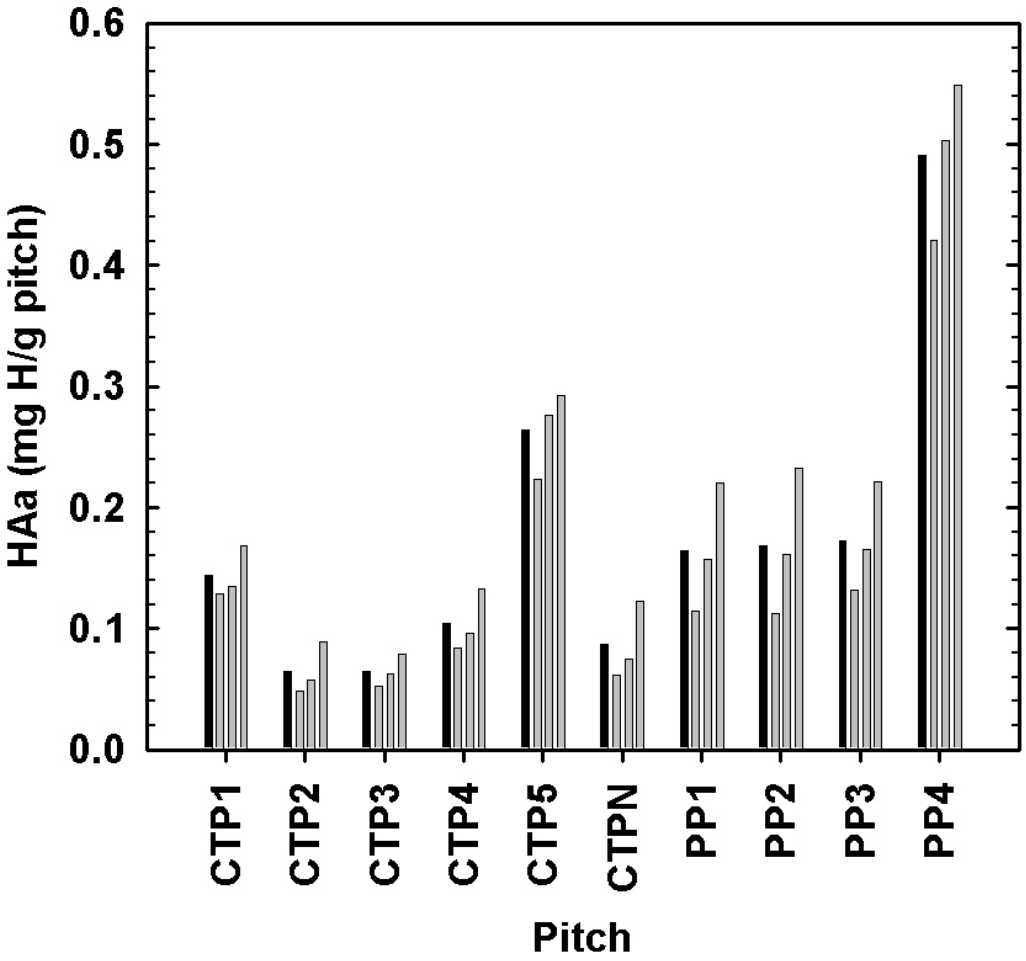

Figure 4.17. Hydrogen acceptor ability (HAa) at 400 °C with a heating rate of 5 °C/min and no soaking time. The black bars are averages of the parallels (grey bars).

4.3 Thermogravimetric Analysis

The weight loss curve and its first derivative (DTG) for coal-tar pitches in the temperature interval from 150 °C and 600 °C are shown in Figure 4.18.

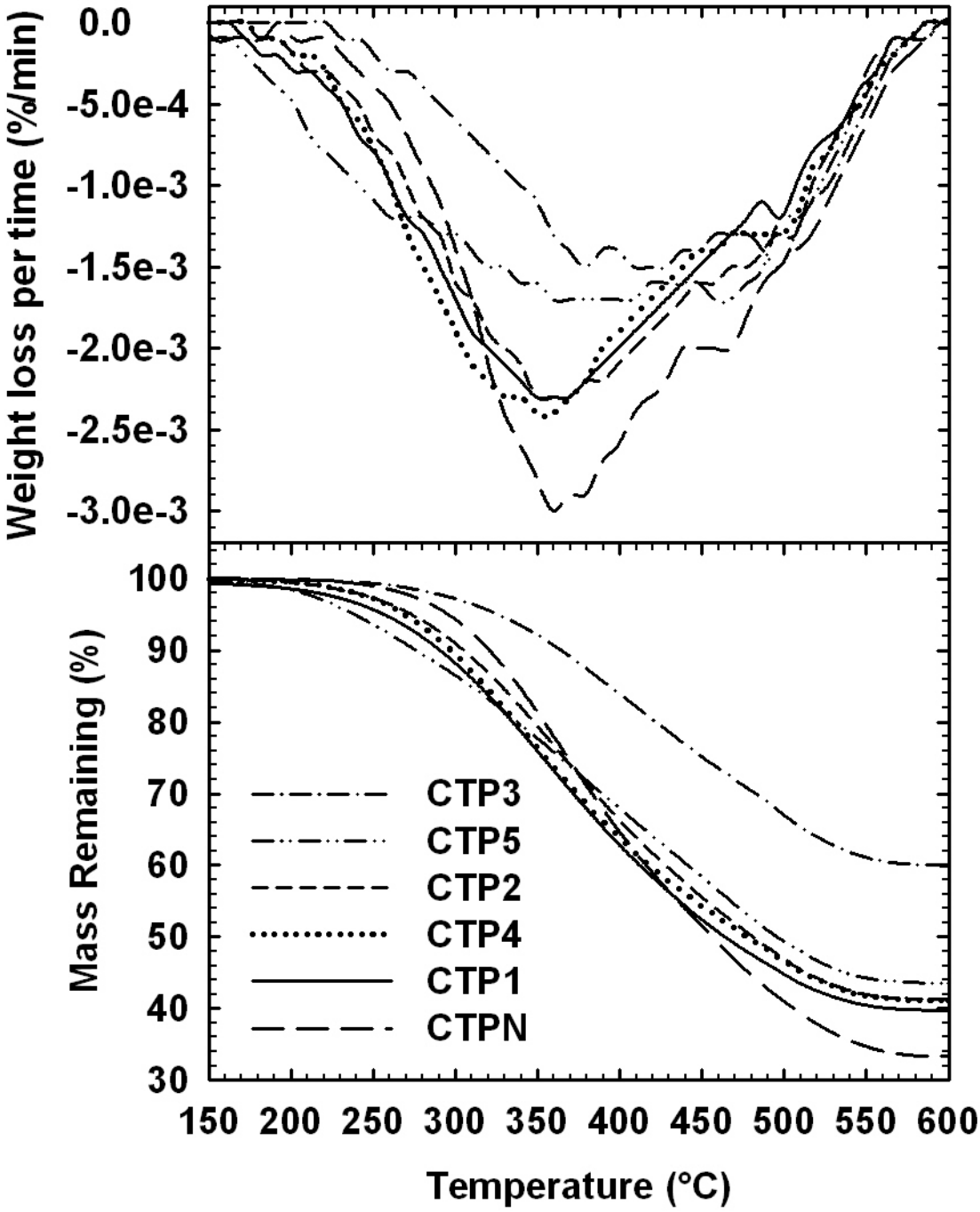

Figure 4.18. Mass remaining versus temperature (bottom) and the first derivative of the weight loss curve (top) for coal-tar pitches. Heating rate of 10 °C/min.

At 600 °C, the pitches have lost more than 96 wt% of the total amount of volatiles released in the entire temperature range up to 1000 °C. Coal-tar pitch 1 (CTP1), CTP2

and CTP4 follow a similar weight loss trend, while CTP3 is differentiated by giving a much higher coke yield than the other pitches due to its high QI content and softening point. The lowest coke yield is exhibited by CTPN which has a very low QI content (Table 3.1). For CTP3 and CTPN the weight loss commences at around 220 ºC which is slightly higher than the other coal-tar pitches. Coal-tar pitch 5 is distinguished due to its relatively high rate of weight loss at temperatures lower than 260 ºC which might indicate the presence of low boiling point compounds or very reactive species which decompose to release volatile fragments. Although the weight loss is high during the initial stages, this pitch has the highest coke yield when excluding CTP3. The first derivatives of the weight loss curves for CTP1, CTP2, CTP4 and CTPN are at their minimum around 360 ºC. This is the temperature where the weight loss curve goes through an inflection point and the volatiles release rate is at a maximum. In comparison, the minima of the weight loss rate curves of CTP3 and CTP5 appear rather broad. The center of this minimum region for CTP5 lies around 390 ºC while it lies at around 410 ºC for CTP3. From about 500 ºC all of the coal-tar pitches show similar but decreasing rates of weight loss until the rate approaches zero at around 600 ºC. At this point the critical stages of carbonization have come to an end and a semi-coke has been formed.

The petroleum pitches have lost more than 97 wt% of their volatiles at 600 ºC. The weight loss and rate of weight loss are shown in Figure 4.19. Petroleum pitch 2 (PP2) and PP3 behave quite similarly upon pyrolysis and the weight loss commences around 170 ºC. At this temperature, the weight loss of PP4 is already quite significant indicating the presence of low boiling point compounds and possibly very reactive species which might decompose into volatile fragments. Although PP4 loses the greatest proportion of its volatiles below 300ºC, it has the highest coke yield of around 38 wt% at 600 ºC. The petroleum pitches behave quite differently from the coal-pitches as the weight loss rate curves go through two minima, the first appearing around 260 ºC for PP4 and around 325 ºC for PP2 and PP3. The second and most intense minimum appear between 425 and 445 ºC. At around 550 ºC, the weight loss rate has reached a stable level. Petroleum pitch 1 (PP1) can be clearly differentiated from the other petroleum pitches. The derivative of the weight loss curve has a shape which is more similar to CTPN with one intense minimum around 365 ºC. The peak has, however, a shoulder from about 410 ºC to 475 ºC. Some of the coal-tar pitches also have a small shoulder in the region 450 to 500 ºC but it is not as pronounced as for PP1. The weight loss for PP1 continues at a relatively high rate until around 570 ºC. Petroleum pitch 1 (PP1) has a coke yield of 33 wt% at 600 ºC which is the lowest of the petroleum pitches and similar to that of CTPN.

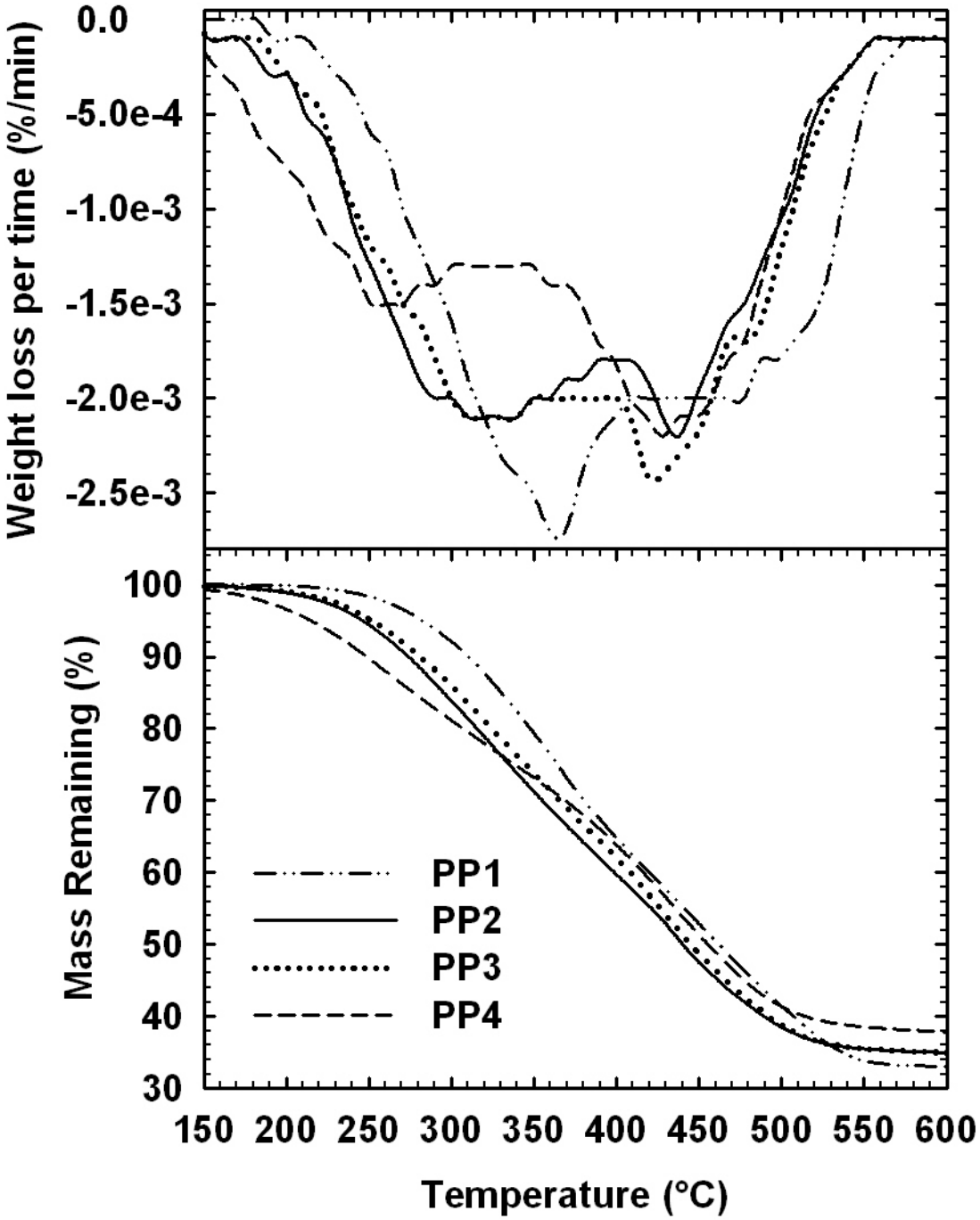

Figure 4.19. Mass remaining versus temperature (bottom) and the first derivative of the weight loss curve (top) for petroleum pitches. Heating rate of 10 ºC/min.

4.4 Optical Texture Analysis

Color images of the optical texture of the eleven pitch cokes which have been studied are shown on the following pages. Each image depicts the texture of one coke grain. Grains that were fairly representative have been picked out.

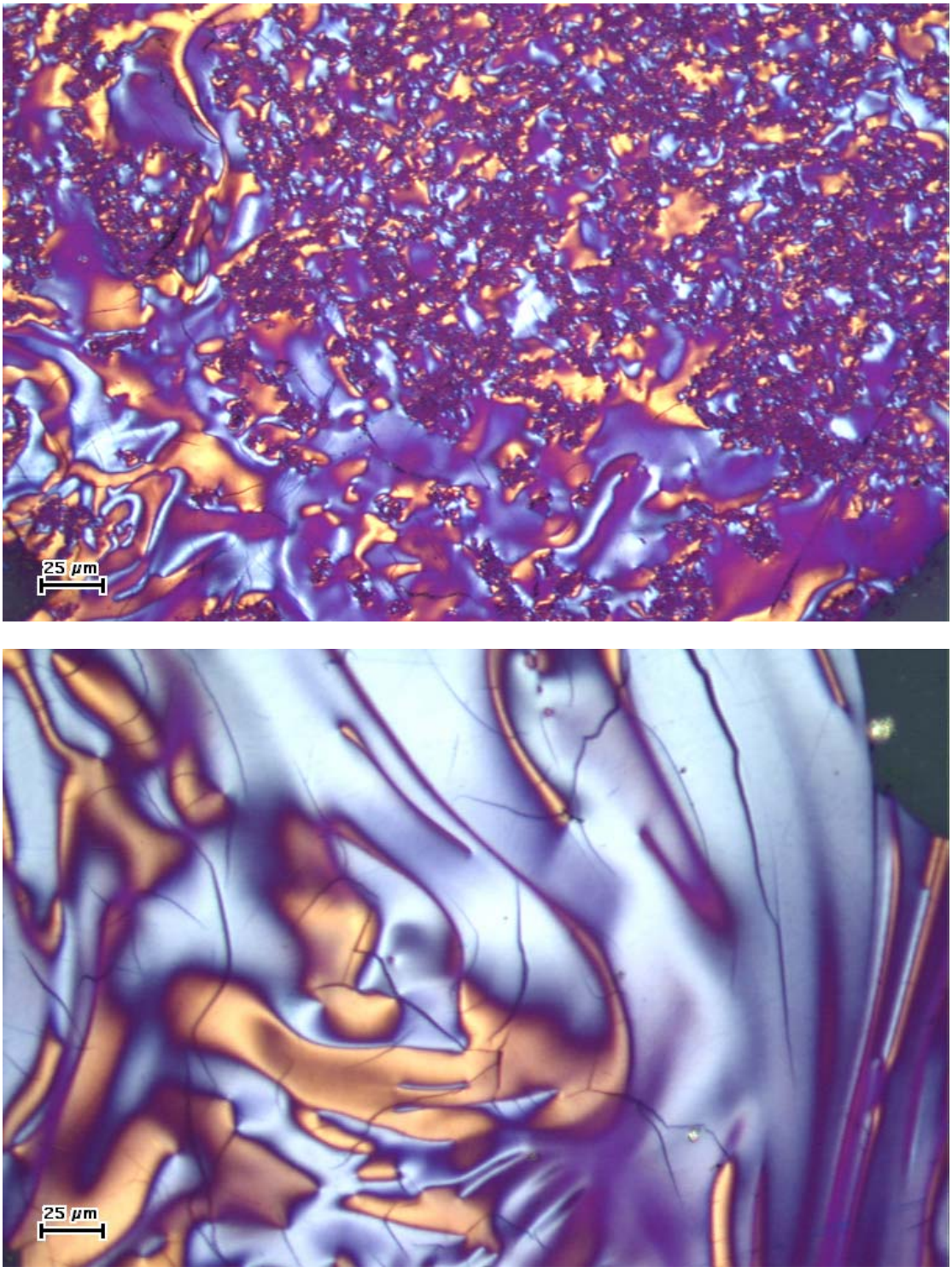

Figure 4.20. Optical texture of CTP1 (12.9 wt% QI) coke (top) and CTP1N (0.6 wt% QI) coke (bottom). CTP1N has been prepared by filtration of CTP1. Note the cracks.

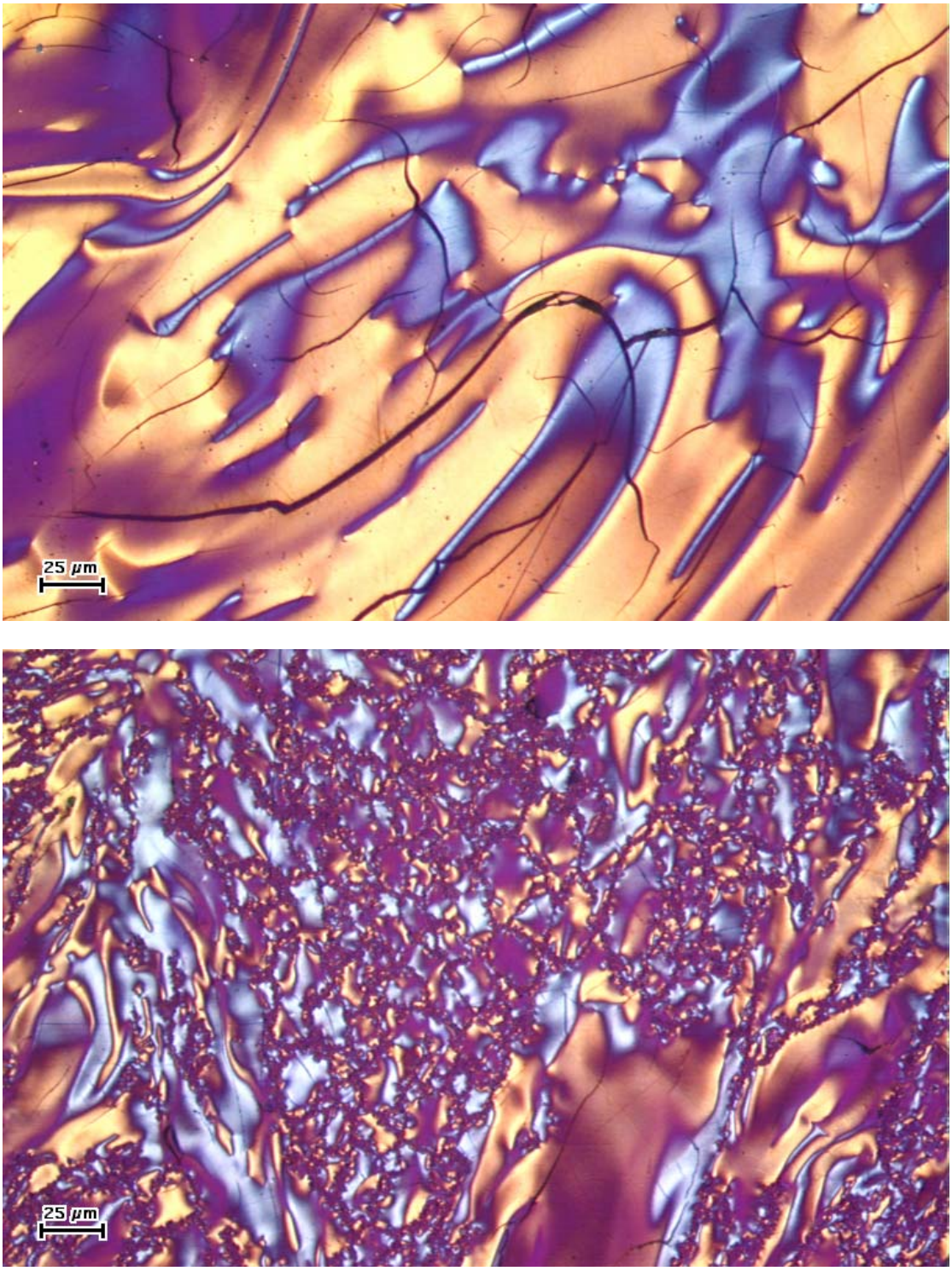

Figure 4.21. Optical texture of CTPN (0.6 wt% QI) coke (top) and CTP2 (9.6 wt% QI) coke (bottom). Cracks appear in the large anisotropic domains of the CTPN coke. The CTP2 coke has a heterogeneous texture showing areas of relatively developed anisotropic domains along with regions of isotropic material (QI) and small-sized anisotropic domains.

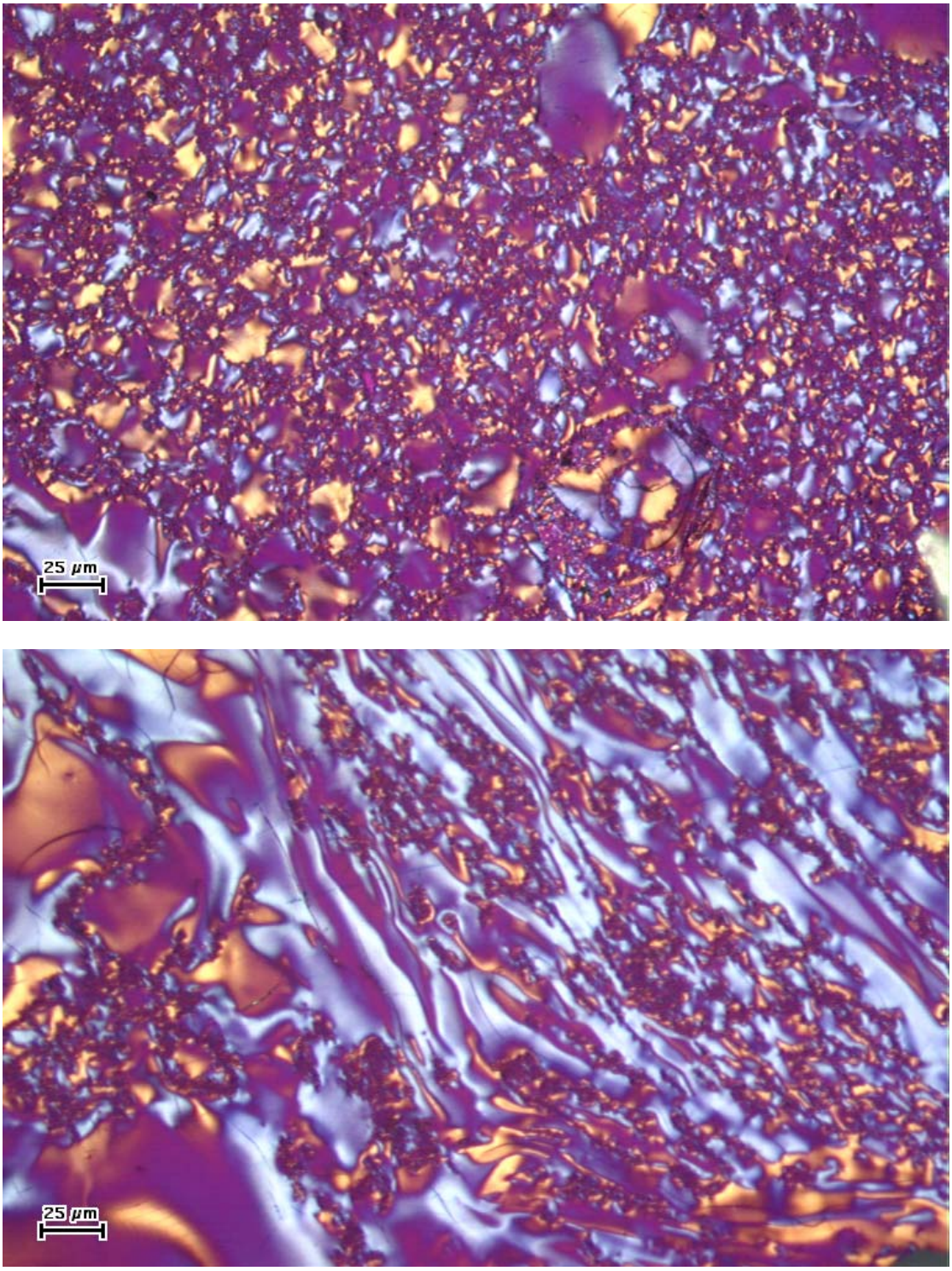

Figure 4.22. Optical texture of CTP3 (25.0 wt% QI) coke (top) and CTP4 (6.6 wt% QI) coke (bottom).

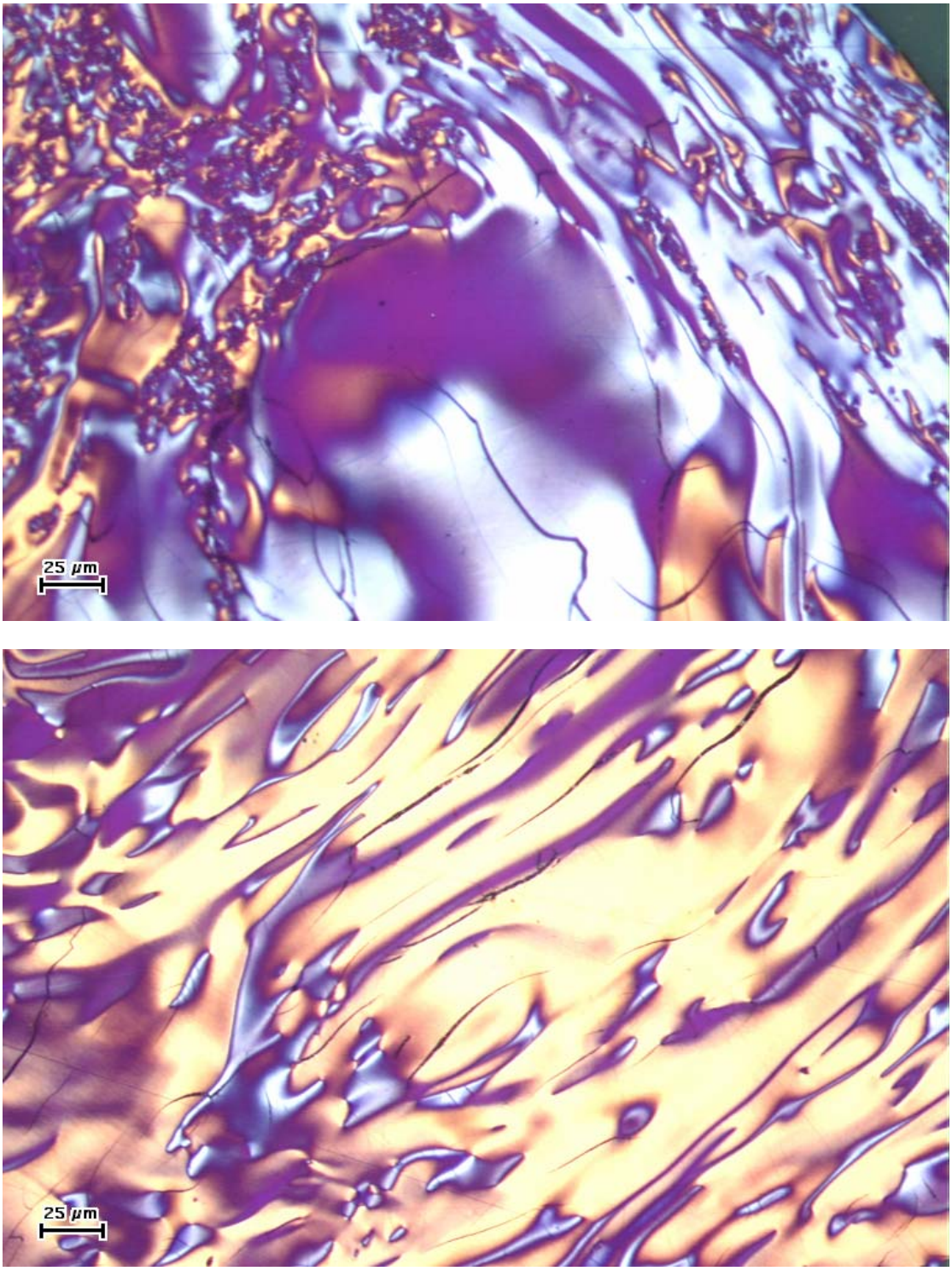

Figure 4.23. Optical texture of CTP5 (4.7 wt% QI) coke (top) and PP1 coke. PP1 is a petroleum pitch. Note that the cracks in the petroleum pitch coke are fewer and smaller than for the QI free coal-tar pitch cokes (CTP1N and CTPN).

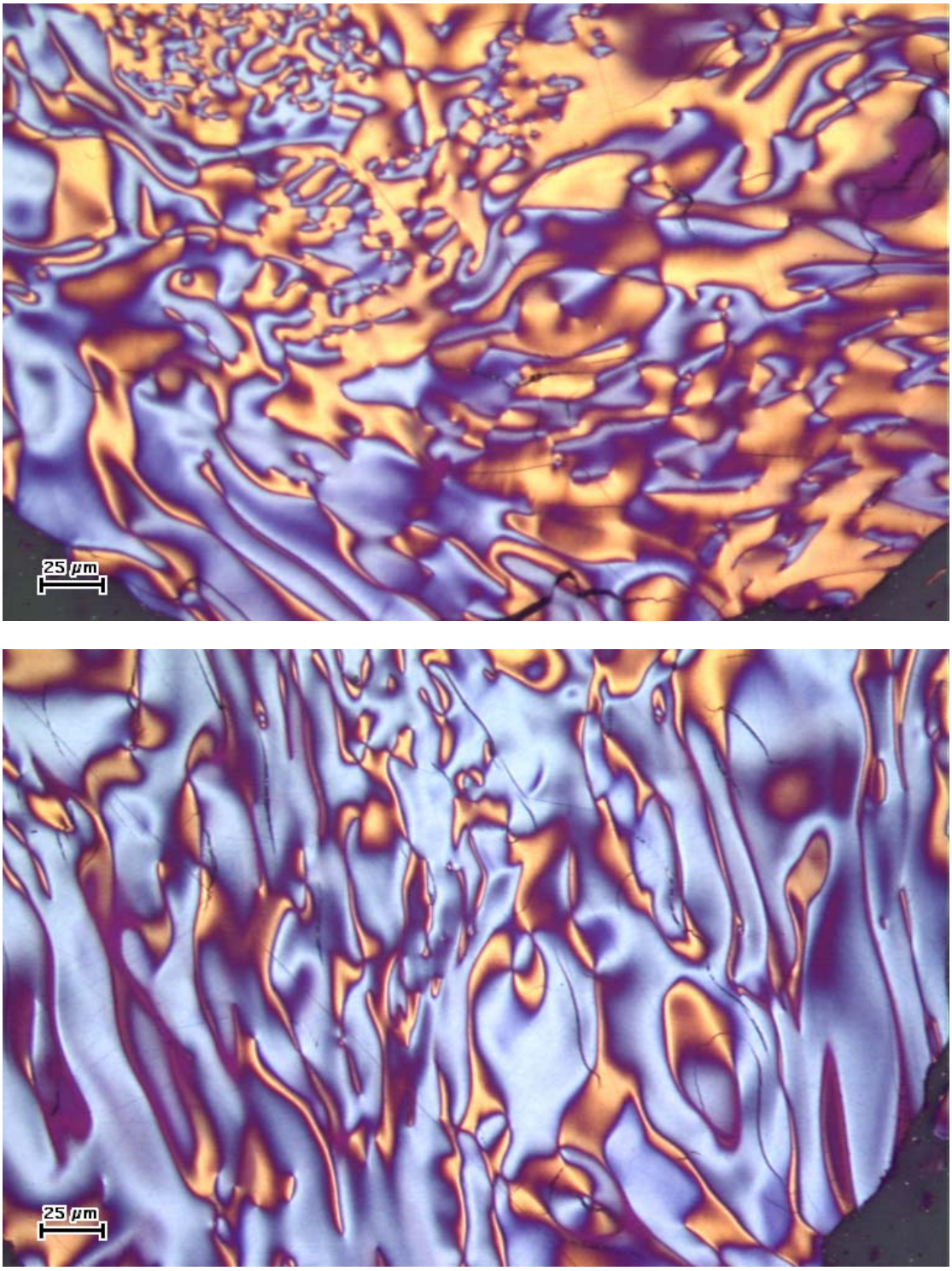

Figure 4.24. Optical texture of PP2 coke (top) and PP3 coke (bottom).

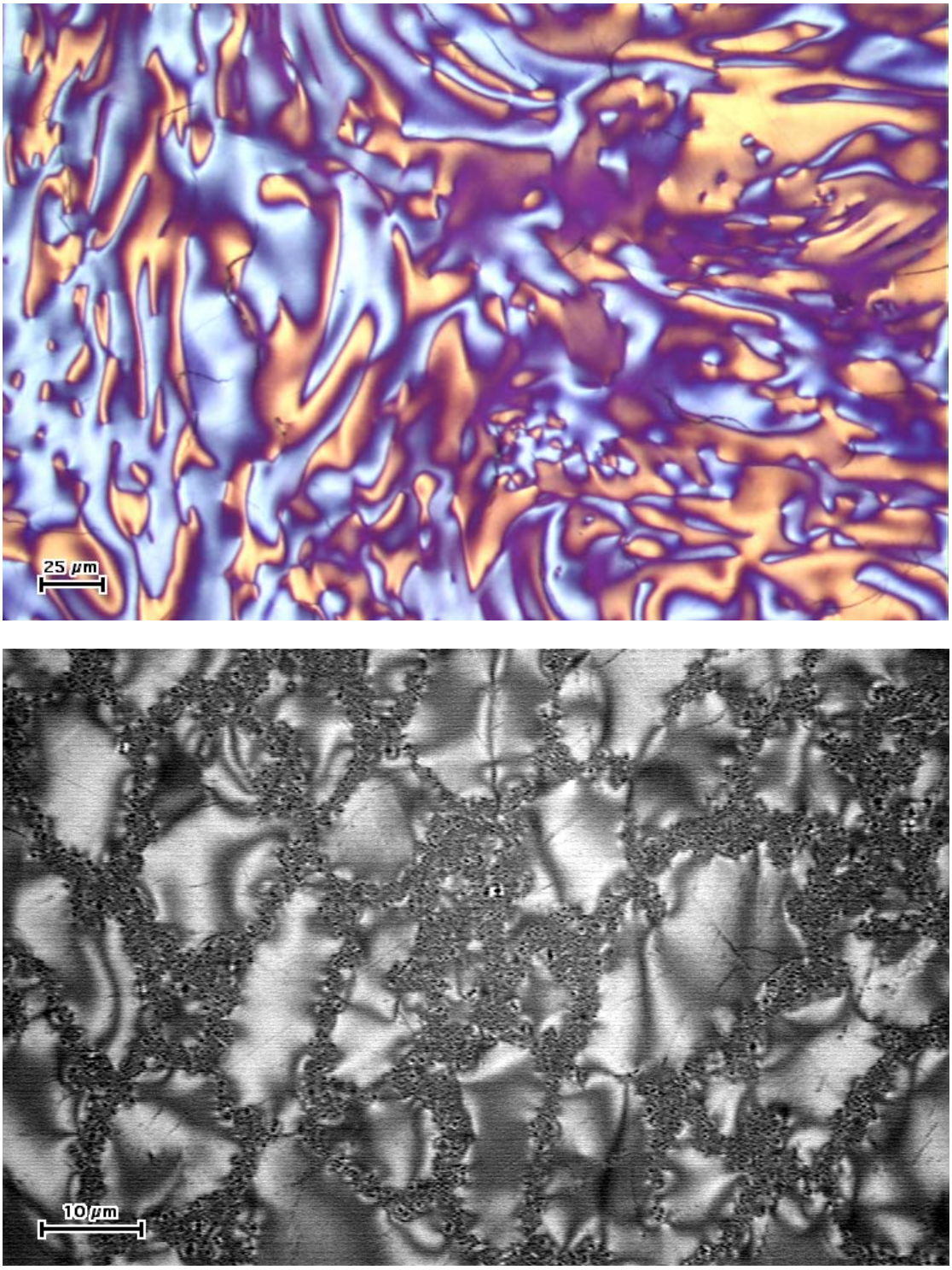

Figure 4.25. Optical texture of PP4 coke (top) and CTP1 (12.9 wt%) coke (bottom) at a higher magnification (1000x). This image is taken without the half-wave retarder plate and therefore appears in grey-scale. Note the clusters of QI material surrounding the irregularly shaped anisotropic domains in the CTP1 coke.

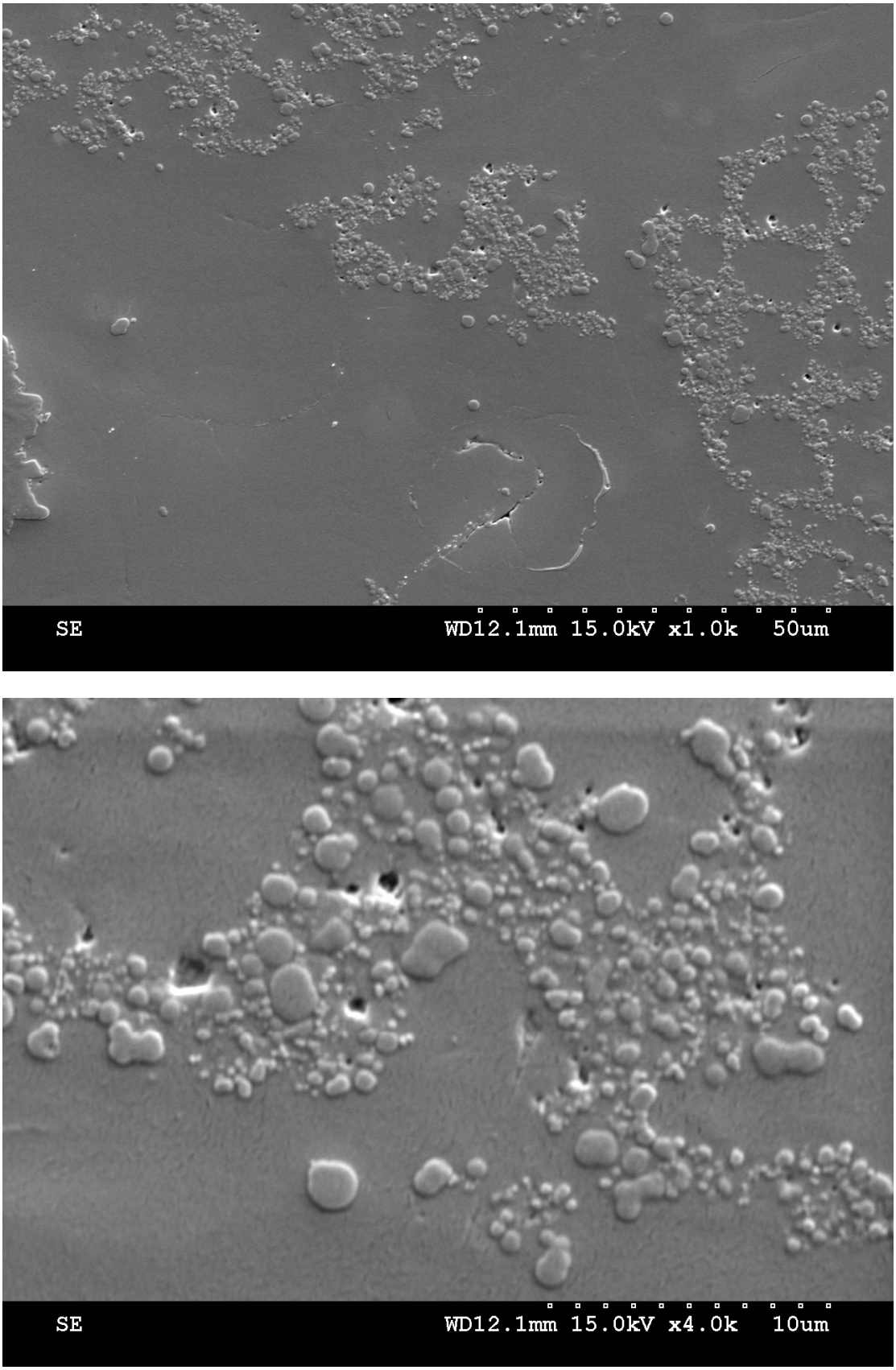

Figure 4.26. Secondary electron image of the polished surface of a CTP1 (12.9 wt% QI) coke grain showing the arrangement of the QI particles (1000x). Bottom picture shows an agglomeration of QI particles from the same coke grain (4000x) The QI particles are harder than the rest of the coke matrix creating a relief effect after polishing.

The high QI coal-tar pitches like CTP1, CTP2 and CTP3 form a heterogeneous coke structure of relatively small irregularly shaped anisotropic domains and clusters of QI. As can be seen from the scanning electron images (Figure 4.26), the QI particles vary in size from a couple of micrometers down to roughly 100 nanometers and below. Coal-tar pitch 4 (CTP4) and CTP5 develop larger anisotropic domains. Regions of QI clusters and small-sized anisotropic domains are present in these pitch cokes as well but these regions are smaller and not as dominant in the structure. In particular, the QI free coal-tar pitches and PP1, but also the other petroleum pitches, develop cokes of large fairly aligned optical domains. Cracks appear in the QI free coal-tar pitch cokes. These cracks are also present in the larger optical domains of the other coal-tar pitches. Interestingly, the petroleum pitch cokes seem to be nearly crack-free.

The results from the optical texture analysis are presented in Figure 4.27 (Mosaic Index) and Figure 4.28 (Fiber Index). Tukey's pairwise comparisons have been used to test if differences in the mean mosaic index (Table 4.5) and the mean fiber index (Table 4.6) were significant.

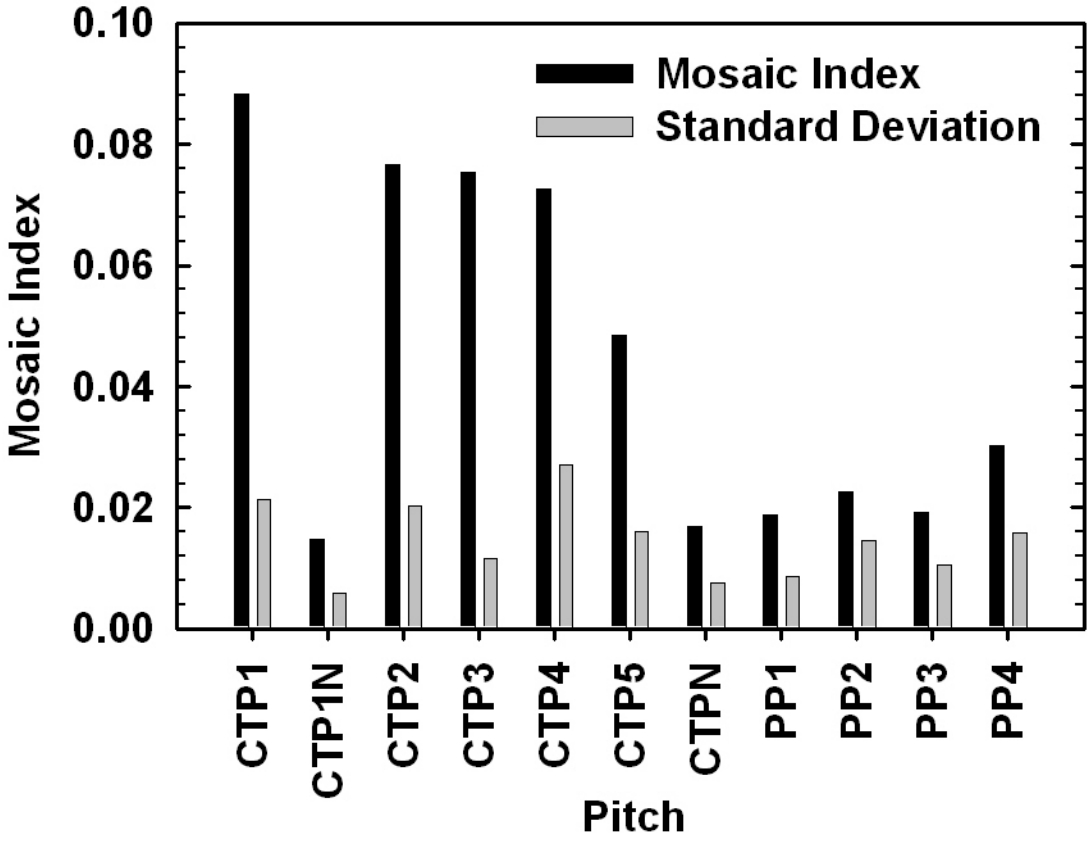

Figure 4.27. Mosaic Index (black bars) for pitch cokes heat treated at 550 ºC. Standard deviation also given (grey bars). A fine textured (small optical domain size) coke structure will yield a high Mosaic Index.

The QI free coal-tar pitch cokes and the petroleum pitch cokes all exhibit a low mosaic index. Coal-tar pitch 1 has the highest mosaic index of all the cokes while CTP2, CTP3 and CTP4 fall in the same region. Coal-tar pitch 5 (CTP5) falls in an intermediate region exhibiting a mosaic index which is significantly different from all the other pitch cokes. The pitch coke of PP4 has a significantly higher mosaic index than the three other petroleum pitch cokes. Petroleum pitch 1 exhibits the lowest

mosaic index of the petroleum pitch cokes but the differences to PP2 and PP3 are not significant.

Table 4.5. Tukey's pairwise comparisons for the Mosaic Index of pitch cokes. Family error rate of 5 %. Significant difference marked "+", non-significant difference marked "-".

	CTP1	CTP1N	CTP2	CTP3	CTP4	CTP5	CTPN	PP1	PP2	PP3
CTP1N	+									
CTP2	+	+								
CTP3	+	+	-							
CTP4	+	+	-	-						
CTP5	+	+	+	+	+					
CTPN	+	-	+	+	+	+				
PP1	+	-	+	+	+	+	-			
PP2	+	+	+	+	+	+	-	-		
PP3	+	-	+	+	+	+	-	-	-	
PP4	+	+	+	+	+	+	+	+	+	+

The petroleum pitch cokes and the QI free pitch cokes exhibit high fiber indexes. CTP3 has the lowest fiber index of all the pitches but the difference to CTP1 is not significant. The CTP5 pitch coke falls in an intermediate region and has a fiber index

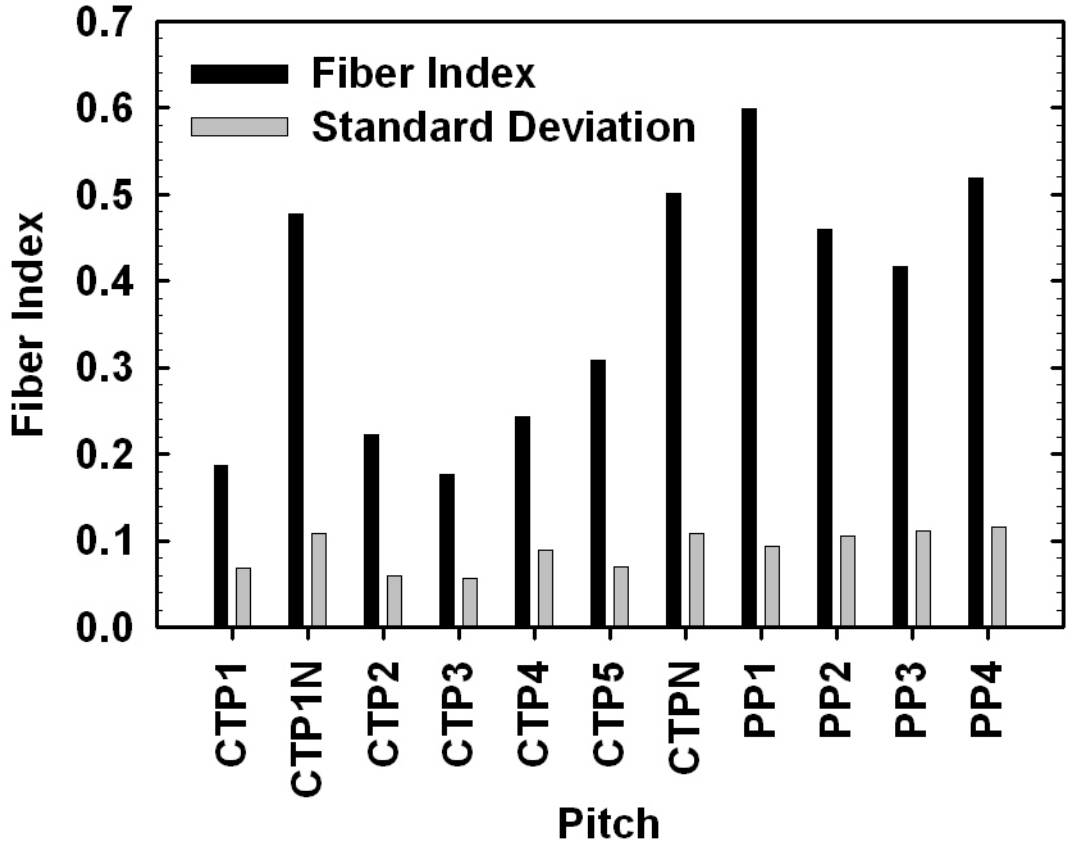

Figure 4.28. Fiber Index (black bars) for pitch cokes heat treated at 550 ºC. Standard deviation is also given (grey bars). A coke structure where the optical domains are arranged parallel (high degree of domain anisotropy) to each other will yield a high Fiber Index.

which is significantly different from all the other pitches. Petroleum pitch 1 exhibits the highest fiber index of the petroleum pitches. The lowest fiber index of the petroleum pitch cokes is exhibited by PP3. The difference between the fiber index of PP2 and PP3 is significant.

Table 4.6. Tukey's pairwise comparisons for the Fiber Index of pitch cokes. Family error rate of 5 %. Significant difference marked "+", non-significant difference marked "-".

	CTP1	CTP1N	CTP2	CTP3	CTP4	CTP5	CTPN	PP1	PP2	PP3
CTP1N	+									
CTP2	-	+								
CTP3	-	+	+							
CTP4	+	+	-	+						
CTP5	+	+	+	+	+					
CTPN	+	-	+	+	+	+				
PP1	+	+	+	+	+	+	+			
PP2	+	-	+	+	+	+	+	+		
PP3	+	+	+	+	+	+	+	+	+	
PP4	+	+	+	+	+	+	-	+	+	+

4.5 X-ray Diffraction

Powder samples of the pitch cokes heat treated at 1150 °C for four hours were studied by X-ray diffraction. The diffraction profiles are shown in Figure 4.29, Figure 4.30 and Figure 4.31. The three figures are drawn in exactly the same scale making direct comparisons possible.

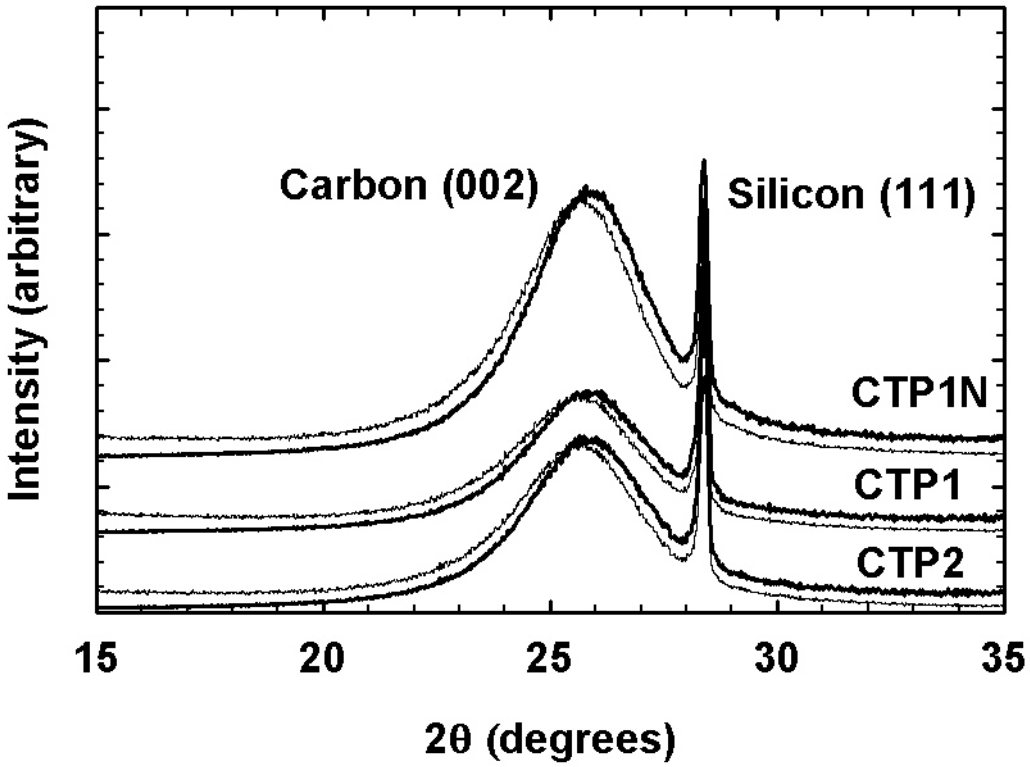

Figure 4.29. Observed and intensity corrected X-ray diffraction profiles for coal-tar pitch cokes heat treated at 1150 °C for 4 hours. The profiles shifted slightly to the right (in bold) are intensity corrected for Lorentz, polarization, absorption and carbon atom scattering factors. Silicon added as internal standard (10 wt%).

The intensity correction of the observed diffraction profiles causes a significant shift in the broad (002) carbon peak position to a higher angle. This will therefore influence the calculated d_{002} interlayer spacing by lowering its value. However, the intensity correction did not influence the full-width half maximum (FWHM) and thus the average crystallite size (L_c) calculated from the Scherrer equation to a significant extent.

The pitch cokes have similar diffraction profiles with the maximum of the broad (002) carbon peak located around 25.9° (2θ). The full-width half maximum varies between a minimum of 2.98° for CTPN and a maximum of 3.36° for PP4. In general, the carbon peak is wider for the petroleum pitches than the coal-tar pitches. The exception is PP1, which has a slightly narrower and more defined carbon peak compared to the other petroleum pitches (Figure 4.31). Coal-tar pitch N (CTPN) and CTP1N, which have very low QI contents (Table 3.1), are distinguished due to higher intensity carbon peaks which seem to be narrow at half height compared to the other coal-tar

pitches. However, it is difficult to make any direct comparisons of the full-width half maximum by just observing the X-ray diffraction profiles. The carbon peak of CTP3 is less intense than the peak of CTPN (Figure 4.30), but the full-width half maximums of the two peaks as found by profile fitting are very similar. The calculated average crystallite size (L_c) and the interlayer spacing (d_{002}) are presented in Figure 4.32 and Figure 4.33, respectively. Two or three parallels were measured for each pitch coke. The steps of mixing silicon and pitch coke and specimen packing were repeated for each parallel.

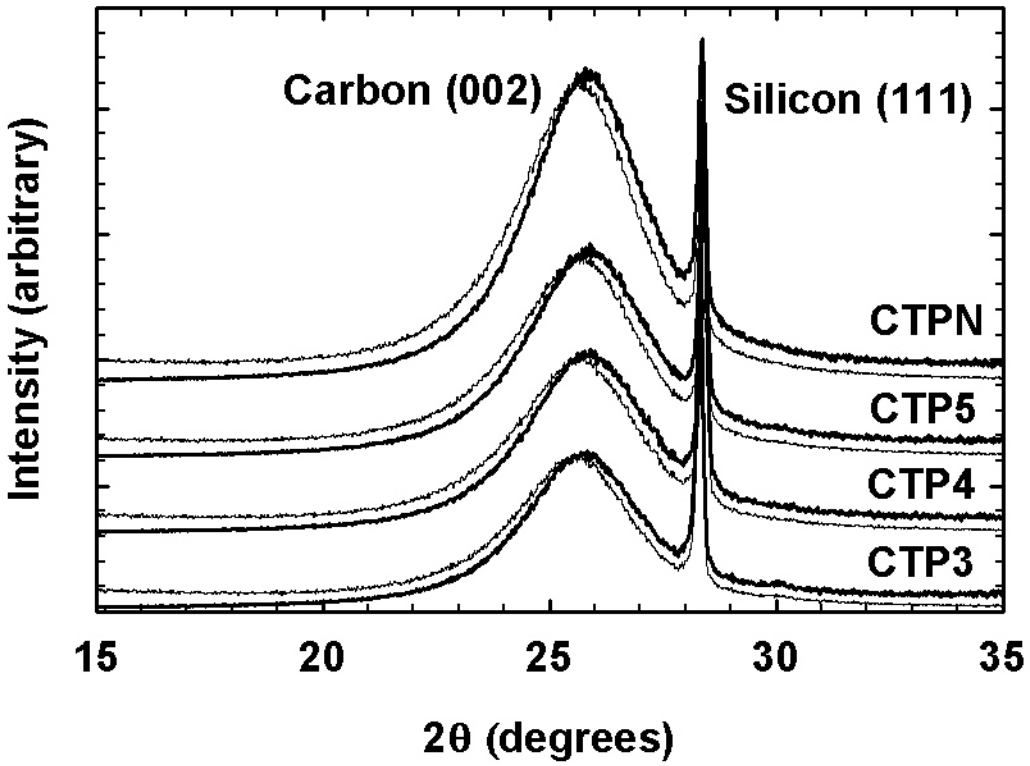

Figure 4.30. Observed and intensity corrected X-ray diffraction profiles for coal-tar pitch cokes heat treated at 1150 °C for 4 hours. The profiles shifted slightly to the right (in bold) are intensity corrected for Lorentz, polarization, absorption and carbon atom scattering factors. Silicon added as internal standard (10 wt%).

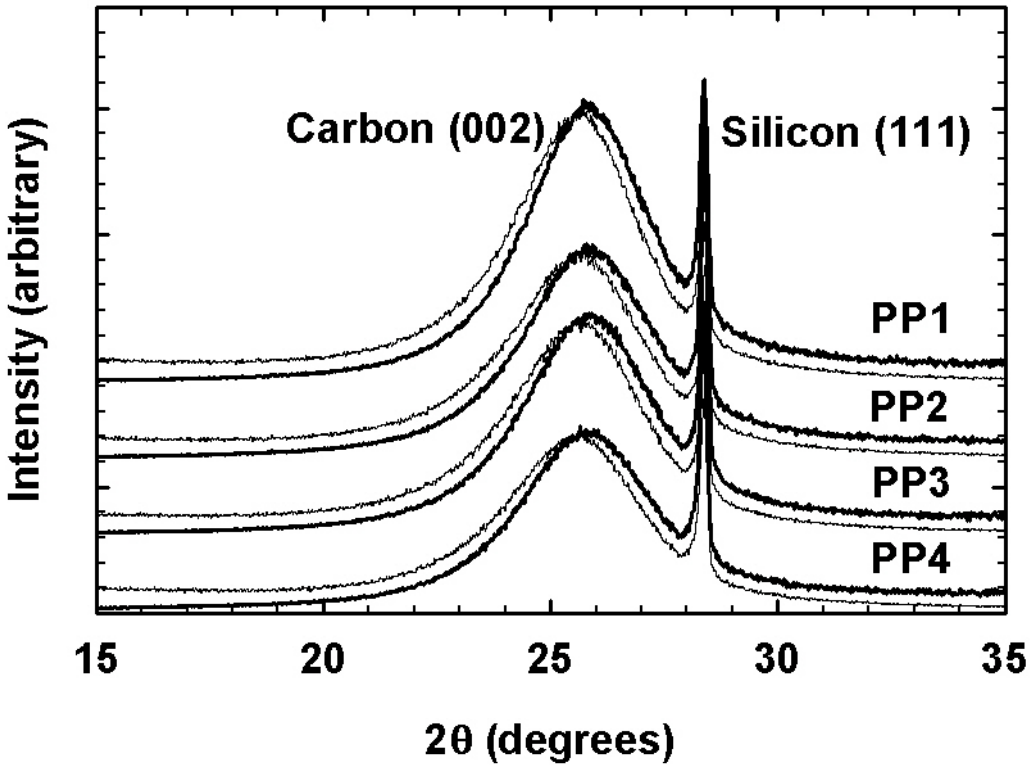

Figure 4.31. Observed and intensity corrected X-ray diffraction profiles for petroleum pitch cokes heat treated at 1150 °C for 4 hours. The profiles shifted slightly to the right (in bold) are intensity corrected for Lorentz, polarization, absorption and carbon atom scattering factors. Silicon added as internal standard (10 wt%).

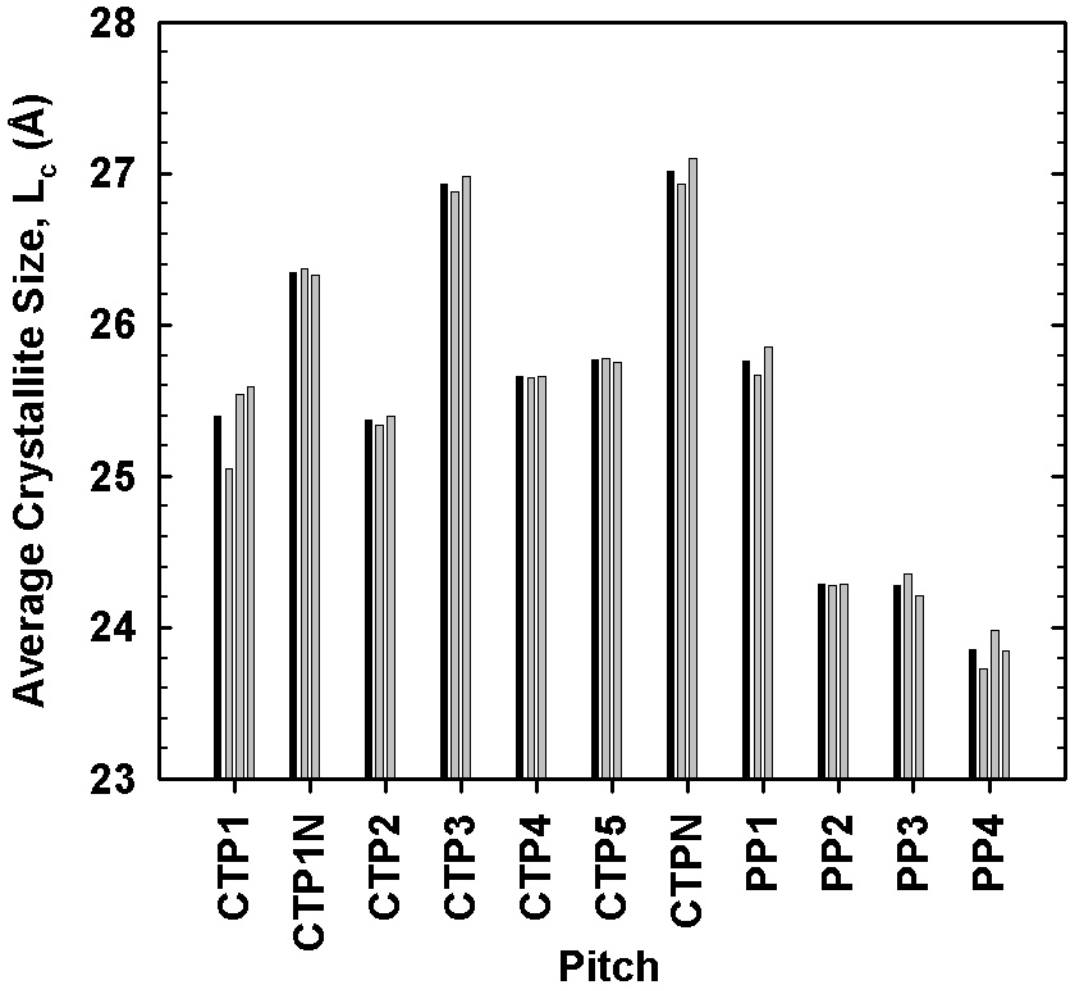

Figure 4.32. Average crystallite size (L_c) for pitch cokes heat treated at 1150 °C for 4 hours. The black bars are averages of the parallels (grey bars).

The two pitches with very low QI contents, CTP1N and CTPN, and CTP3 are different from the other pitches forming cokes of relatively high average crystallite size. The rest of the coal-tar pitches and PP1 fall in an intermediate region while the three remaining petroleum pitches form cokes of relatively low stack heights (L_c). Petroleum pitch 4 forms a coke of lower L_c-value than PP2 and PP3 but the difference was not found to be significant using Tukey's pairwise comparisons with a family error rate of 5 %.

The coke formed from PP4 exhibits the highest interlayer spacing and the lowest stack height indicating a less ordered structure than the other pitch cokes. However, there does not seem to be any straight correlation between L_c and d_{002}. The interlayer spacing from the CTP3 coke is one of the highest and was not significantly different from the PP4 coke. It is interesting that there is a significant difference between the interlayer spacing of the CTP1 and the CTP1N cokes as CTP1N is the pitch prepared by QI removal from CTP1.

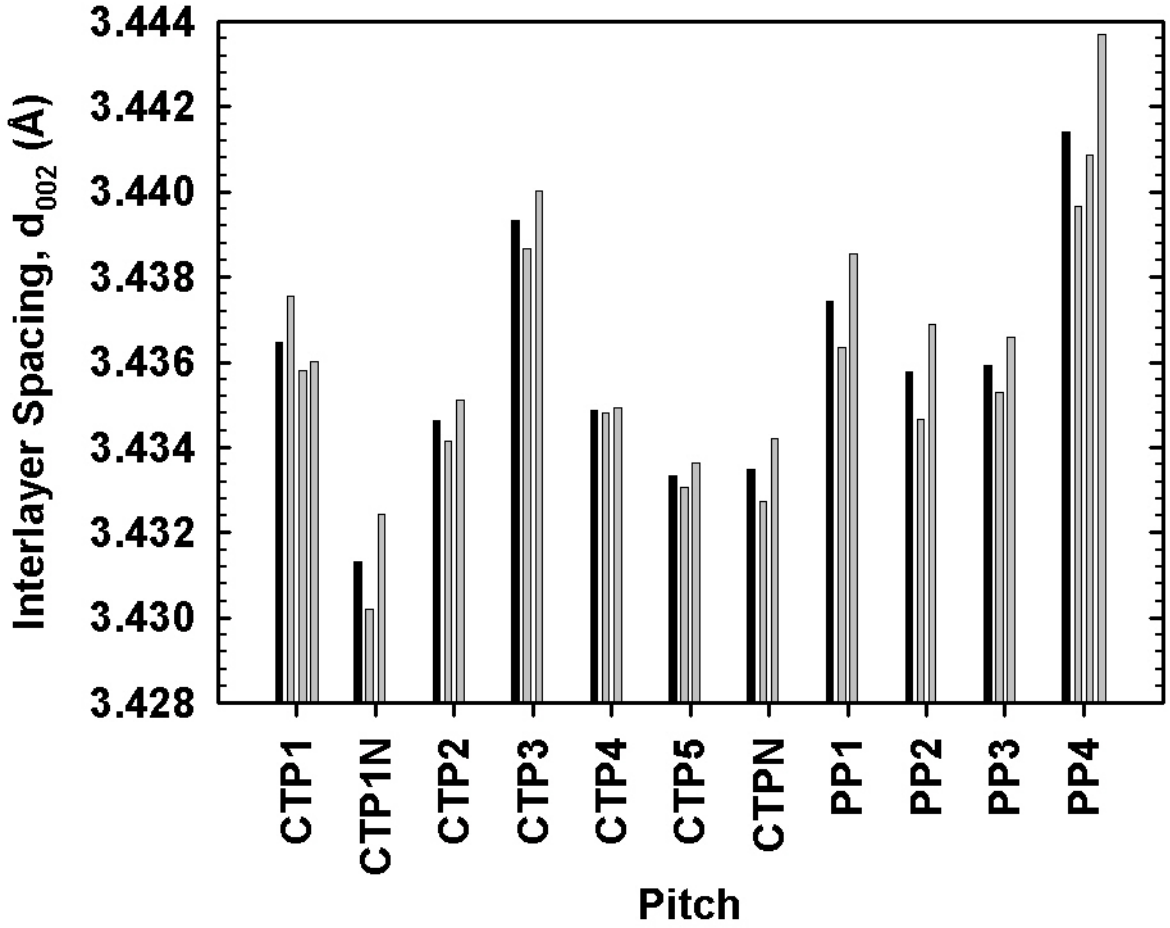

Figure 4.33. Average interlayer spacing (d_{002}) for pitch cokes heat treated at 1150 °C for 4 hours. The black bars are averages of the parallels (grey bars).

5 DISCUSSION

5.1 Nuclear Magnetic Resonance

The structure of pitch cokes is directly linked to the properties of the mesophase at the time of solidification. These properties are in turn mainly dependent on the chemical characteristics of the parent pitch. The composition of the pitch will thus to a large extent govern the reactivity during thermal treatment. A thermally reactive pitch is expected to undergo a rapid transformation through polymerization of constituents at relatively low temperatures. In this case, either mesophase will not be formed or the growth and coalescence of mesophase will take place under low fluidity/high viscosity conditions leading to an isotropic pitch coke or a pitch coke of small optical domains. On the other hand, if the pitch has a low thermal reactivity, the formation, growth and coalescence of mesophase may be postponed and take place at a higher temperature where the viscosity of the pyrolysis system is low and an anisotropic coke of large well-developed optical domains is formed.

Hydroaromatic and naphthenic rings in hydroaromatic species are of particular interest as they have been recognized as principal hydrogen donor groups by Clarke, Rantell and Snape [57]. Donatable hydrogen in the pitch may stabilize free radicals formed by thermal rupture of bonds in reactive species during carbonization and thereby lower the thermal reactivity. The concentration of donatable hydrogen is not directly connected to the total concentration of hydrogen in the pitch as a large proportion of the aliphatic hydrogen may also be present in alkyl side chains. The hydrogen located in alkyl side chains is not donatable and would on the contrary be expected to lead to an increased intermolecular reactivity of the pitch. According to Greinke [45], it is generally believed that the initiation of polymerization in pitch involves primarily the reaction of the less stable alkyl group when compared to the more stable aromatic hydrogens. The first step in the dehydrogenative polymerization of pitch, the formation of bi-aryls, is very likely rate determining. The aromatic hydrogen abstraction by radicals formed in the early stages of carbonization by cleavage of alkyl side chains probably has an important influence on the thermal reactivity. Structural changes in oligomers prepared from model compounds like naphthalene, tetralin, biphenyl and their alkyl substituted homologues suggested that radicals formed from thermal cleavage of alkyl groups would accelerate condensation reactions [76]. The length of the alkyl side chains was found to influence the rate of condensation reactions of the oligomers. Longer side chains resulted in a rapid increase in ring size which in turn led to a low fluidity of the reaction system and consequently a fine mosaic structure of the resulting coke. Both the length and number of alkyl substituents may thus be important factors which influence the thermal reactivity of pitches.

The purpose of the NMR analysis is to identify and quantify structures in the pitch which are considered to either increase or decrease the thermal reactivity.

5.1.1 Concentration of Donatable Hydrogen

The concentration of donatable hydrogen in pitches can be estimated from the aliphatic region of the ^{1}H NMR spectra and the ^{13}C NMR spectra (DEPT). The distribution of aliphatic hydrogen and carbon (DEPT) is given in Figure 4.2 and Figure 4.6, respectively. Description of the various types of hydrogen is given in Table 3.5 while description of the carbon chemical shift regions is shown in Table 3.6.

Examples of model compounds that contain donatable hydrogen are shown in Figure 5.1 while model compounds that do not are shown in Figure 5.2. The potentially donatable hydrogen is mainly located in the H_F (3) and $H_{\beta 2}$ (6) bands of the ^{1}H NMR spectra (see Figure 3.1). In addition, a proportion of the hydrogen in the $H_{\alpha 1}$ band is donatable. The $H_{\alpha 1}$ band contains both hydrogen in methylene groups in hydroaromatic rings (5c) which is donatable and hydrogen located in methylene (5b) or methyl groups (5a) in alkyl side chains which is not.

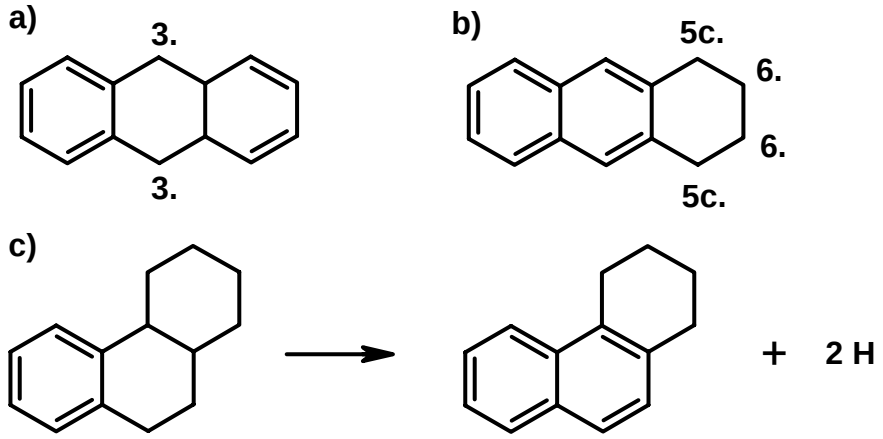

Figure 5.1. Model compounds containing donatable hydrogen.
a) Dimethylenic bridge (H_F): 3,
b) Methylene group in α position ($H_{\alpha 1}$): 5c , 2. Methylene group in β position ($H_{\beta 2}$): 6,
c) Partial dehydrogenation resulting in conversion of naphthenic ring to hydroaromatic ring.

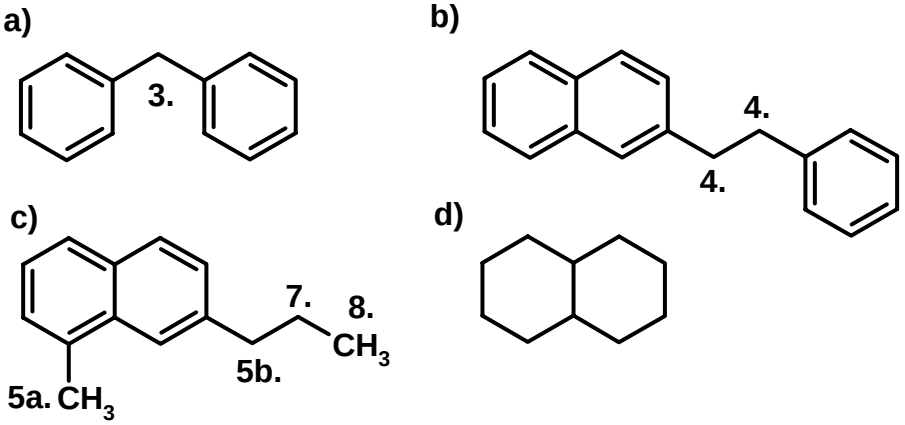

Figure 5.2. Model compounds that do not contain donatable hydrogen.
a) Single methylene bridge (H_F): 3, b) Ethylene bridge (H_A): 4,
c) Hydrogen located in alkyl side chains. Methylene group in α position ($H_{\alpha 1}$): 5a, b,
Methylene group in β position ($H_{\beta 1}$): 7, Methyl group in γ position (H_{γ}): 8.
d) Polynaphthenic (saturate) methylene groups which may contribute to the $H_{\beta 2}$ band.

Clarke, Rantell and Snape [57] have found a saturate content of around 6 wt% in a hydrogenated anthracene oil by silica gel adsorption chromatography. The concentration of saturates (Figure 5.2, d) in pitches is probably considerably lower due to their more aromatic character and has been neglected. If it is assumed that all the hydrogen in the $H_{\beta 2}$ band is located in hydroaromatic rings, the proportion of hydrogen in cyclic methylene groups in α position to an aromatic ring should be equal to the proportion of $H_{\beta 2}$ type hydrogen (Figure 5.1, b). One half of the hydrogen located in methylene groups in hydroaromatic rings is considered donatable and the concentration of such hydrogen in the pitches can thus be estimated as follows:

$$H_{donatable} = \frac{(H_F + 2 \cdot H_{\beta 2})}{2} \cdot \%H \qquad \textbf{(5-1)}$$

where %H is the weight percent of hydrogen in the pitches determined by elemental analysis (Table 3.2).

The estimated concentration of donatable hydrogen in the pitches according to Equation 5-1 is shown in Figure 5.3.

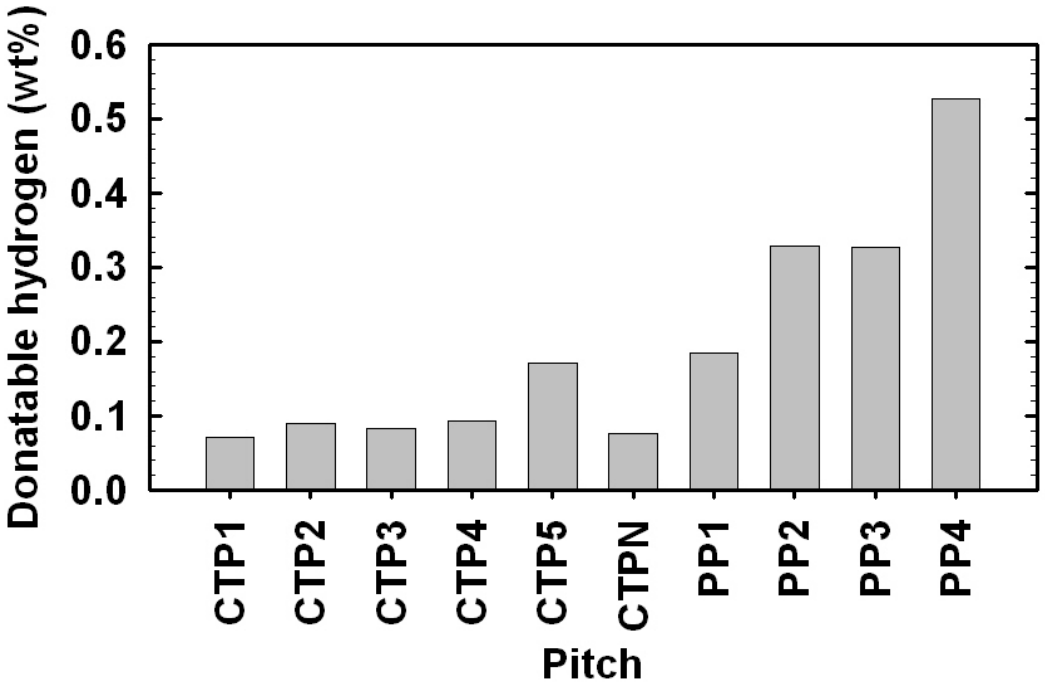

Figure 5.3. Concentration of donatable hydrogen estimated from ^{1}H NMR spectra of pitches.

The expression given above (Equation 5-1) is similar to the expression used by Clarke, Rantell and Snape [57] in the estimation of donatable hydrogen in a hydrogenated anthracene oil. They do, however, not consider the hydrogen located in the H_F band as potentially donatable. Hydrogen located in methylene single bridges linking two aromatic structures, Ar-CH_2-Ar' (Figure 5.2, a) is not potentially donatable as these bridges are expected to undergo cleavage leading to free radical fragments (Figure 2.5). On the other hand, hydroaromatic species like for instance 9,10-dihydroanthracene where two aromatic rings are linked by two methylene bridges (dimethylenic bridge), may donate hydrogen (Figure 5.1, a) [77]. It is, however, not possible to distinguish hydrogen in dimethylenic bridges from the hydrogen located in

a methylene single bridge (Ar-CH_2-Ar') as the methylene hydrogen in both cases will have a similar chemical shift in the H_F band. If single methylene bridges are abundant in the pitches, the inclusion of hydrogen in the H_F band would lead to an overestimation of the concentration of donatable hydrogen. The amount of these single bridges is unknown and the concentration of donatable hydrogen shown in Figure 5.3 must accordingly be taken as a rough estimate. Clarke, Rantell and Snape [57] also consider naphthenic rings to contain potentially donatable hydrogen (Figure 5.1, c). The $H_{\beta 1}$ and H_γ bands may thus also contain donatable hydrogen. However, naphthenic rings are considered to be present in quite low amounts in pitches and all the hydrogen in these bands has been assumed to be present in alkyl side chains. Accordingly, hydrogen located in naphthenic rings has not been included in the estimation of donatable hydrogen (Equation 5-1). If naphthenic rings in hydroaromatic species are present in significant amounts, it would lead to an underestimation of donatable hydrogen.

The concentration of donatable hydrogen can also be estimated from the aliphatic carbon fractions determined from the ^{13}C NMR (DEPT) spectra (Figure 4.6). Examples of model compounds that contain donatable hydrogen are shown in Figure 5.4 while model compounds that do not are shown in Figure 5.5. The potentially donatable hydrogen is mainly located in dimethylenic bridges (3), hydroaromatic rings (4b), naphthenic rings (also 4b) and in hydroaromatic rings with alkyl substituents (7) (see Figure 3.3).

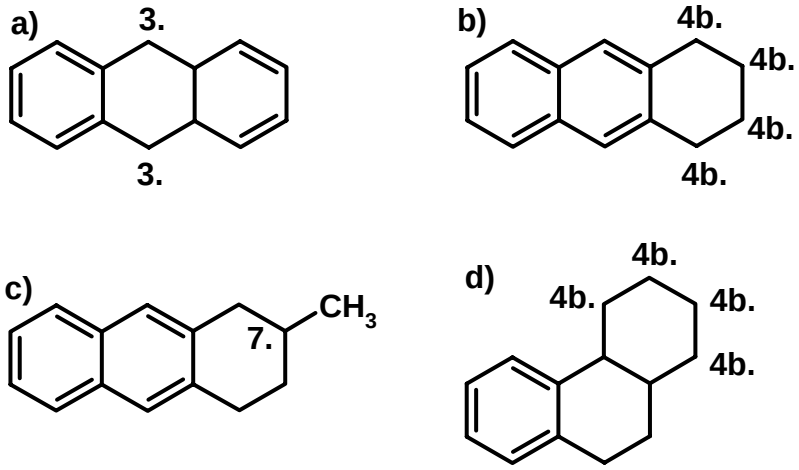

Figure 5.4. Model compounds containing donatable hydrogen.
a) Dimethylenic bridge ($C_{\alpha 2}$): 3, b) Methylene group in hydroaromatic ring (CH_2): 4b,
c) Aliphatic carbon connected to one hydrogen (CH_{al}): 7,
d) Methylene group in naphthenic ring (CH_2): 4b.

The fraction of methylene groups in alkyl side chains, which do not contain donatable hydrogen, can be taken as equal to the fraction of terminal methyl (t-CH_3) groups (Figure 5.5, c) assuming that the alkyl side chains are not more than 2 carbon atoms long [57]. This approximation is quite rough, especially for PP4 which has an estimated average alkyl side length of more than 2 (Figure 5.8), and would lead to an overestimation of the amount of methylene groups which contain donatable hydrogen.

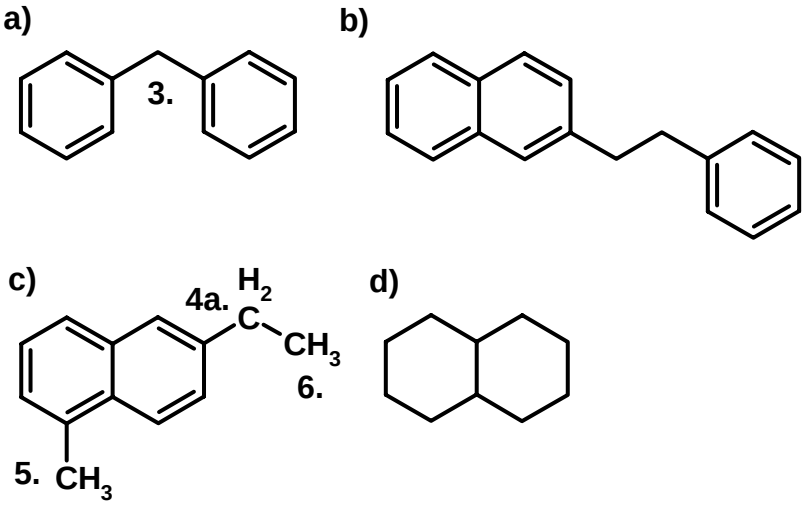

Figure 5.5. Model compounds that do not contain donatable hydrogen.
a) Single methylene bridge ($C_{\alpha 2}$): 3, b) Ethylene bridge (CH_2),
c) Alkyl substituents. Methylene group (CH_2): 4a, α methyl group (α-CH_3): 5 and terminal methyl group (t-CH_3): 6.
d) Polynaphthenic (saturate) methylene (CH_2).

The concentration of saturates (Figure 5.5, d), which has not been determined, is considered to be low in pitches and methylene groups in polynaphthenic structures have been neglected. If it is assumed that all methylene groups which are not located in alkyl side chains and all aliphatic CH groups (CH_{al}, Figure 5.4, c) can donate one hydrogen, the concentration of donatable hydrogen can be estimated from Equation 5-2. The amount of methylene groups in alkyl side chains (taken equal to t-CH_3) has been subtracted from the total amount of methylene groups in the expression below:

$$H_{donatable} = \left[C_{\alpha 2} + (CH_2 - \text{t-}CH_3) + CH_{al}\right] \cdot \frac{\%C \cdot 1.008}{12.01} \qquad \textbf{(5-2)}$$

where %C is the weight percent of carbon in the pitches determined by elemental analysis (Table 3.2).

The estimated concentration of donatable hydrogen in the pitches determined from the DEPT spectra is shown in Figure 5.6.

The expression given above is similar to the expression used by Clarke, Rantell and Snape [57] in the estimation of donatable hydrogen in a hydrogenated anthracene oil. They do, however, not consider the $C_{\alpha 2}$ (Figure 3.3) band to contain methylene groups which can donate hydrogen. This is true in the case of single methylene bridges (Figure 5.5, a) but not for dimethylenic bridges (Figure 5.4, a) which contain donatable hydrogen. It is not possible to distinguish methylene groups in single bridges from those located in dimethylenic bridges as the methylene groups in both cases will give rise to a signal in the $C_{\alpha 2}$ band. The amount of single methylene bridges is unknown and the concentration of donatable hydrogen shown in Figure 5.6 must accordingly be taken as a rough estimate. Methylene groups located in ethylene bridges (Figure 5.5) do not contain donatable hydrogen and would on the

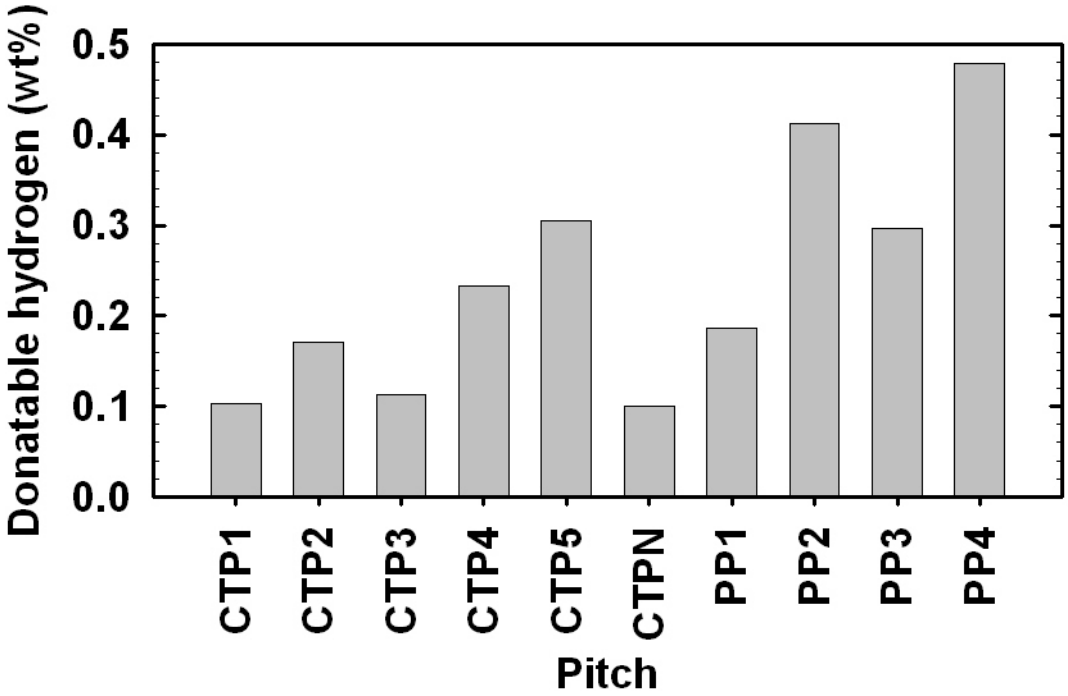

Figure 5.6. Estimated concentration of donatable hydrogen in pitches from DEPT ^{13}C NMR spectra.

contrary be expected to undergo cleavage leading to the formation of free radicals (Figure 2.5). Such methylene groups can not be distinguished from hydrogen donor methylene groups in hydroaromatic or naphthenic rings in hydroaromatic species. If ethylene bridges are abundant in the pitches, this would lead to an overestimation of the concentration of donatable hydrogen.

The estimation of donatable hydrogen from the ^{1}H NMR spectra and the ^{13}C NMR (DEPT) spectra correlate fairly well. This correlation is displayed in Figure 5.7.

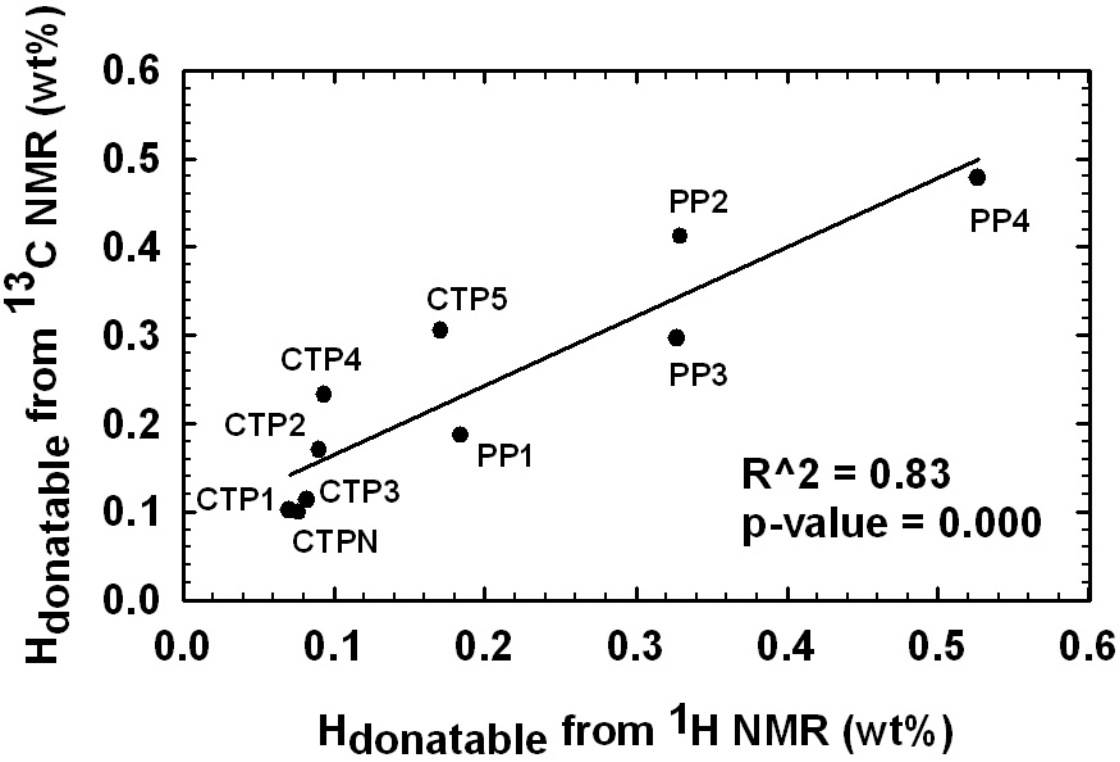

Figure 5.7. Relationship between the concentration of donatable hydrogen estimated from the ^{1}H NMR and ^{13}C NMR (DEPT) spectra.

The concentration of donatable hydrogen is underestimated from the DEPT spectra compared to the ^{1}H NMR spectra by a factor of 0.8. The average concentration of donatable hydrogen determined from both methods would rank the pitches in the following order from the lowest to the highest supply of donatable hydrogen:

CTP1 ≤ CTPN ≤ CTP3 < CTP2 < CTP4 < PP1 < CTP5 << PP3 < PP2 << PP4.

5.1.2 Alkyl Side Chains

The petroleum pitches have a more hydroaromatic and naphthenic structure which is reflected in a higher estimated concentration of donatable hydrogen (Figure 5.3 and Figure 5.6) compared to the coal-tar pitches. However, less than 35 % of the aliphatic hydrogen is potentially donatable. The rest of the hydrogen is assumed to be located in alkyl side chains or ethylene bridges (H_A). The fraction of α methyl or α methylene hydrogen in alkyl side chains can be taken as equal to the difference between the $H_{\alpha 1}$ and $H_{\beta 2}$ bands (see Section 5.1.1). In addition, all hydrogen located in the $H_{\beta 1}$ and H_{γ} bands is assumed to present in alkyl side chains. The average length of alkyl substituents (n) can be estimated according to the following expression [67]:

$$n = \frac{(H_{\alpha 1} - H_{\beta 2}) + H_{\beta 1} + H_{\gamma}}{(H_{\alpha 1} - H_{\beta 2})} \qquad \textbf{(5-3)}$$

The expression given above (Equation 5-3) is similar to the expression used by Dickinson [79] in the estimation of the average length of substituents. Hydrogen located in the H_F and H_A bands and in hydroaromatic rings (taken equal to $H_{\beta 2}$) has been excluded as only the average alkyl side length is considered in Equation 5-3.

The average alkyl side chain length of the pitches is shown in Figure 5.8.

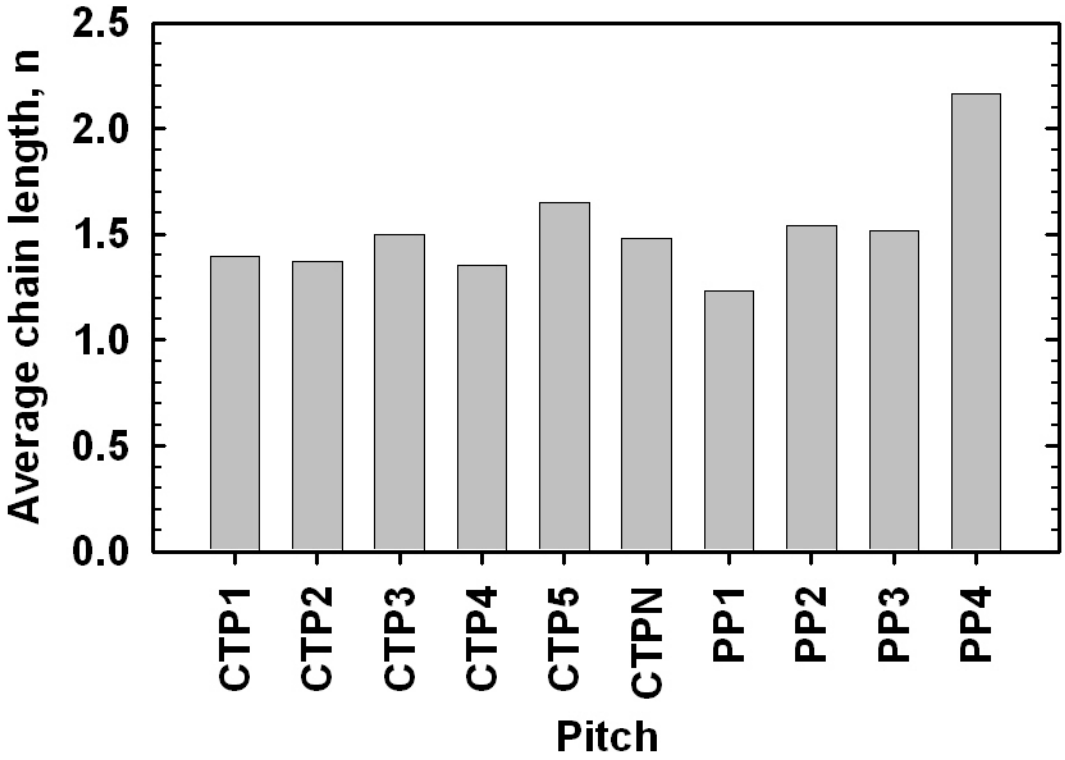

Figure 5.8. Estimated average length of alkyl side chains from ^{1}H NMR spectra of pitches.

The alkyl side chains of PP4 are markedly longer compared to the other pitches. The other pitches have fairly similar average alkyl side chain lengths. Coal-tar pitch 5 (CTP5) has a slightly higher average alkyl side chain length than the other coal-tar pitches. Petroleum pitch 1 (PP1) has the shortest average alkyl side chain length of all the pitches and is probably abundant in methyl substituents.

5.1.3 Aromatic Hydrogen and Carbon

The coal-tar pitches have a significantly higher aromatic hydrogen fraction than the petroleum pitches (Figure 4.2). Coal-tar pitch 5 is distinguished from the other pitches of coal-tar origin due to its relatively low aromatic hydrogen fraction of 0.70. The other coal-tar pitches have aromatic hydrogen fractions which lie in a quite narrow range from 0.83 for CTP4 to 0.87 for CTPN. Petroleum pitch 1 has a more aromatic character than the other petroleum pitches with an aromatic hydrogen fraction of 0.57 compared to the other petroleum pitches which have relatively similar aromatic hydrogen fractions in the range of 0.46 to 0.49. The relative fraction of H_{ar2} is similar for PP2 and PP3 but lower than PP1 and all the coal-tar pitches indicating a less pericondensed structure and a lower relative amount of aromatic hydrogen in sterically hindered positions (see Figure 3.1). The fraction of H_{ar2} is markedly lower for PP4 than all the other pitches. Coal-tar pitch 5 has a lower H_{ar2} fraction than the other pitches of coal-tar origin indicating a structure which more resembles that of the petroleum pitches.

The aromaticity (aromatic carbon fraction), as determined from the conventional ^{13}C NMR spectra, is quite similar for the coal-tar and petroleum pitches (Figure 4.4). This is surprising as the atomic hydrogen to carbon ratio (H/C) from the elemental analysis (Table 3.2) differ significantly for the two groups of pitches. The aromatic hydrogen fraction is also markedly higher for the coal-tar pitches which should suggest a higher carbon aromaticity (Figure 4.2). A lower H/C ratio should generally be connected with a higher aromaticity. Maroto-Valer, Andrésen and Snape [78] have found a very good linear relationship between the H/C ratio and aromaticity determined by solid state ^{13}C NMR for 15 bituminous coal samples. Although this relationship was found for coal samples, there is a strong indication from the elemental analysis performed in the present work that the aromaticities for pitches and especially those of coal-tar origin have been underestimated from the conventional ^{13}C NMR spectra. The signals in the aliphatic carbon region for the coal-tar pitches were quite weak with a resulting poor signal to noise ratio. This may have resulted in uncertainty in the determination of peak areas. There is an unexpectedly low difference between the total aliphatic carbon fraction from the conventional ^{13}C NMR spectra (Figure 4.4) and from the DEPT spectra (Figure 4.6). This is suspicious as the aliphatic fraction should be much higher from the quantification of the DEPT spectra as only the hydrogenated aromatic carbons are visible when using this pulse sequence. The distribution of carbons in the aliphatic region differ significantly in the conventional ^{13}C NMR spectra and the DEPT spectra. The fraction of terminal methyl groups (t-CH_3) is much higher in the conventional ^{13}C NMR spectra, especially for the coal-tar pitches. This might indicate an overestimation of the aliphatic carbon fractions in the conventional ^{13}C NMR spectra.

Aliphatic carbon connected to one hydrogen (CH_{al}, Figure 3.3) which was found to be present in significant amounts in PP2, PP3 and PP4, could only be distinguished in the DEPT spectra due to the phase difference of 180º between CH or CH_3 and CH_2. In general, the resolution seems to be better in the DEPT spectra and the quantifications seem more reliable. However, the aromatic carbon distribution must be based on the data obtained from the conventional ^{13}C NMR spectra as the DEPT sequence only reveals protonated aromatic carbon.

According to Dickinson [79], the fraction of protonated aromatic carbon (Figure 3.3, 2b) can be estimated from the following relation.

$$CH_{ar} = 12 \cdot H_{ar} \cdot H \qquad \textbf{(5-4)}$$

where H is the weight fraction of hydrogen determined by elemental analysis and H_{ar} is the fraction of aliphatic hydrogen from the ^{1}H NMR spectra.

Based on the estimated fraction of protonated aromatic carbon (Equation 5-4), an indirect calculation of the aromaticity (total aromatic carbon fraction) can be made from the DEPT spectra as this sequence only reveals the protonated aromatic carbons. The expression for the estimation of the aromaticity (f_a) from the DEPT spectra is shown below:

$$f_a = \frac{C_{ar}}{C_{ar} + C_{al} \cdot CH_{ar}} \qquad \textbf{(5-5)}$$

where C_{al} is the aliphatic carbon fraction from integration of the DEPT spectra (Figure 4.6). The aromatic carbon fraction (C_{ar}) is equal to 1 – C_{al} while CH_{ar} is the protonated aromatic carbon fraction estimated from Equation 5-4.

The indirectly determined aromaticities from the DEPT spectra are shown in Figure 5.9. For comparison, the aromaticities directly determined from the conventional carbon spectra (Figure 4.4) are also shown.

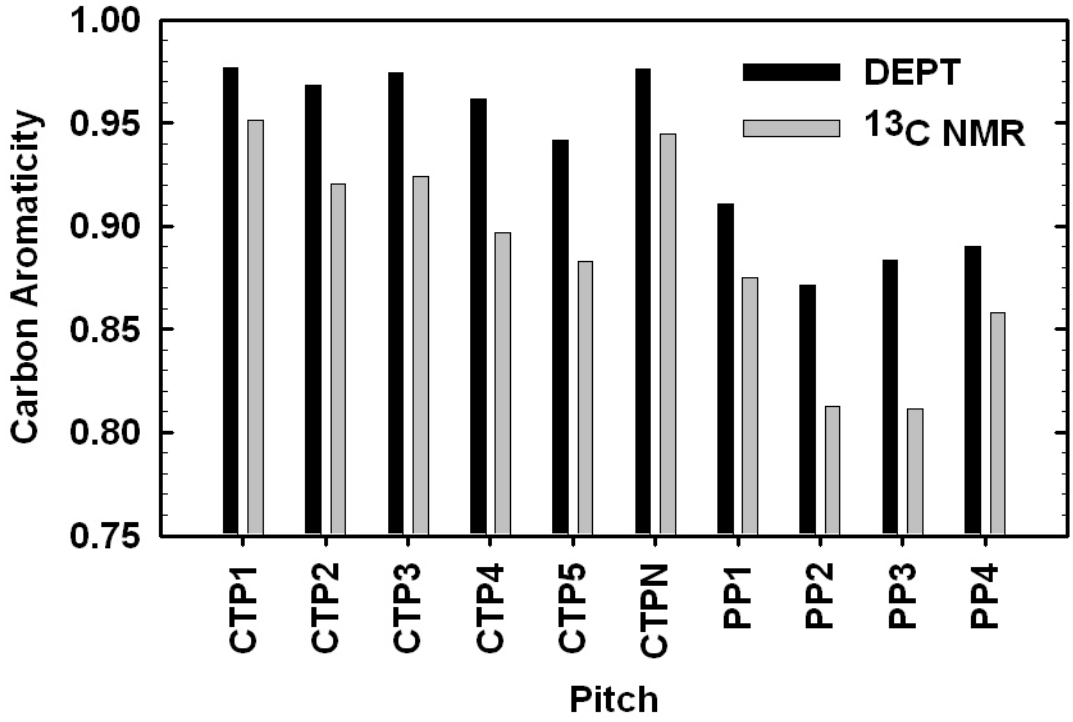

Figure 5.9. Carbon aromaticity (f_a) of pitches determined directly from conventional ^{13}C NMR spectra (grey bars) and indirectly from DEPT spectra (black bars). The total fraction of aromatic carbon (aromaticity) has been estimated from the DEPT spectra using Equation 5-4 and Equation 5-5.

The linear correlation between carbon aromaticity and H/C atomic ratio from elemental analysis was tested and is displayed in Figure 5.10.

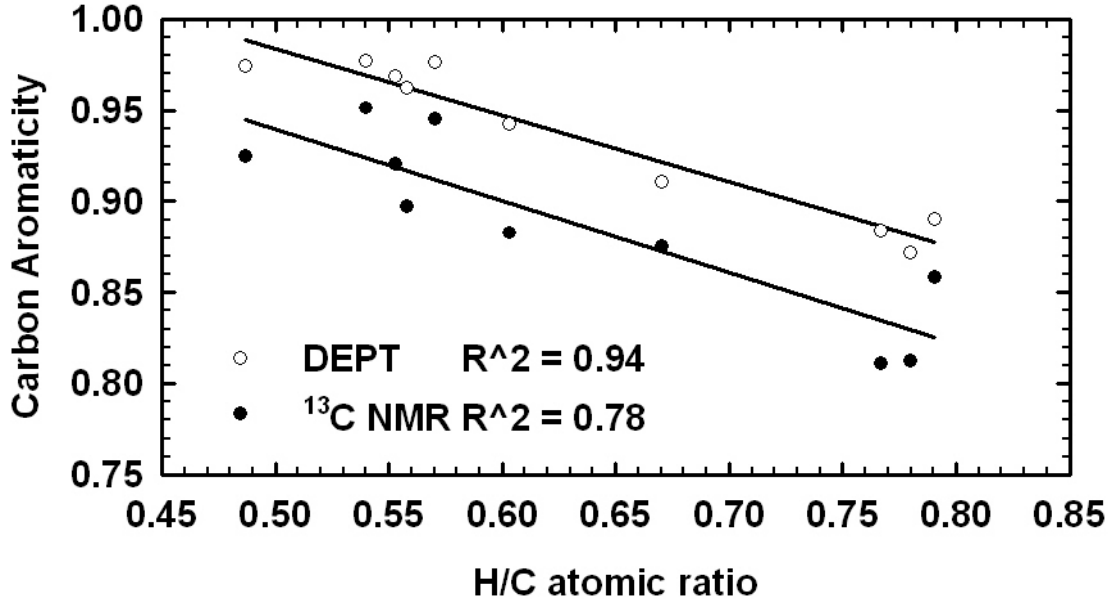

Figure 5.10. Linear relationship between H/C atomic ratio and carbon aromaticity (f_a) both directly determined from conventional ^{13}C NMR spectra (black dots) and indirectly determined from DEPT spectra (white dots).

A good fit was observed between the aromaticities indirectly calculated from the DEPT spectra and the hydrogen to carbon ratio. The H/C ratio from elemental analysis might therefore give a good indication of the aromaticity of pitches. The estimated correlation obtained indirectly from the DEPT spectra has the equation shown below:

$$f_a = 1.17 - 0.367 \cdot H/C \qquad \textbf{(5-6)}$$

where f_a is the aromaticity and H/C is the atomic ratio of hydrogen to carbon obtained from elemental analysis.

The petroleum pitches have lower carbon aromaticities (Figure 5.9) than the coal-tar pitches. This is mainly due to the more alkylated structure but also the more hydroaromatic and naphthenic character. Petroleum pitch 1 (PP1) has a more aromatic character than the other petroleum pitches. Except for CTP5, the coal-tar pitches show quite similar aromaticities, but CTP4 is slightly less aromatic than CTP1, CTP2, CTP3 and CTPN. Coal-tar pitch 5 falls in a region between the other coal-tar pitches and the pitches of petroleum origin.

The aromatic carbon fraction can be sub-divided into four groups. These are protonated carbon (CH_{ar}, Equation 5-4), carbon joined to aliphatic side chains, catacondensed carbon including carbon with aromatic substituents and pericondensed carbon. For reference, the aromatic carbon types are illustrated in Figure 5.11. The relative amount of aromatic carbon within each of these groups can be estimated using the equations given by Dickinson [79] shown below. Notations used for the aromatic

carbon fractions are the same as those used by Díaz and Blanco [67]. The fractions of $C_{ar1,2}$ and $C_{ar1,3}$ were determined from the conventional ^{13}C NMR spectra (Figure 4.4).

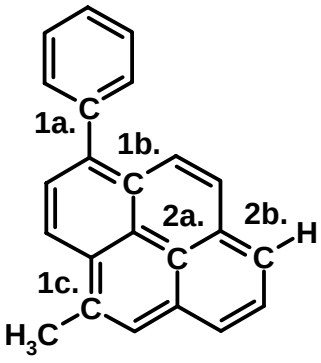

Aromatic carbon with aromatic substituent, C_{ar2}: 1a.

Catacondensed aromatic carbon, C_{ar2}: 1b.

Aromatic carbon joined to aliphatic group, C^s_{ar}: 1c.

Pericondensed aromatic carbon, C_{ar3}: 2a.

Protonated aromatic carbon, CH_{ar}: 2b.

Figure 5.11. Illustration of aromatic carbon fractions.

$$C^s_{ar} = C \cdot C_{al} / n_{sub} \quad \textbf{(5-7)}$$

where C is the weight fraction of carbon determined by elemental analysis and n_{sub} is the average length of the substituents (^1H NMR, Figure 4.2). The aliphatic carbon fraction, C_{al}, is determined indirectly from the DEPT spectra (1-f_a in Figure 5.9).

$$n_{sub} = \frac{H_\alpha + H_\beta + H_\gamma}{H_\alpha} \quad \textbf{(5-8)}$$

$$C_{ar3} = C \cdot C_{ar1,3} - (CH_{ar}) \quad \textbf{(5-9)}$$

$$C_{ar2} = C \cdot C_{ar1,2} - C^s_{ar} \quad \textbf{(5-10)}$$

where C is the weight fraction of carbon determined from elemental analysis.

It must be noted that the relations above are simplified as they do not take the heteroatom content into consideration. The aromatic carbon distribution shown in Figure 5.12 is therefore just a rough estimate. The sum of the four estimated sub-fractions, is even lower than the aromatic carbon fraction determined from the conventional ^{13}C NMR spectra indicating uncertainty in the estimations. However, the sub-fractions is considered to give fairly representative relative information on the distribution of different types of aromatic carbon in the pitches.

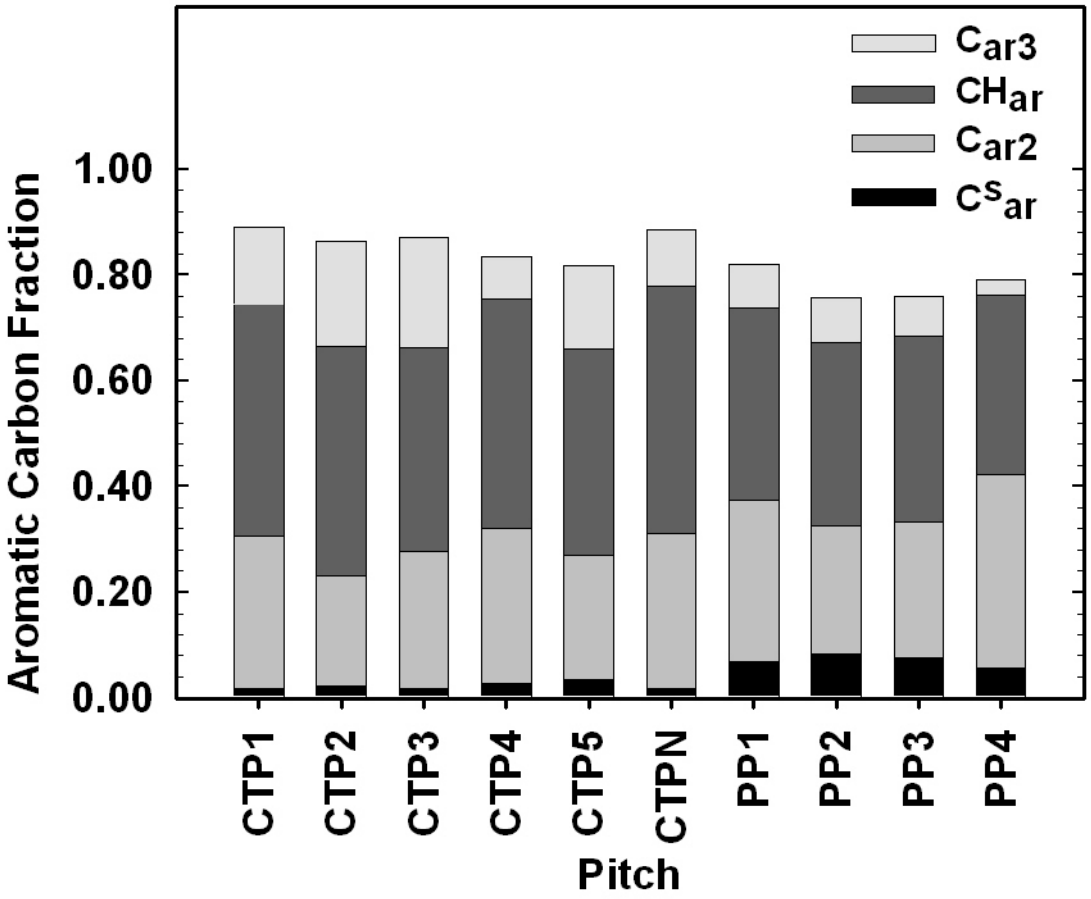

Figure 5.12. Estimated distribution of aromatic carbon fractions. Carbon joined to aliphatic chains (C^s_{ar}), catacondensed carbon and carbon with aromatic substituents (C_{ar2}), protonated carbon (CH_{ar}) and pericondensed carbon (C_{ar3}).

The fraction of substituted aromatic carbon (C^s_{ar}) is as expected higher for the petroleum pitches than for the coal-tar pitches. A high proportion of alkyl substituents would be expected to lead to a higher thermal reactivity as the aromatic carbon to aliphatic carbon bond is relatively weak. Petroleum pitch 4 (PP4) has a slightly lower concentration of alkyl substituents than the other pitches of petroleum origin but the average alkyl side chain length is markedly longer (Figure 5.8). Coal-tar pitch 5 (CTP5) has a higher degree of substitution than the other pitches of coal-tar origin. The sharp signal in the DEPT spectra of CTP5, PP2, PP3 and PP4 at around 30.5 ppm (Figure 4.5 and Appendix Section) is indicative of a high amount of methylene groups in alkyl side chains. All of the coal-tar pitches have a higher proportion of protonated aromatic carbon than the petroleum pitches. Except for CTP4, the coal-tar pitches are richer in pericondensed aromatic carbon (C_{ar3}, Figure 5.12) possibly indicating that the aromatic structures are larger on the average compared to the petroleum pitches.

Aromatic carbon linked to oxygen, nitrogen and sulphur could not be distinguished in the carbon NMR spectra. Oxygen-linked aromatic carbons would probably give rise to signals downfield from the cut-off point (160 ppm) of the defined aromatic region. There were observed no clear signals at higher chemical shifts than around 150 ppm. Pitch constituents containing heteroatoms are generally concentrated in the heavier pitch fractions [18]. The concentration of such compounds might therefore be very low in the CS_2 soluble fraction of the pitches which has been investigated in the

present work. This could be an explanation for the failure in the detection of aromatic carbons connected to heteroatoms. The solubility of the pitches in carbon disulphide has not been tested in the present work. As mentioned earlier, Guillén *et al.* [64] found that the extraction yield of six coal-tar pitches in CS_2 was between 67.1 wt% and 80.4 wt%. The CS_2 insoluble fraction of the pitches contains molecules of high molecular weight which would lead to an increase in the aromaticity. Differences in solubility between pitches mean that the NMR spectra are not directly comparable. However, it is considered that the CS_2 soluble fraction gives fairly representative structural information about the pitches which is valuable for comparative purposes, especially with regards to the periphery of the constituents. Information about the hydroaromatic and naphthenic character and degree and nature of alkyl substituents is particularly relevant in the discussion of the thermal reactivity of the pitches.

5.2 Hydrogen Donor and Acceptor Abilities

5.2.1 Hydrogen Donor Ability

The transfer of hydrogen from CTP1 and CTP2 to anthracene was investigated for soaking times ranging from 10 minutes to 13 hours (Figure 4.7) at 400 ºC. Both pitches show a similar trend but CTP2 exhibits a slightly higher HDa for all the investigated heat treatment times. The relationship between HDa and soaking time is linear within the first hour of heat treatment for both pitches (Figure 4.8). After the first hour, the rate of hydrogen transfer decreases. A decrease in reaction rate can be expected because the supply of donor hydrogen will be consumed by the reaction system and free radicals formed in the later stages of the carbonization process are "stabilized" by re-polymerization. At longer heat treatment times, the recovery rate of anthracene decreases which indicates that anthracene or the hydrogenated reaction products, 9,10-dihydroanthracene (DHA) and 1,2,3,4-tetrahydroanthracene (THA), undergo further reactions to form other products. This would also lead to an observed decreasing kinetic trend. Minor amounts of methylanthracenes found in the chromatograms (Figure 3.5) suggest that alkylation reactions have occurred. Ideally, anthracene should only form DHA and THA in the donor ability test. This is, however, not the case in the hydrogen donor ability test performed at 8 hours soaking time (Figure 4.11) as demonstrated by the relatively low observed recovery rates shown in Table 4.1. The low recovery rates of anthracene at 8 hours soaking probably suggests that this heat treatment is too severe. The less severe heat treatment where the pitch/anthracene mix was heated at 5 ºC/min to 400 ºC with no soaking time (Figure 4.12) is probably more suitable due to the high recovery rates of anthracene which are above 93 % for all of the pitches (Table 4.3). Only minor amounts of THA is formed in addition to the major hydrogenated product DHA. This is an advantage as the formation mechanism of THA is poorly understood. It also seems like the formation of THA is accompanied by a decrease in recovery rate of anthracene which suggests that a complex reaction pathway is involved. The mechanism of DHA formation in the presence of a hydrogen donor is better understood. Formation of DHA occurs via hydrogen transfer at the central carbon atoms in anthracene (9- and 10- positions). Calculations based on orbital theory of the different carbon positions in anthracene show that the formation of DHA should be the dominant reaction [80].

The hydrogen donor ability test performed at the less severe heat treatment was more successful in differentiating the pitches but it does only give a measure of the hydrogen donor ability of the pitches during the initial stages of carbonization. However, the beginning steps of aromatic growth are considered to be particularly important for the pyrolysis behavior of pitches. The hydrogen donor ability measured after heat treatment to 400 ºC with no soaking has therefore been chosen as the parameter reflecting the self-stabilization of pitches during carbonization.

The hydrogen donor ability does clearly not only reflect the concentration of donatable hydrogen estimated from the ^{1}H and ^{13}C NMR spectra of the pitches. A likely explanation for this apparent inconsistency is that potential donatable hydrogen in particularly reactive pitches will be preferentially consumed by free radicals and heteroatom acceptor sites instead of being transferred to anthracene. Good examples are PP4 and CTP5 which both have high concentration of donatable hydrogen but at

the same are expected to be reactive due to a high amount of alkyl substituents, a long average chain length and a high oxygen content. Both of these pitches therefore exhibit a relatively low HDa. The hydrogen donor ability does not only reflect the supply of donatable hydrogen but also to a certain extent the thermal reactivity of pitches.

5.2.2 Hydrogen Acceptor Ability

The hydrogen acceptor ability test performed at 400 ºC with 8 hours soaking time Figure 4.16) was more successful than the corresponding donor ability test in differentiating the pitches. The hydrogen transfer from the hydrogen donor compound, 1,2,3,4-tetrahydronaphthalene (tetralin), to CTP1 and CTP2 was investigated for soaking times ranging from 10 minutes to 12 hours (Figure 4.13). The hydrogen acceptor ability of CTP2 is lower for all investigated heat treatment times compared to CTP1. The hydrogen transfer from tetralin to the two pitches occurs continuously over the entire soaking time range but with decreasing kinetics. A decrease in the rate of hydrogen transfer is expected as free radical species will eventually re-polymerize and the number of acceptor sites for hydrogen transfer from tetralin will be reduced. Compared to the donor ability reaction, the acceptor ability reaction shows a less pronounced decrease in reaction rate. This is probably due to the high thermal stability of tetralin and the dehydrogenated reaction product, naphthalene. The decreasing kinetics of naphthalene formation from dehydrogenation of tetralin in the presence of pitch at 400 ºC for longer soaking times is therefore considered to be representative of an actual decrease in activity of the pyrolysis system. A standard heat treatment of 8 hours was chosen for the acceptor ability to represent not only the beginning stages of carbonization but also the development in the carbonization system with an increase in the severity of thermal treatment (longer soaking time). The results are shown in Figure 4.16. However, minor amounts of 1-methylindan (~ 0.8 wt%) and butylbenzene (~ 0.7 wt%) were found in the residue after the reaction between the pitches and tetralin at 400 ºC and 8 hours soaking time. Methylindan is probably formed from thermal rearrangement of tetralin while butylbenzene is formed from ring opening of tetralin [81]. The amounts of these compounds have not been taken into consideration when calculating the hydrogen acceptor ability from the ratio of the peak areas of naphthalene and tetralin from the chromatograms. This means that the hydrogen acceptor ability has been slightly over-estimated as a minor amount of the tetralin added to the reaction tube initially has undergone thermal rearrangement/ring opening instead of dehydrogenating to give naphthalene. The over-estimation would, however, be within the experimental error and would also be similar for all the pitches. It is therefore considered that the results obtained for the hydrogen acceptor abilities at 400 ºC and 8 hours heat treatment time are suitable for comparison of the pitches.

The hydrogen acceptor ability test was also performed under less severe heat treatment conditions with a heating rate of 5 ºC/min to 400 ºC with no soaking time (Figure 4.17). During the initial stages of carbonization, PP4 but also CTP5 are distinguished due to their significantly higher ability to abstract hydrogen from tetralin when compared to the other pitches within the same group (*i.e.* petroleum or coal-tar pitch). This strongly suggests that PP4 and CTP5 are highly reactive and form

a large number of thermally induced free radicals which are stabilized by hydrogen transfer from tetralin during the initial stages of carbonization.

Only minor amounts of naphthalene was formed after heat treatment to 400 ºC with no soaking time. The tetralin peak was huge compared to the naphthalene peak in the chromatograms. The hydrogen acceptor ability is calculated from the ratio of these two peaks. A quantification based on such a huge peak difference is not desirable. The reproducibility of the acceptor ability at the less severe heat treatment was relatively poor. The ratio between the hydrogen and acceptor ability which will be discussed below is therefore based on the results obtained after heat treatment of the pitch/tetralin mix for 8 hours.

5.2.3 Hydrogen Donor and Acceptor Ability and Thermal Reactivity

A correlation between the hydrogen donor and acceptor ability might be expected if both of these parameters individually reflect the thermal reactivity of the pitches. This was obviously not the case as demonstrated by the plot of HDa (400 ºC, no soaking time) versus HAa (400 ºC, 8 hours soaking time) shown in Figure 5.13. The complete absence of correlation between the hydrogen donor ability and the acceptor ability strongly suggests that the two parameters mainly represent two separate properties where both are linked to the thermal reactivity of the pitch. The hydrogen donor ability reflects the ability of the pitch to modify the pyrolysis system while the hydrogen acceptor ability on the other hand reflects the transformation of the pitch itself. It is important to consider both the hydrogen donor ability and acceptor ability at the same time.

The ratio between the hydrogen donor and acceptor ability, HDa/HAa, has been proposed as a parameter reflecting the extent of the modifying ability of a pitch in the co-carbonization with coal by Iyama and co-workers [82, 83]. They found a good correlation between this parameter and the optical texture of cokes from the co-carbonization of pitch and coal. A higher ratio of HDa to HAa resulted in improved fluidity conditions of the pyrolysis system and larger optical texture of the coke.

In the present work, the ratio between the hydrogen donor and acceptor ability will be used as a measure of the thermal reactivity of pitches. The HDa/HAa ratio is shown in Figure 5.14. Pitches with a high HDa/HAa ratio are expected to have a high ability to modify the carbonization system by hydrogen transfer relative to the amount of thermally induced radicals formed. Extensive polymerization of the pitch during the early stages of the carbonization process is thus prevented and the growth and coalescence of mesophase can take place under low viscosity/high fluidity conditions resulting in an anisotropic (large optical domains) coke structure. Pitches with a relatively low HDa/HAa ratio on the other hand, are expected to form a more isotropic (small optical domains) coke. It must be stressed that the HDa/HAa ratio should not be viewed as an equilibrium constant as the pyrolyzing pitch system is irreversibly dynamic.

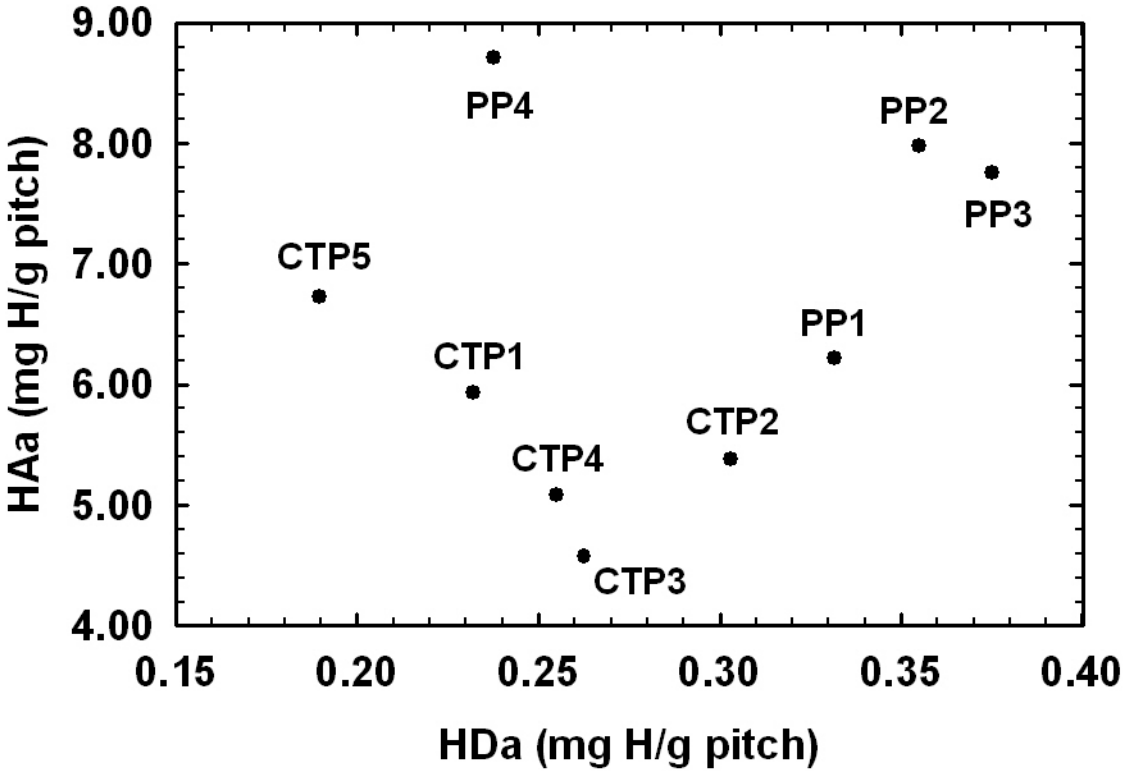

Figure 5.13. Hydrogen donor ability (400 ºC, no soaking time) versus hydrogen acceptor ability (400 ºC, 8 hours soaking time).

The HDa and HAa parameters (mg H/g pitch) of two pitches which differ in QI content would not be directly comparable as the particulate matter is not expected to take part in the hydrogen transfer reactions. Both the HDa and the HAa would be underestimated for a pitch containing particulate matter compared to a pitch which does not contain any QI. An advantage of the HDa/HAa ratio is that it is independent on the sample weight and would thus be comparable for two pitches that differ in the content of material that does not take part in the hydrogen transfer reactions.

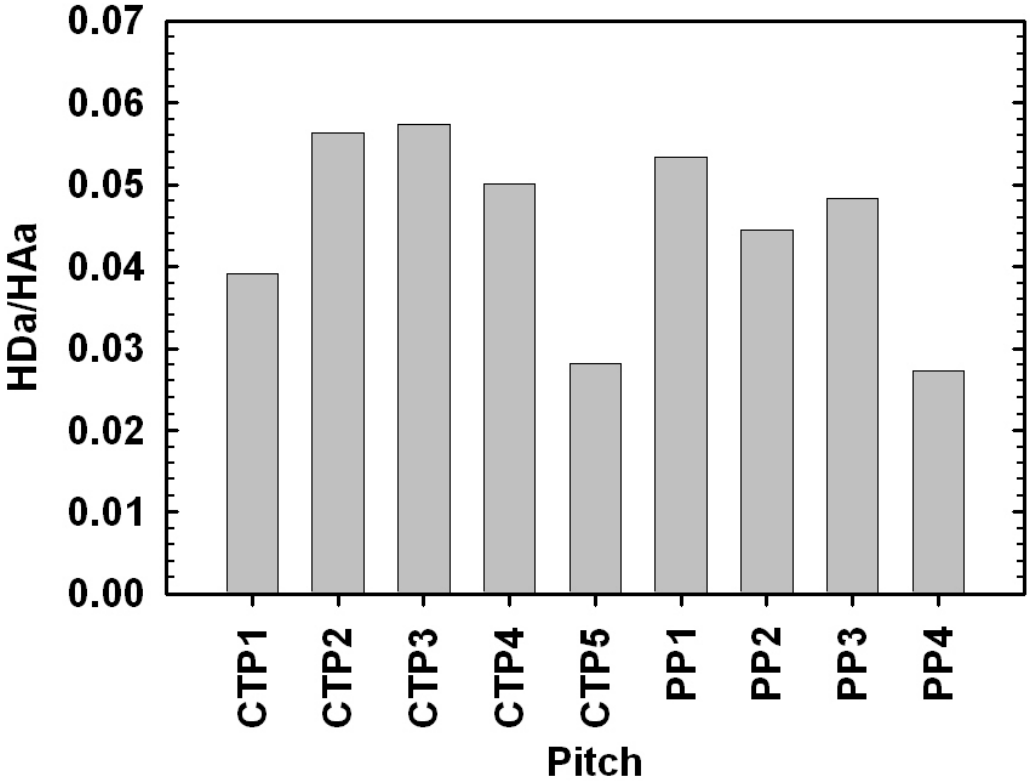

Figure 5.14. Ratio between hydrogen donor ability (400 ºC, no soaking time) and hydrogen acceptor ability (400 ºC, 8 hours soaking time), HDa/HAa.

The low HDa/HAa ratios of CTP5 and PP4 suggest that these pitches are particularly reactive. The coal-tar pitches, despite their higher aromaticity, are not considered to be generally less reactive than the petroleum pitches based on the HDa/HAa ratio. Petroleum pitch 1 (PP1) is expected to be the most stable of the petroleum pitches. Although the difference is quite small, PP2 is expected to more reactive than PP3.

The acceptor ability at 400 ºC and 8 hours soaking time was not determined for CTPN. However, from the acceptor ability test performed under the less severe heat treatment conditions, CTPN is expected to fall in the same range as CTP2 and CTP3 an exhibit a low HAa. The donor ability of CTPN is similar to CTP2 and CTP3. It would thus be expected that CTPN would be in the same thermal stability range as CTP2 and CTP3 by exhibiting a high HDa/HAa ratio. With the exception of PP2 and PP3, a linear correlation between the acceptor abilities measured at the two different heat treatments was found.

5.3 Thermogravimetric Analysis

The processes occurring during thermal treatment of pitches are reflected in the release of volatiles. A relation between the amounts and timing of volatiles release and the thermal reactivity of pitches would therefore be expected.

It is particularly difficult to discuss the differences in thermal behavior among the coal-tar pitches on the sole basis of the weight loss curves (Figure 4.18) due to the varying QI contents. The QI material is mostly expected to be non-volatile matter and a high QI content would lead to a high coke yield. It is, however, interesting to note that CTP5 has a higher coke yield at 600 ºC than the other coal-tar pitches with the exception of CTP3 (25.0 wt% QI) despite the low QI content of only 4.7 wt%. The differences between the volatiles release behavior of the pitches are clearer from the first derivative of the weight loss curves. It is clear that the volatiles release commences at an earlier stage for CTP5 than the other pitches of coal-tar origin. This is probably due to the distillation of thermally stable low molecular weight species but may also partly be explained by the release of fragments from the cracking of alkyl side chains. The relatively high release rate of volatiles up to around 400 ºC is probably connected with the high thermal reactivity of CTP5. A similar weight loss behavior is displayed by PP4 (Figure 4.19) which is also considered to be particularly reactive. The weight loss commences at a much earlier stage than the other petroleum pitches, especially PP1. The DTG curve of PP4 shows a local minimum, corresponding to a maximum in volatiles release rate, at around 270 ºC. This might be connected with thermal rupture of long reactive alkyl side chains. The temperature seems quite low for these kinds of reactions to occur though. It would have been of great interest to analyze the volatiles as their nature may reveal important information about the thermal processes occurring in the pitch. A similar local minimum is also observed for PP2 and PP3 but at a higher temperature of around 330 ºC. It is likely that this minimum is connected to the cleavage of longer side chains. The weight loss of PP1 commences at a later stage than the other pitches of petroleum origin and the first and main maximum lies at around 360 ºC and is probably related to thermal rupture of methyl groups which are abundant in this pitch. Aromatic growth is thus delayed to a higher temperature and consequently take place under higher fluidity conditions. A more ordered coke structure is therefore expected to be obtained from PP1. The other petroleum pitches have a second maximum between 430 and 440 ºC. At this stage, low molecular weight species that have been formed from radical fragments stabilized by hydrogen transfer are distilled. After this minimum, the volatiles release rate decreases quite rapidly to around 550 ºC where the weight loss ends. Petroleum pitch 1 does not have a clear second minimum in the DTG curve but the rate of volatiles release is relatively high until it starts to decrease around 480 ºC. The release of volatiles continues until around 570 ºC. The high thermal stability of PP1 would mean that the temperature range where the fluidity of the pyrolysis system remains high extends to a higher temperature compared to the other petroleum pitches. As the release of volatiles takes place at a relatively high rate until a green coke is formed, PP1 has a higher total weight loss and the coke yield of this pitch is consequently the lowest. The high reactivity of PP4 would, on the other hand, lead to extensive cross-linking at an earlier stage, an increase in viscosity and the formation of a more isotropic (small optical domains) green coke at a lower temperature. The

temperature interval where the release of volatiles takes place at a relatively high rate would thus be reduced which would result in a higher coke yield.

The coke yields of pitches from the thermogravimetric analysis are lower than the coke yields given in Table 3.1. This is due to the different conditions of carbonization. In the thermogravimetric analysis, the carbonization is performed under a flow of inert gas. The volatiles are thus readily carried away by the gas flow. In the standardized (ISO 6998) method, carbonization is performed in ceramic crucibles fitted with a lid. The volatiles are thus not free to escape and may condense as coke leading to a higher coke yield.

The weight loss behavior of the pitches can be compared by studying the percentage of the total volatile matter (1000 ºC) released within a certain temperature range. A correlation has been found between the HDa/HAa ratio and the percentage of volatile matter released between 300 and 500 ºC (VM300-500). This correlation is displayed in Figure 5.15.

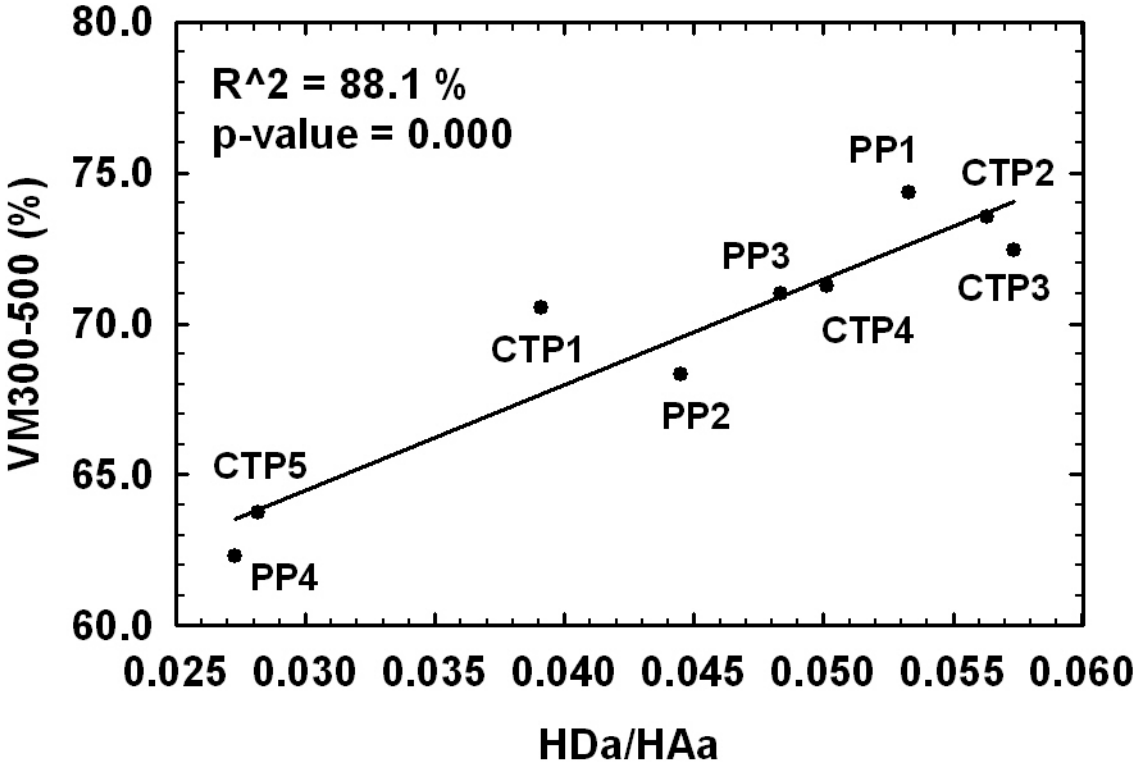

Figure 5.15. Correlation between HDa/HAa ratio and the percentage of volatile matter released between 300 and 500 ºC (VM300-500).

Thermally reactive pitches exhibiting a low HDa/HAa ratio will have a high activity at low temperatures which is reflected in a large amount of volatiles released during the early stages of carbonization. Low boiling point pitch molecules are distilled and fragmentation species resulting from for instance thermal rupture of weak bonds to long alkyl side chains or bridges between aromatic structures lead to a relatively high amount of volatiles being released at low temperatures. If on the other hand the pitch has a high thermal stability, fragmentation species will be stabilized by hydrogen transfer and retained in the pyrolysis system. The resulting thermally stable molecules

of relatively low molecular weight may then act as solvating vehicles maintaining a low viscosity in the system and may also be important as hydrogen shuttling agents. When the system has reached a critical stage for mesophase growth and coalescence, these smaller thermally stable molecules (non-mesogens) are eventually distilled resulting in a high amount of volatile matter released at relatively high temperatures and an ordered anisotropic coke structure will be formed. For the more reactive pitches, the high loss of volatiles during the early stages of carbonization will result in a more rapid increase in viscosity and the resulting coke will be less ordered with smaller optical domains.

Thermally reactive pitches like PP4 and CTP5 have lost more than 66 wt% of their total amount of volatiles released at a rather modest temperature of 300 ºC. In comparison, more stable pitches like PP1 and CTP2 have lost less than 27 wt% at the same stage. Results from the thermogravimetric analysis indicate that important reactions which in the later stages of carbonization govern the initiation, growth and coalescence of mesophase occur to a significant extent already at modest temperatures of less than 300 ºC. It is unlikely that the entire weight loss below 300 ºC is exclusively due to distillation of low molecular weight species initially present in the pitch.

5.4 Optical Texture of Green Pitch Cokes

The standard deviation of the mosaic index is large for all of the pitch cokes ranging from around 15 % for CTP3 and up to 64 % for PP2 (Figure 4.27). This is not due to a an unacceptably high experimental uncertainty but indicates that there is a large variation in optical texture among the pitch coke grains. Due to the number of grains analyzed (144), a statistically significant difference between the average mosaic index of most of the pitch cokes was observed (Table 4.5). A relatively high standard deviation of the mosaic index would therefore indicate that the pitch coke structure is inhomogeneous and areas of varying optical texture exist within one pitch coke. The petroleum pitch cokes generally have a higher relative standard deviation of the mosaic index compared to the coal-tar pitches. This is seemingly inconsistent as the coal-tar pitch cokes have a heterogeneous structure where larger anisotropic domains co-exist with clusters of QI particles and very fine mosaic areas. The mosaic index of each grain is calculated as the average of the mosaic index of 24 sub-frames. The variation in optical texture might thus be greater within each grain for the coal-tar pitch cokes, but the average mosaic index of each grain shows a lesser extent of variation than for the petroleum pitch cokes.

The standard deviation of the fiber index is generally smaller than the standard deviation of the mosaic index and ranges from about 16 % for PP1 and to about 37 % for CTP4. The standard deviation of the fiber index is slightly smaller for the petroleum pitch cokes than the coal-tar pitch cokes. This indicates a greater similarity of parallel alignment of optical domains between grains for the petroleum pitches. The orientation of the optical domains of the coal-tar pitch cokes are more random due to the influence of the QI particles which tend to hinder the growth, coalescence and alignment of mesophase. Both the mosaic index and the fiber index reflect the anisotropy of the pitch coke. The correlation between these two parameters is displayed in Figure 5.16.

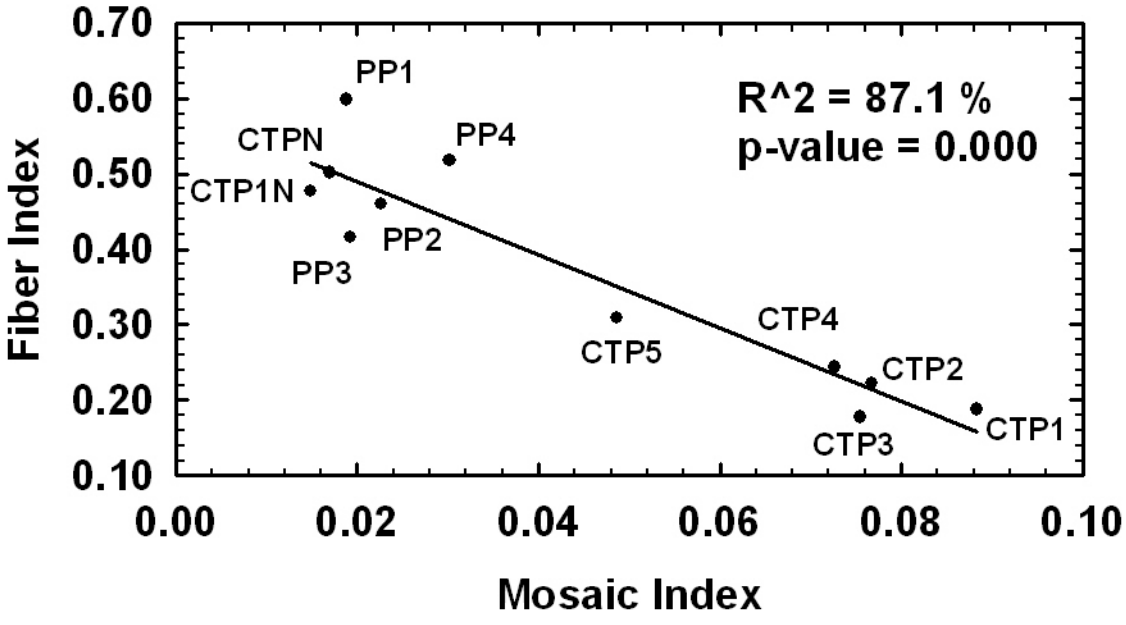

Figure 5.16. Correlation between mosaic index and fiber index of pitch cokes.

The petroleum pitch cokes and the QI free coal-tar pitches, CTP1N and CTPN, fall in the same region with a relatively low mosaic index and high fiber index. These pitch cokes thus have relatively large well-aligned optical domains. The other QI containing coal-tar pitches fall in the same region exhibiting a relatively high mosaic index and low fiber index which indicates smaller average size and a more random orientation of the optical domains. The pitch coke obtained from CTP5, which has a relatively low QI content of 4.7 wt%, has a coke structure between the other two groups of pitch cokes.

It might seem inconsistent that PP4, which is expected to have a high thermal reactivity, exhibits a relatively high fiber index. A likely explanation for this inconsistency is that the alignment of optical domains is also dependent on the evolution of volatiles during the later stages of carbonization. The mesophase constituents of PP4 may still have alkyl side chains left which are cleaved at higher temperatures. The flow of volatiles would be expected to align the optical domains parallel to the large pores formed as the viscosity of the pyrolysis system increases abruptly and a coke is irreversibly formed. A high fiber index is thus not necessarily connected with a low thermal reactivity of the pitch.

Due to the major influence of particulate matter (QI particles) on the growth and coalescence of the mesophase, a straight correlation between the thermal reactivity estimated by the HDa/HAa parameter and the size of optical texture (mosaic index) of cokes obtained from QI containing pitches would not be expected. However, for the petroleum pitches a correlation was observed (Figure 5.17).

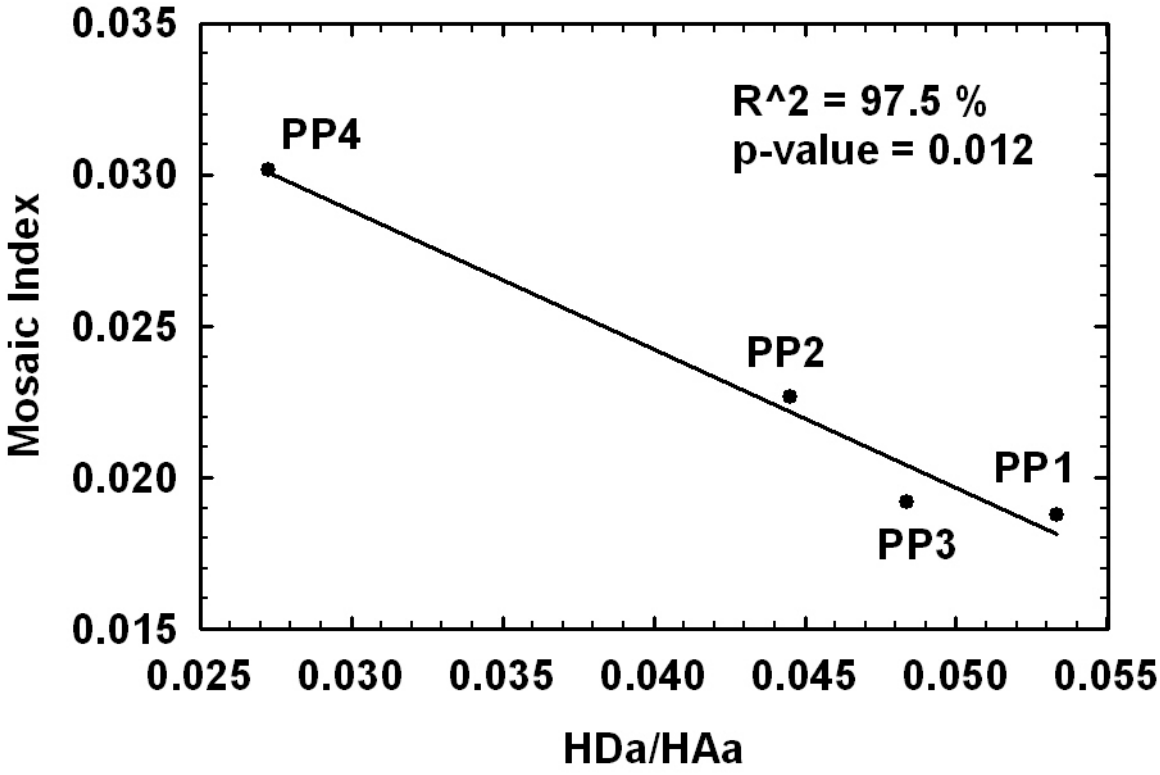

Figure 5.17. Correlation between HDa/HAa ratio and mosaic index for petroleum pitch cokes.

From the considerations given in Chapter 5.2.3, CTPN would be expected to have a HDa/HAa ratio which is slightly higher than PP1. The mosaic index of the CTPN coke is also slightly lower than the PP1 coke and CTPN might thus fit quite well in the linear correlation shown above (Figure 5.17).

The coke obtained from the pitch prepared by QI removal from CTP1 which is labeled CTP1N exhibits the lowest mosaic index of all the pitch cokes. This might be unexpected since CTP1 was considered to have a quite high thermal reactivity from its relatively low HDa/HAa ratio. From the elemental analysis (Table 3.2), the oxygen content of CTP1 is 0.63 wt%. It has been reduced to 0.22 wt% for CTP1N after QI removal. This indicates that the oxygen is concentrated in the QI fraction and CTP1N might thus have a reduced thermal reactivity compared to CTP1. It is thus likely that the QI fraction not only acts physically by obstructing the growth and coalescence of mesophase but may also be chemically active. Solid QI particles with oxygenated functional groups or heteroaromatic structures containing oxygen which due to their large size are insoluble in quinoline may act as acceptor sites for hydrogen thus increasing the thermal reactivity. The oxygenated functional groups in the QI material may play an important role in the adherence to the growing mesophase.

Granda *et al.* [84] have also found that the oxygen is concentrated in the QI fraction separated by filtration of a coal-tar pitch. Interestingly, they found that an increased content of QI particles in the coal-tar pitch matrix of C/C composites resulted in a higher air reactivity. The QI particles themselves were found to be more susceptible to oxidation by air than the anisotropic pitch coke matrix. An increased QI content was also found to reduce the size of the optical domains (fine mosaic) which further increased the air reactivity.

The effect of the QI on the development of optical texture is clearly demonstrated by the difference in structure of the pitch cokes obtained from CTP1 and CTP1N. Upon carbonization, the QI free CTP1N gives a coke of large optical texture. The QI containing CTP1 on the other hand, gives a mixed structure of predominantly fine mosaic coke with inclusions of areas of larger and more developed optical domains. The SEM pictures (Figure 4.26) of the CTP1 coke clearly reveals how the QI particles encircle small optical domains. Tiny areas of pitch coke is observed between the QI particles. The black and white image taken at a high magnification (Figure 4.25, bottom picture) shows how the QI particles tend to form clusters between the optical domains.

Relatively large cracks were observed in the larger optical domains of the pitch cokes. The nature and cause of these cracks have not been the subject of a detailed study. It is, however, believed that they are caused by shrinkage due to the release of volatiles after a green coke has been irreversibly formed. The cracks are particularly pronounced in the cokes obtained from CTP1N and CTPN (Figure 4.20 and Figure 4.21, bottom picture) but are also observed in the larger optical domains of for instance the CTP5 coke (Figure 4.23). Interestingly, the petroleum pitch cokes are virtually crack-free. An explanation might be that the petroleum pitch coke structure is less dense than the coal-tar pitch coke structure thus providing pathways for the release of volatiles. Alkyl side chains may still be present at the green coke stage of the petroleum pitches resulting in a less dense structure.

5.5 X-ray Diffraction

At the green coke stage, the coherent domains are small, less than 1.0 nm in diameter, consisting of a stack of two or three graphene (aromatic sheets) layers [85]. The long-range order of these coherent domains is established at the green coke stage and fixes irreversibly structural features like carbon porosity, density and graphitizability. The processes taking place in the fluid stage of carbonization which are governed by the thermal reactivity of the pitch are thus expected to have a critical influence on the properties of the final carbon artifact.

In the present work, the green cokes obtained after carbonization of pitches to 550 ºC were further heat treated (calcined) to 1150 ºC. The average crystallite size (L_c) of the calcined pitch cokes were measured by X-ray diffraction. It must be pointed out that the term "crystallite" is misleading. The so-called crystallites represent domains where the graphene sheets are stacked parallel to each other. These domains are connected by distorted or turbostratic carbon and are as such not separate crystallites. Due to its common use, the term "average crystallite size", is, however, used in the present work.

The average coherent stacks of the calcined pitch cokes consist of between 7 and 8 graphene layers (L_c divided by d_{002}). With the exception of the PP1 coke, the petroleum pitch cokes have smaller average crystallite sizes than the coal-tar pitches. This might seem inconsistent with the results from the optical texture analysis. It is, however, important to distinguish between optical anisotropy and anisotropy at a level below the resolution of light. The less developed microstructure of the petroleum pitch cokes compared to the coal-tar pitch cokes is thus not necessarily inconsistent with the higher degree of optical anisotropy of these cokes. Although there is not a good linear relationship between the HDa/HAa ratio and L_c-values of the petroleum pitch cokes, the trend observed at an optical level of the green cokes is reflected in the microstructure. The coke obtained from the least reactive of the four pitches, PP1, has a significantly higher crystallite size than the other petroleum pitch cokes. Cokes obtained from PP2 and PP3 showed very similar optical textures and also have almost identical average crystallite sizes. The most reactive petroleum pitch, PP4, which developed a significantly more fine mosaic green coke than the other pitches of petroleum origin, has the significantly lowest L_c value of all the pitch cokes. The QI free pitches, CTPN and CTP1N, which developed green cokes of the highest optical domain size, also have larger average crystallite sizes than the petroleum pitch cokes.

The other coal-tar pitch cokes, with the exception of the coke obtained from CTP3, have similar average crystallite sizes and the differences are not statistically significant. It is likely that the structure of the QI material will differ from the rest of the pitch coke and thus influence the average crystallite size. The nature of the QI material of CTP3 (25.0 wt%) might differ from the other coal-tar pitches. This pitch has probably been subjected to a severe heat treatment as the high softening point (187 ºC) suggests. The QI material in CTP3 might thus be more ordered (large amount of secondary QI) compared to the other coal-tar pitches and contribute to the significantly higher average crystallite size observed for the coke obtained from this pitch.

The interlayer spacing (Figure 4.33), d_{002}, does not seem to correlate with pitch properties or pitch coke structures investigated in the present work. The reproducibly was poorer than for the average crystallite size and the interlayer spacing is probably not a good parameter for observing structural differences between calcined cokes obtained from different pitches.

5.6 Comparison of Pitch and Pitch Coke Properties

The properties of the pitches and the pitch cokes have been summarized in Table 5.1 displayed on the next page. References to these properties are given below the table.

In general, the estimated concentration of donatable hydrogen is higher for the petroleum pitches than the pitches of coal-tar origin. This is due to the generally more hydroaromatic structure of the petroleum pitches. Coal-tar pitch 5 (CTP5) is distinguished from the other coal-tar pitches due to its higher concentration of donatable hydrogen which even exceeds that of PP1. This pitch also has a higher fraction of aromatic carbon with aliphatic substituents (C^{s}_{ar}). A relatively high fraction of aliphatic substituents is generally connected with a high concentration of donatable hydrogen in the pitches.

The average length of alkyl side chains is similar for the pitches of coal-tar origin with the exception of CTP5. The higher concentration of donatable hydrogen, the higher fraction of aliphatic substituents and the longer length of alkyl side chains of CTP5 are reflected in a lower aromatic hydrogen fraction, lower carbon aromaticity and higher H/C atomic ratio compared to the other pitches of coal-tar origin. Coal-tar pitch 5 (CTP5) is also distinguished from the other coal-tar pitches due to a higher oxygen content. Oxygen acceptor sites are believed to deplete the supply of donatable hydrogen and leave free radicals free to recombine [77]. Despite the relatively high concentration of donatable hydrogen, CTP5 is considered to have a higher thermal reactivity than the other coal-tar pitches due to a more alkylated structure, longer average alkyl side chain length and a higher oxygen content. The high thermal reactivity of CTP5 is reflected in a low HDa/HAa ratio, *e.g.* this pitch has a limited ability to modify the carbonization system by hydrogen transfer relative to the amount of free radicals formed. Coal-tar pitch 5 (CTP5) is also distinguished from the other pitches of coal-tar origin due to its low relative amount of volatiles released between 300 and 500 ºC (VM300-500). This is connected to a high thermal reactivity, reflected in a high volatiles release rate during the early stages of carbonization. The coke yield of CTP5 is, however, only slightly lower than the other coal-tar pitches with the exception of CTP3. The high coking value of CTP3 is linked to a high QI content and high softening point which may be a result of severe heat treatment of this pitch.

A pitch which exhibits a high thermal reactivity is expected to form a coke of small optical domains which is reflected in a high mosaic index. However, the coke obtained from carbonization of CTP5 has a lower mosaic index than the other coal-tar pitches with the exception of CTPN. This is probably due to the relatively low QI content of CTP5. Even though the QI material has a profound influence on the optical texture, it is not possible to relate the QI content directly to the optical texture. However, if CTP3 (extreme case) is not considered, a fairly good linear relationship ($R^2 = 0.91$) between the mosaic index and the QI content of the coal-tar pitches is found. Coal-tar pitch N (CTPN) which is considered to have a low thermal reactivity develops a pitch coke of large (low mosaic index) and aligned (high fiber index) optical domains in a similar manner to PP1 due to its low QI content.

Table 5.1. Selected pitch and pitch coke properties. For overview, the properties have been defined as either low, medium or high. Low values: *Italic font*, medium values: normal font and high values: **Bold font**. Properties which are distinctly different within the pitch group (*e.g.* coal-tar or petroleum pitch) are boxed.

Pitch	Donatable hydrogen (wt%) (1)	C^s_{ar} (2)	Average alkyl side chain length, n (3)	Aromatic hydrogen fraction, H_{ar} (4)	Carbon aromaticity, f_a (5)	H/C atomic ratio (6)	Oxygen content (wt%) (6)	HDa/HAa ratio (7)	Softening Point (°C) (8)	β-fraction (wt%) (TI – QI) (8)	Quinoline Insolubles (QI) (wt%) (8)	VM300-500 (9)	Coking Value (wt%) (8)	Mosaic Index (10)	Fiber Index (11)	Average crystallite size, L_c (Å) (12)
CTP1	*0.09*	*0.018*	1.4	**0.86**	**0.98**	*0.54*	0.63	0.039	*110.7*	19.7	**12.9**	70.5	61.0	**0.088**	*0.19*	25.4
CTP2	*0.13*	0.024	1.4	**0.83**	**0.97**	*0.55*	*0.25*	**0.056**	119.7	20.5	**9.6**	**73.5**	60.1	**0.077**	*0.22*	25.4
CTP3	*0.10*	*0.018*	1.5	**0.83**	**0.97**	*0.49*	*0.44*	**0.057**	**187.2**	**28.0**	**25.0**	**72.4**	**78.1**	**0.075**	*0.18*	**26.9**
CTP4	0.16	0.029	1.4	**0.83**	**0.96**	*0.56*	0.86	0.050	118.4	**26.5**	6.6	71.2	59.7	**0.073**	*0.24*	25.7
CTP5	0.24	0.036	**1.7**	0.70	0.94	0.60	**1.24**	*0.028*	116.5	**27.9**	4.7	*63.7*	60.4	0.049	0.31	25.8
CTPN	*0.09*	*0.018*	1.5	**0.87**	**0.98**	*0.57*	*0.23*	ND	120.0	22.0	*0.6*	**78.9**	60.4	*0.017*	**0.50**	**27.0**
PP1	0.19	**0.069**	*1.2*	0.57	0.91	0.67	*0.00**	**0.053**	123.1	*7.3*	*0.1*	**74.3**	*54.4*	*0.019*	**0.60**	25.8
PP2	**0.37**	**0.083**	1.5	*0.47*	*0.87*	**0.78**	*0.00**	0.044	*112.3*	*13.4*	*0.3*	68.3	*48.1*	*0.023*	0.46	*24.3*
PP3	**0.31**	**0.076**	1.5	*0.49*	*0.88*	**0.77**	*0.00**	0.048	120.3	*11.8*	*0.2*	71.0	*50.4*	*0.019*	0.42	*24.3*
PP4	**0.50**	**0.057**	**2.2**	*0.46*	*0.89*	**0.79**	**1.67**	*0.027*	*109.2*	*10.2*	*0.0*	*62.3*	*46.9*	0.030	**0.52**	*23.9*

1) Figure 5.7, 2) Figure 5.12, 3) Figure 5.8, 4) Figure 4.2, 5) Figure 5.9 (DEPT), 6) Table 3.2, 7) Figure 5.14, 8) Table 3.1, 9) Figure 5.15, 10) Figure 4.27, 11) Figure 4.28 and 12) Figure 4.32. * Sum of C, H, N and S from the elemental analysis (Table **3**.**2**) exceeded 100 wt%.

Petroleum pitch 4 (PP4) is distinguished due to its high concentration of donatable hydrogen. This pitch also has a lower fraction of aliphatic substituents than the other pitches of petroleum origin. Even though the number of substituents is lower for PP4, the average alkyl side chain length is markedly higher than all the other pitches possibly suggesting a higher thermal reactivity. In general, it seems like a high concentration of donatable hydrogen is connected to a more alkylated structure. The concentration of donatable hydrogen as estimated from the NMR spectra does therefore not seem to be a good measure of the thermal stability of pitches on its own. The oxygen content of PP4 is particularly high and this pitch is expected to have a relatively high thermal reactivity. This is reflected in a low HDa/HAa ratio. The low relative amount of volatiles released between 300 and 500 ºC (VM300-500) also suggests that PP4 has a high thermal reactivity during the initial stages of carbonization. The amount of particulate matter (primary QI) is very low or negligible for all the petroleum pitches and the optical texture of the petroleum pitch cokes should thus be mainly dependent on their thermal reactivity. A correlation between the size of optical texture and the HDa/HAa ratio is therefore expected and was found for the petroleum pitches. Petroleum pitch 1 (PP1) is considered to be the least reactive (high HDa/HAa ratio) of the petroleum pitches. It has a considerably lower alkyl side chain length than the other pitches. Methyl substituents may be thermally more stable than ethyl groups or longer substituents. The more aromatic character of PP1 is reflected in a lower H/C atomic ratio, higher fraction of aromatic hydrogen and a higher carbon aromaticity compared to the other petroleum pitches. Petroleum pitch 2 (PP2) and PP3 have similar structural features and also exhibit a similar thermal behavior. However, PP2 is considered to be slightly more reactive than PP3 due to a higher fraction of aliphatic substituents and a less aromatic character. Hence, PP2 develops a pitch coke structure of slightly smaller optical domains (higher mosaic index) than PP3.

The coal-tar pitches have markedly higher β-fractions (TI-QI) than the pitches of petroleum origin. This might indicate a higher proportion of high molecular weight species in the coal-tar pitches. However, due to the more alkylated structure of the petroleum pitches they may be more soluble in toluene. The coal-tar pitches also contain a higher amount of heteroatomic constituents which may be less soluble in toluene. The β-fraction does not seem to give information on the thermal reactivity of pitches and does not seem to be related to the structure of the coke obtained from the pitches.

A high mosaic index is generally connected to a low fiber index. However, the pitch coke obtained from PP4 has a relatively high fiber index and high mosaic index compared to the other petroleum pitches. This apparent inconsistency may be explained by the cleavage alkyl side chains in the late stages of carbonization resulting in the release of gases which align the optical domains.

The average crystallite size (L_c) of the calcined pitch cokes is fairly similar for all the pitches but statistically significant differences were observed. The nature of the QI material probably has an influence on the L_c-values of the cokes obtained from the coal-tar pitches. There is a tendency for the petroleum pitches that a high average crystallite size is connected to a more well-developed (lower mosaic index) green coke structure. Petroleum pitch 1 (PP1), which was considered to be the least

thermally reactive, has a higher average crystallite size compared to the other pitches of petroleum origin.

CONCLUDING REMARKS

The hydrogen donor (HDa) and acceptor ability (HAa) tests were successful in differentiating the pitches. The ratio between these two parameters, HDa/HAa, was chosen as a parameter reflecting the thermal reactivity of pitches. A high ratio is connected to a low thermal reactivity whereas a low ratio is connected to a high thermal reactivity. For the petroleum pitches, a good correlation was found between the size of optical texture in the green cokes obtained and the HDa/HAa ratio. A high HDa/HAa ratio (low thermal reactivity) was connected to a green coke structure of larger more well-developed optical domains. The evaluation of hydrogen transfer properties may thus be a rapid and relatively simple way of estimating the thermal reactivity of petroleum pitches and may give a guideline for the selection of binder pitches. However, for the pitches of coal-tar origin, the most influential factor on the coke structure was the particulate matter (QI) which reduced the size of optical domains. A correlation between the HDa/HAa ratio and the size of optical domains was therefore not found for the coal-tar pitches. With the exception of one coal-tar pitch (extreme case, 25 wt% QI), a fairly good correlation was observed between the QI content and the size of optical texture of the green cokes obtained from the pitches of coal-tar origin. A QI-free coal-tar pitch developed a coke of large optical domains similar to the petroleum pitches.

All the green cokes heat treated to 1150 ºC (calcined) had a relatively similar average crystallite size (L_c) as determined by X-ray diffraction. However, there was a tendency for the petroleum pitches that a high average crystallite size was connected to a more well-developed structure (larger domains) at the green coke stage.

Considerations on the thermal reactivity of pitches from ^{1}H NMR and ^{13}C NMR spectroscopy in conjunction with elemental analysis could generally be related to the HDa/HAa ratio. A high amount of alkyl substituents and especially longer alkyl side chains and a high content of oxygen as determined by elemental analysis were considered to lead to an increased thermal reactivity. Pitches which had a high estimated concentration of potentially donatable hydrogen due to a more hydroaromatic structure were also generally richer in reactive alkyl substituents. A high concentration of donatable hydrogen was therefore not necessarily connected to a higher thermal stability. The coal-tar pitches were as expected found to be more aromatic than the pitches of petroleum origin. A good correlation between the H/C atomic ratio and the aromaticity of pitches was observed. Elemental analysis may thus be a rapid and convenient way of estimating the aromaticity of pitches.

The processes taking place during thermal treatment of pitches are reflected in the release of volatiles. A correlation was observed for all the pitches between the relative weight loss between 300 and 500 ºC (VM300-500) and the HDa/HAa ratio. Pitches which had a high thermal reactivity experienced a relatively high weight loss before 300 ºC. For the pitches of lower thermal reactivity, the weight loss was postponed to the more critical stages of carbonization thus resulting in a higher VM300-500 parameter. A high HDa/HAa ratio was connected to a high relative weight loss between 300 and 500 ºC.

REFERENCES

[1] Haupin W.E. "Electrochemistry of the Hall-Heroult process for aluminum smelting", *J Chem Educ, 60 (1983),279-282.*
[2] Zander M. "Pitch Characterization for Industrial Applications", In Introduction to Carbon Technologies. Marsh H., Heintz E.A. and Rodríguez-Reinoso F. (1997),425-459. University of Alicante, Alicante.
[3] Oya A. "High Density Isotropic Graphites and Glassy Carbons", In Introduction to Carbon Technologies. Marsh H., Heintz E.A. and Rodríguez-Reinoso F. (1997),561-595. University of Alicante, Alicante.
[4] Yokono T. and Marsh H. "Protium NMR study of the co-carbonization of hydrogenated anthracene oil with coal-tar pitch and coal", *Fuel, 59 (1980),362-364.*
[5] Gray R.J. and Krupinski K.C. "Pitch Production", In Introduction to Carbon Technologies. Marsh H., Heintz E.A. and Rodríguez-Reinoso F. (1997),329-423. University of Alicante, Alicante.
[6] Schobert H.H. and Song C. "Chemicals and materials from coal in the 21st century", *Fuel, 81 (2001),15-32.*
[7] Acuna C., Marzin R., De Oteyza M. and Perruchoud R.C. "Petroleum pitch, a real alternative to coal tar pitch as binder material for anode production", *Light Metals (Warrendale, Pennsylvania), (1997),549-554.*
[8] Turner N.R., Alsop S.H., Malmros O., Whittle D., Hansen B.E., Stenby E.H. and Andersen S.I. "Development of petroleum enhanced coal tar pitch in Europe", *Light Metals (Warrendale, PA, United States), (2001),565-572.*
[9] Gipson J.D. "Chapter 9", In Proceedings for the 6th Great Lakes Carbon Corporation Carbon Conference. (2000),Great Lakes Carbon Corporation.
[10] Newman J.W. "Petroleum Derived Carbons", In ACS Symposium Series. Deviney M.L. and O'Grady T.M. 21 (1976),52. American Chemical Society, Washington, D.C.
[11] Mochida I., Whitehurst D.D. and Sakanishi K. "Catalysis of Coal Liquefication", In Sciences of Carbon Materials. Marsh H. and Rodríguez-Reinoso F. (2000),637-662. University of Alicante, Alicante.
[12] Andresen J.M., Burgess C.E., Pappano P.J. and Schobert H.H. "New directions for non-fuel uses of anthracites", *Fuel Processing Technology, 85 (2004),1373-1392.*
[13] Andresen J.M., Zhang Y., Burgess C.E. and Schobert H.H. "Synthesis of pitch materials from hydrogenation of anthracite", *Fuel Processing Technology, 85 (2004),1361-1372.*
[14] Zander M. and Collin G. "A review of the significance of polycyclic aromatic chemistry for pitch science", *Fuel, 72 (1993),1281-1285.*
[15] Boenigk W., Haenel M.W. and Zander M. "Structural features and mesophase formation of coal-tar pitch fractions obtained by preparative size exclusion chromatography", *Fuel, 69 (1990),1226-1232.*
[16] Zander M. "On the composition of pitches", *Fuel, 66 (1987),1536-1539.*
[17] Parker J.E., Johnson C.A.F., John P., Smith G.P., Herod A.A., Stokes B.J. and Kandiyoti R. "Identification of large molecular mass material in high temperature coal tars and pitches by laser desorption mass spectroscopy", *Fuel, 72 (1993),1381-1391.*
[18] Zander M. "On the nitrogen-containing constituents of coal-tar pitch", *Fuel, 70 (1991),563-565.*
[19] Marsh H., Latham C.S. and Gray E.M. "The structure and behavior of QI material in pitch", *Carbon, 23 (1985),555-570.*

[20] Sørlie M. and Tørklep K.T. In Extended Abstracts 17th Biennal Conference on Carbon. (1985),328. American Carbon Society, Lexington.
[21] Rand B., Hosty A.J. and West S. "Physical Properties of Pitch Relevant to the Fabrication of Carbon Materials", In Introduction to Carbon Science. Marsh H. (1989),75-103. Butterworth, London.
[22] Meier M.W. "Anodes: The Impact of Raw Material Quality and Anode Manufacturing Parameters on the Behaviour in Electrolysis", In The 23rd International Course on Process Metallurgy of Aluminium. Øye H.A. (2004),203. Tapir Uttrykk, Trondheim.
[23] Zander M. "Recent advances in pitch characterization", *Fuel, 66 (1987),1459-1466.*
[24] Zander M., Alscher A., Boenigk W. and Haenel M.W. "Average molecular weight and molecular weight distribution of coal tar pitches: methods of determination and molecular weight/chemical structure relationships", *Light Metals (Warrendale, PA, United States), (1991),597-602.*
[25] Zander M. and Haenel M.W. "Regularities in the fluorescence spectra of coal-tar pitch fractions", *Fuel, 69 (1990),1206-1207.*
[26] Domin M., Li S., Lazaro M.-J., Herod A.A., Larsen J.W. and Kandiyoti R. "Large Molecular Mass Materials in Coal-Derived Liquids by 252Cf-Plasma and Matrix-Assisted Laser Desorption Mass Spectrometry", *Energy & Fuels, 12 (1998),485-492.*
[27] Menendez R., Blanco C., Santamaria R., Dominguez A., Blanco C.G., Suelves I., Herod A.A., Morgan T.G. and Kandiyoti R. "Effects of Air-Blowing on the Molecular Size and Structure of Coal-Tar Pitch Components", *Energy & Fuels, 16 (2002),1540-1549.*
[28] Herod A.A., Zhang S.-F., Carter D.M., Domin M., Cocksedge M.J., Parker J.E., Johnson C.A.F., John P., Smith G.P. and et a. "Matrix-assisted laser desorption/ionization mass spectrometry of pitch fractions separated by planar chromatography", *Rapid Commun Mass Spectrom, 10 (1996),171-177.*
[29] John P., Johnson C.A.F., Parker J.E., Smith G.P., Herod A.A., Li C.Z., Humphrey P., Chapman J.R. and Kandiyoti R. "Molecular masses up to 270,000 in coal and coal-derived products by matrix-assisted laser desorption ionization mass spectrometry (MALDI-MS)", *Fuel, 73 (1994),1606-1616.*
[30] Alula M., Cagniant D. and Rouzaud J.N. "Interactions between pitch constituents in thermal treatment. 1. Behavior of extrographic fractions by heating at 350, 400 and 450 DegC", *Fuel, 68 (1989),995-998.*
[31] Granda M., Bermejo J., Moinelo S.R. and Menendez R. "Application of extrography for characterization of coal tar and petroleum pitches", *Fuel, 69 (1990),702-705.*
[32] Granda M., Menendez R., Moinelo S.R., Bermejo J. and Snape C.E. "Mass spectrometric characterization of polynuclear aromatic nitrogen compounds in coal tar pitches separated by extrography", *Fuel, 72 (1993),19-23.*
[33] Bermejo J., Granda M., Menendez R., Garcia R. and Tascon J.M.D. "Thermal behavior of extrographic fractions of coal tar and petroleum pitches", *Fuel, 76 (1997),179-187.*
[34] Bermejo J., Granda M., Menendez R. and Tascon J.M.D. "Comparative analysis of pitches by extrography and thermal analysis techniques", *Carbon, 32 (1994),1001-1010.*

[35] Guillen M.D., Diaz C. and Blanco C.G. "Characterization of coal tar pitches with different softening points by 1H NMR. Role of the different kinds of protons in the thermal process", *Fuel Processing Technology, 58 (1998),1-15.*
[36] Miyazawa K., Yokono T. and Sanada Y. "High temperature proton NMR study of coal and pitch at the early stages of carbonization", *Carbon, 17 (1979),223-225.*
[37] Azami K., Yokono T., Sanada Y. and Uemura S. "Studies on the early stage of carbonization of petroleum pitch by means of high-temperature proton-NMR and ESR", *Carbon, 27 (1989),177-183.*
[38] Maroto-Valer M.M., Andresen J.M. and Snape C.E. "In situ 1H NMR study of the fluidity enhancement for a bituminous coal by coal tar pitch and a hydrogen-donor liquefaction residue", *Fuel, 77 (1998),921-926.*
[39] Snape C.E., Kenwright A.M., Bermejo J., Fernandez J. and Moinelo S.R. "Evaluation of the aromatic structure of coal tar pitch by solid and solution state NMR", *Fuel, 68 (1989),1605-1608.*
[40] Maroto-Valer M.M., Andresen J.M., Rocha J.D. and Snape C.E. "Quantitative solid-state 13C NMR measurements on cokes, chars and coal tar pitch fractions", *Fuel, 75 (1996),1721-1726.*
[41] Azami K., Yamamoto S., Yokono T. and Sanada Y. "In-situ monitoring for mesophase formation processes of various pitches by means of high-temperature carbon-13 NMR", *Carbon, 29 (1991),943-947.*
[42] Guillen M.D., Iglesias M.J., Dominguez A. and Blanco C.G. "Semi-quantitative FTIR analysis of a coal tar pitch and its extracts and residues in several organic solvents", *Energy & Fuels, 6 (1992),518-525.*
[43] Zander M. "Chemistry and Properties of Coal-tar and Petroleum Pitch", In Sciences of Carbon Materials. Marsh H. and Rodríguez-Reinoso F. (2000),205-258. University of Alicante, Alicante.
[44] Lewis I.C. "Chemistry of carbonization", *Carbon, 20 (1982),519-529.*
[45] Greinke R.A. "Chemical bond formed in thermally polymerized petroleum pitch", *Carbon, 30 (1992),407-414.*
[46] Brooks J.D. and Taylor G.H. "The Formation of some Graphitizing Carbons", In Chemistry and Physics of Carbon. Walker P.L.J. 4 (1968),243-285. Marcel Dekker, Inc., New York.
[47] Marsh H. and Menendez R. "Carbons from pyrolysis of pitches, coals, and their blends", *Fuel Processing Technology, 20 (1988),269-296.*
[48] Oberlin A. "Carbonization and graphitization", *Carbon, 22 (1984),521-541.*
[49] Greinke R.A. and Singer L.S. "Constitution of coexisting phases in mesophase pitch during heat treatment: mechanism of mesophase formation", *Carbon, 26 (1988),665-670.*
[50] Marsh H. and Neavel R.C. "Carbonization and liquid-crystal (mesophase) development. 15. A common stage in mechanisms of coal liquefaction and of coal blends for coke making", *Fuel, 59 (1980),511-513.*
[51] Yokono T., Obara T., Sanada Y., Shimomura S. and Imamura T. "Characterization of carbonization reaction of petroleum residues by means of high-temperature ESR and transferable hydrogen", *Carbon, 24 (1986),29-32.*
[52] Neavel R.C. "Coal plasticity mechanism: inferences from liquefaction studies", *Coal Science, 1 (1982),1-19.*
[53] Kidena K., Murata S. and Nomura M. "Studies on the Chemical Structural Change during Carbonization Process", *Energy & Fuels, 10 (1996),672-678.*

[54] Yokono T., Marsh H. and Yokono M. "Hydrogen donor and acceptor abilities of pitch: proton NMR study of hydrogen transfer to anthracene", *Fuel, 60 (1981),607-611.*
[55] Obara T., Yokono T., Miyazawa K. and Sanada Y. "Carbonization behavior of hydrogenated ethylene tar pitch", *Carbon, 19 (1981),263-267.*
[56] Yokono T., Takahashi N. and Sanada Y. "Hydrogen donor ability (Da) and acceptor ability (Aa) of coal and pitch. 1. Coalification, oxidation, and carbonization paths in the Da-Aa diagram", *Energy & Fuels, 1 (1987),360-362.*
[57] Clarke J.W., Rantell T.D. and Snape C.E. "Estimation of the concentration of donatable hydrogen in a coal solvent by N.M.R", *Fuel, 61 (1982),707-712.*
[58] Uemasu I. and Kushiyama S. "Analysis of 9,10-dihydroanthracene by capillary gas chromatography for evaluation of transferable hydrogen in heavy oils", *J Chromatogr, 368 (1986),387-390.*
[59] Bermejo J., Canga J.S., Guillen M.D., Gayol O.M. and Blanco C.G. "Evidence for hydrogen donor-acceptor behavior of 9,10-dihydroanthracene in thermal reactions with coals and pitches", *Fuel Processing Technology, 24 (1990),157-162.*
[60] Diez M.A., Dominguez A., Barriocanal C., Alvarez R., Blanco C.G. and Canga C.S. "Hydrogen donor and acceptor abilities of pitches from coal and petroleum evaluated by gas chromatography", *J Chromatogr A, 830 (1999),155-164.*
[61] Pajak J. "Hydrogen transfer from Tetralin to coal macerals. Reactivity of macerals", *Fuel Processing Technology, 21 (1989),245-252.*
[62] Machnikowski J., Kaczmarska H., Leszczynska A., Rutkowski P., Diez M.A., Alvarez R. and Garcia R. "Hydrogen-transfer ability of extrographic fractions of coal-tar pitch", *Fuel Processing Technology, 69 (2001),107-126.*
[63] Shao R.L., Lewis I.C. and Chang C.F.J. "A Continuous Method for Producing a Q.I.-Free Liquid Coal Tar Using Cross-flow Ceramic Membranes", In Extended Abstracts, Carbon '02. (2002), Beijing.
[64] Guillen M.D., Blanco J., Canga J.S. and Blanco C.G. "Study of the effectiveness of 27 organic solvents in the extraction of coal tar pitches", *Energy & Fuels, 5 (1991),188-192.*
[65] Brecker L. "Nuclear magnetic resonance of lipid A-the influence of solvents on spin relaxation and spectral quality", *Chem Phys Lipids, 125 (2003),27-39.*
[66] Claridge T.D.W. High-Resolution NMR Techniques in Organic Chemistry. (1999),138. Pergamon Press, Amsterdam.
[67] Diaz C. and Blanco C.G. "NMR: A Powerful Tool in the Characterization of Coal Tar Pitch", *Energy & Fuels, 17 (2003),907-913.*
[68] Blanco C.G., Canga J.S., Dominguez A., Iglesias M.J. and Guillen M.D. "Flame ionization detection relative response factors of some polycyclic aromatic compounds: determination of the main components of the coal tar pitch volatile fraction", *J Chromatogr, 607 (1992),295-302.*
[69] Jorgensen A.D., Picel K.C. and Stamoudis V.C. "Prediction of gas chromatography flame ionization detector response factors from molecular structures", *Anal Chem, 62 (1990),683-689.*
[70] Eidet T. "Reactions on carbon anodes in aluminium electrolysis", In Dr. Ing. Thesis. (1997),NTNU, Trondheim.
[71] Rorvik S., Aanvik M., Sorlie M. and Oye H.A. "Characterization of optical texture in cokes by image analysis", *Light Metals (Warrendale, Pennsylvania), (2000),549-554.*

[72] Iwashita N., Park C.R., Fujimoto H., Shiraishi M. and Inagaki M. "Specification for a standard procedure of X-ray diffraction measurements on carbon materials", *Carbon, 42 (2004),701-714.*
[73] Dahn J.R., Sleigh A.K., Shi H., Reimers J.N., Zhong Q. and Way B.M. "Dependence of the electrochemical intercalation of lithium in carbons on the crystal structure of the carbon", *Electrochim Acta, 38 (1993),1179-1191.*
[74] ASTM. "D 5187 - 91: Standard Test Method for Determination of Crystallite Size (L_c) of Calcined Petroleum Coke by X-Ray Diffraction", *ASTM International, (1997),188-191.*
[75] Walpole R.E., Myers R.H., Myers S.L. and Ye K. "Section 13.6 Multiple Comparisons", Probability & Statistics for Engineers & Scientists, 7. edtition. (2002),479-480. Prentice-Hall, Inc., New Jersey.
[76] Ida T., Akada K., Okura T., Miyake M. and Nomura M. "Carbonization of methylene-bridge aromatic oligomers - effect of alkyl substituents", *Carbon, 33 (1995),625-631.*
[77] Clemens A.H. and Matheson T.W. "Further studies of Gieseler fluidity development in New Zealand coals", *Fuel, 71 (1992),193-197.*
[78] Maroto-Valer M.M., Andresen J.M. and Snape C.E. "Verification of the linear relationship between carbon aromaticities and H/C ratios for bituminous coals", *Fuel, 77 (1998),783-785.*
[79] Dickinson E.M. "Structural comparison of petroleum fractions using proton and carbon-13 NMR spectroscopy", *Fuel, 59 (1980),290-294.*
[80] Walker P.L.J. "Carbon: an old but new material revisited", *Carbon, 28 (1990),261-279.*
[81] Hooper R.J., Battaerd H.A.J. and Evans D.G. "Thermal dissociation of tetralin between 300 and 450 DegC", *Fuel, 58 (1979),132-138.*
[82] Yokono T., Obara T., Iyama S. and Sanada Y. "Hydrogen donor and acceptor ability of coal and pitch -factors governing mesophase development from low rank coal during carbonization", *Carbon, 22 (1984),623-624.*
[83] Iyama S., Yokono T. and Sanada Y. "Development of anisotropic texture in co-carbonization of low rank coal with pitch evaluation from hydrogen donor and acceptor abilities of coal and pitch", *Carbon, 24 (1986),423-428.*
[84] Granda M., Casal E., Bermejo J. and Menendez R. "The influence of primary QI on the oxidation behaviour of pitch-based C/C composites", *Carbon, 39 (2001),483-492.*
[85] Bourrat X. "Structure in Carbons and Carbon Artifacts", In Sciences of Carbon Materials. Marsh H. and Reinoso-Rodriguez F. (2000),1-90. University of Alicante, Alicante.

APPENDIX

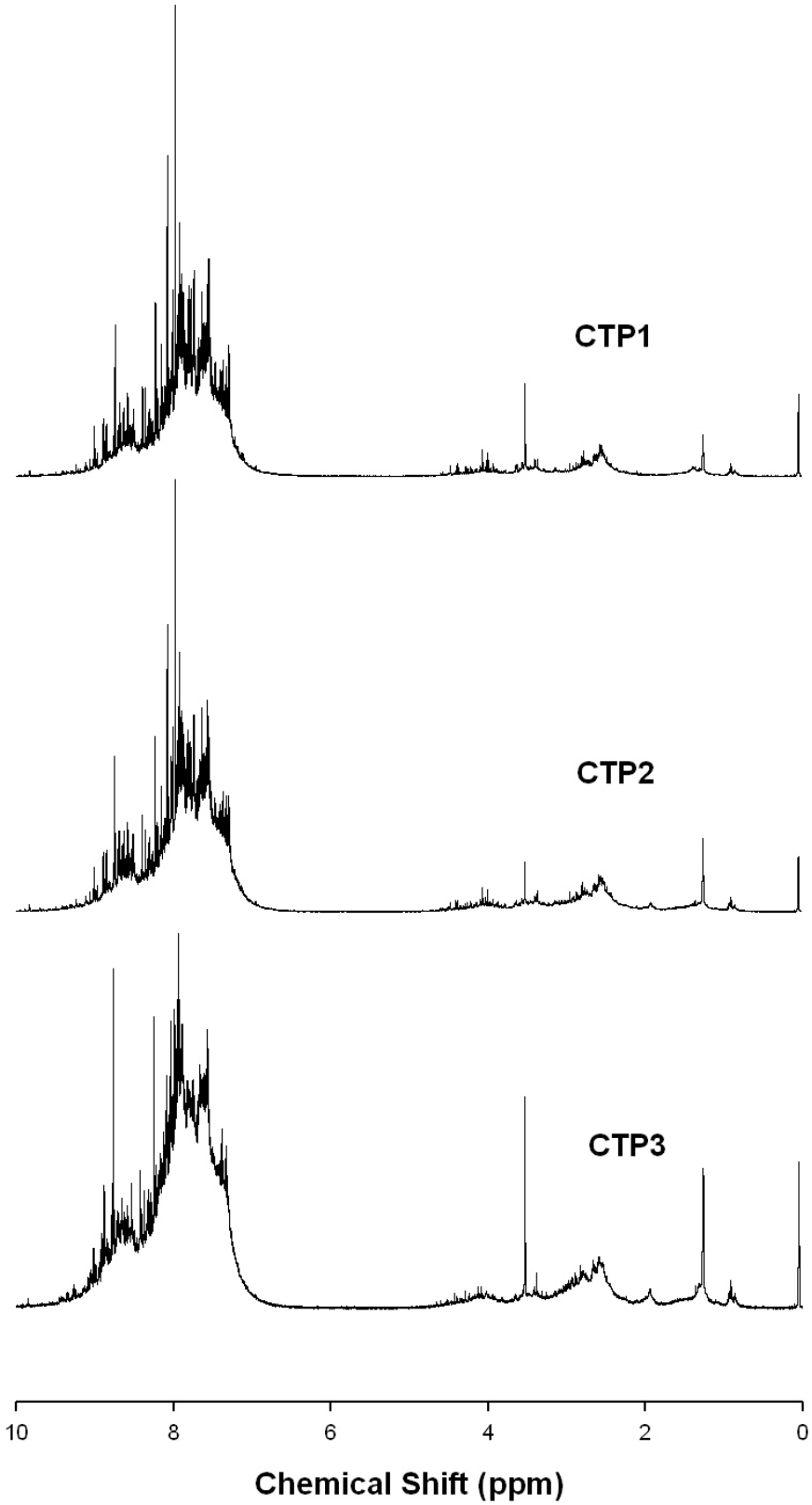

Figure A.1.1. ^{1}H NMR spectra of CTP1, CTP2 and CTP3.

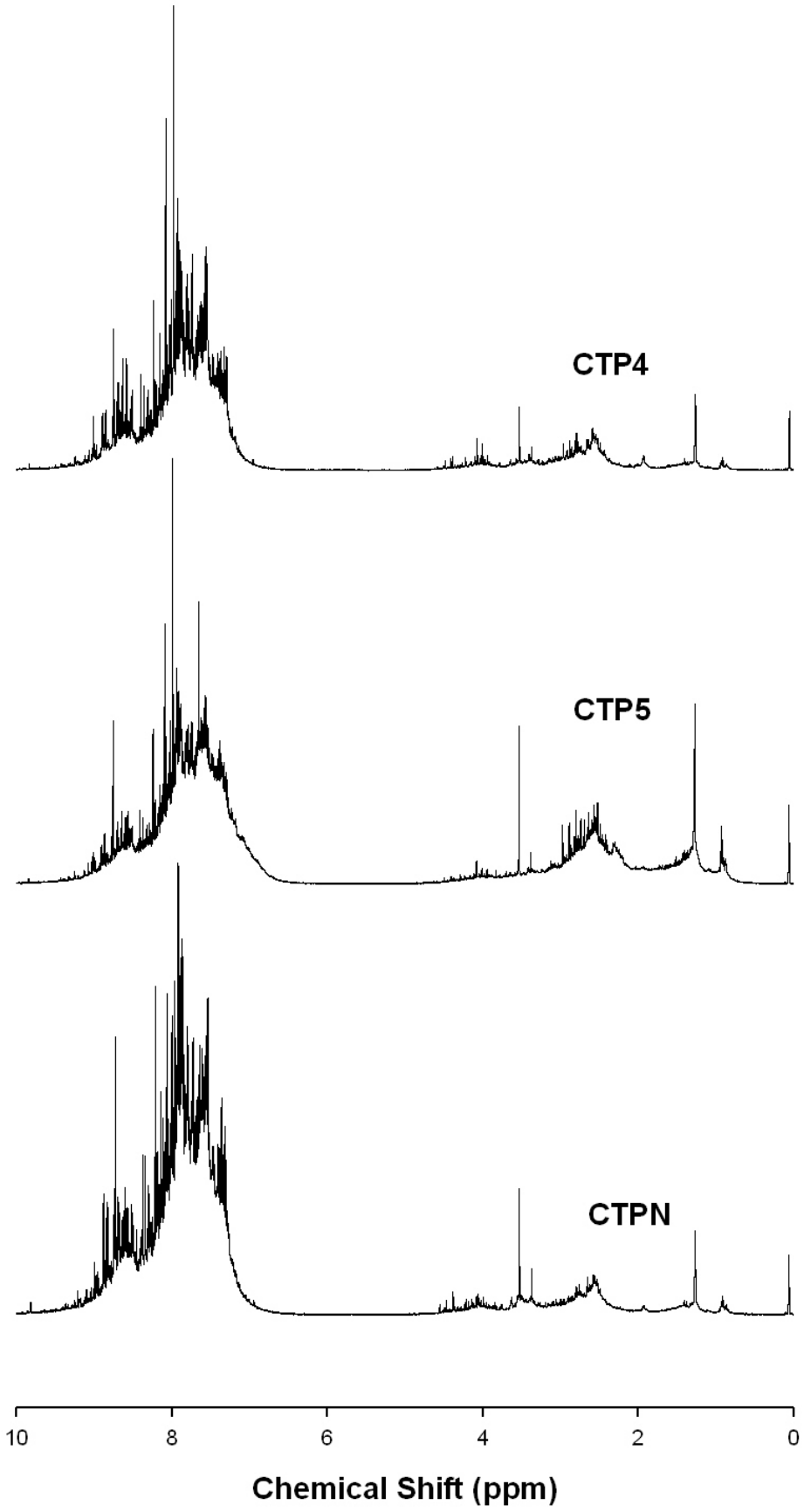

Figure A.1.2. ^{1}H NMR spectra of CTP4, CTP5 and CTPN.

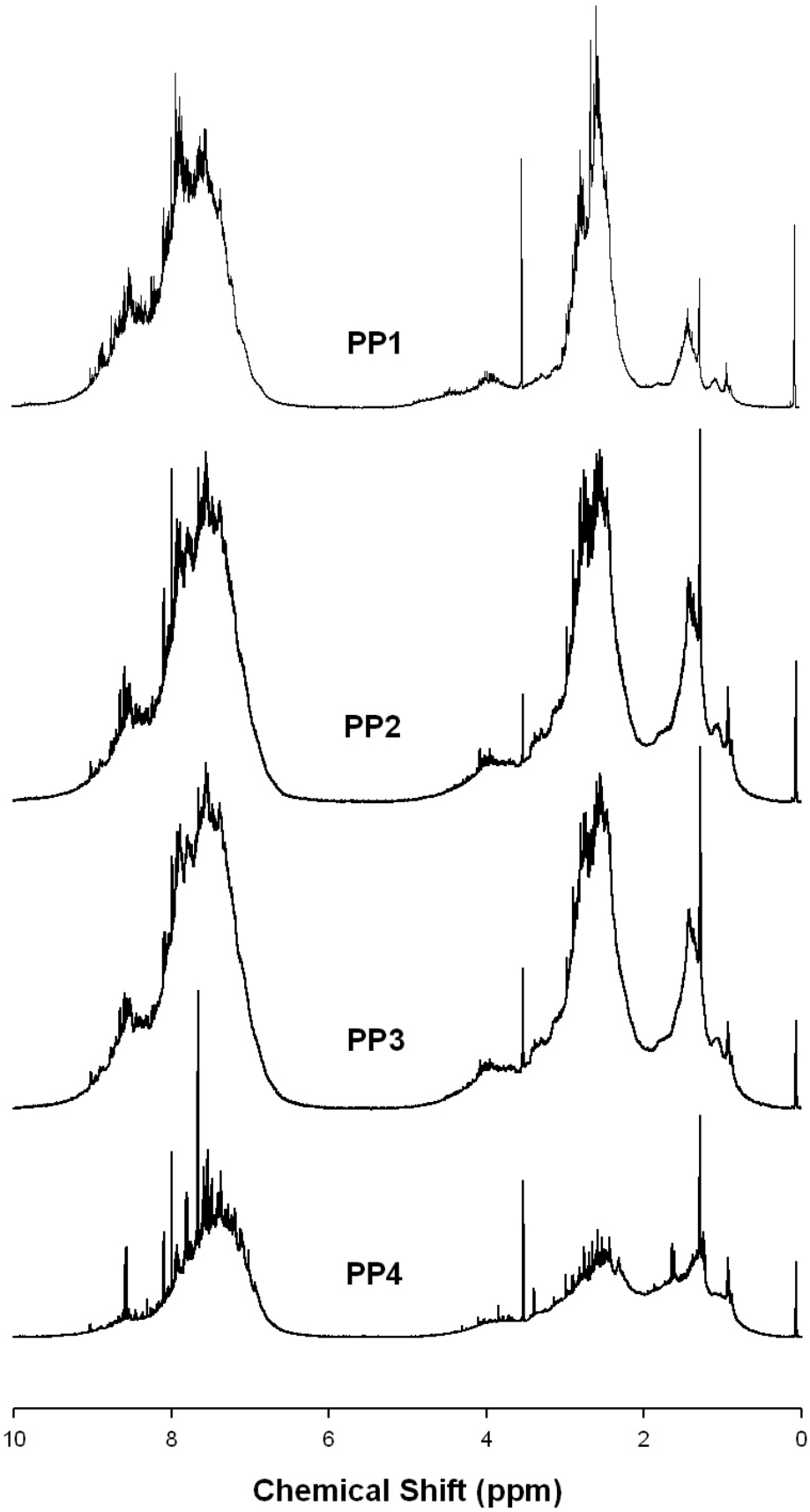

Figure A.1.3. ^{1}H NMR spectra of PP1, PP2, PP3 and PP4.

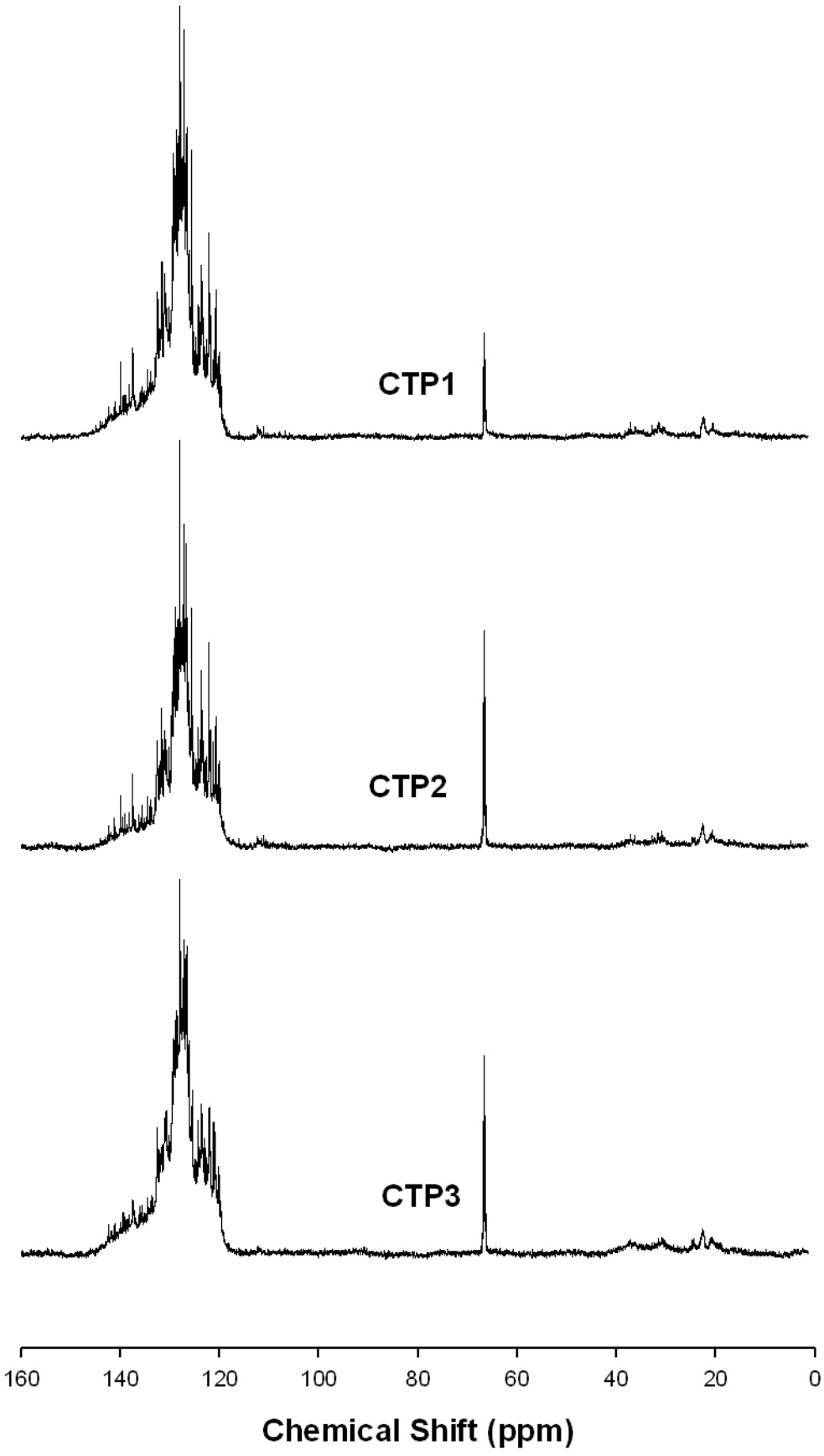

Figure A.2.1. ^{13}C NMR spectra of CTP1, CTP2 and CTP3.

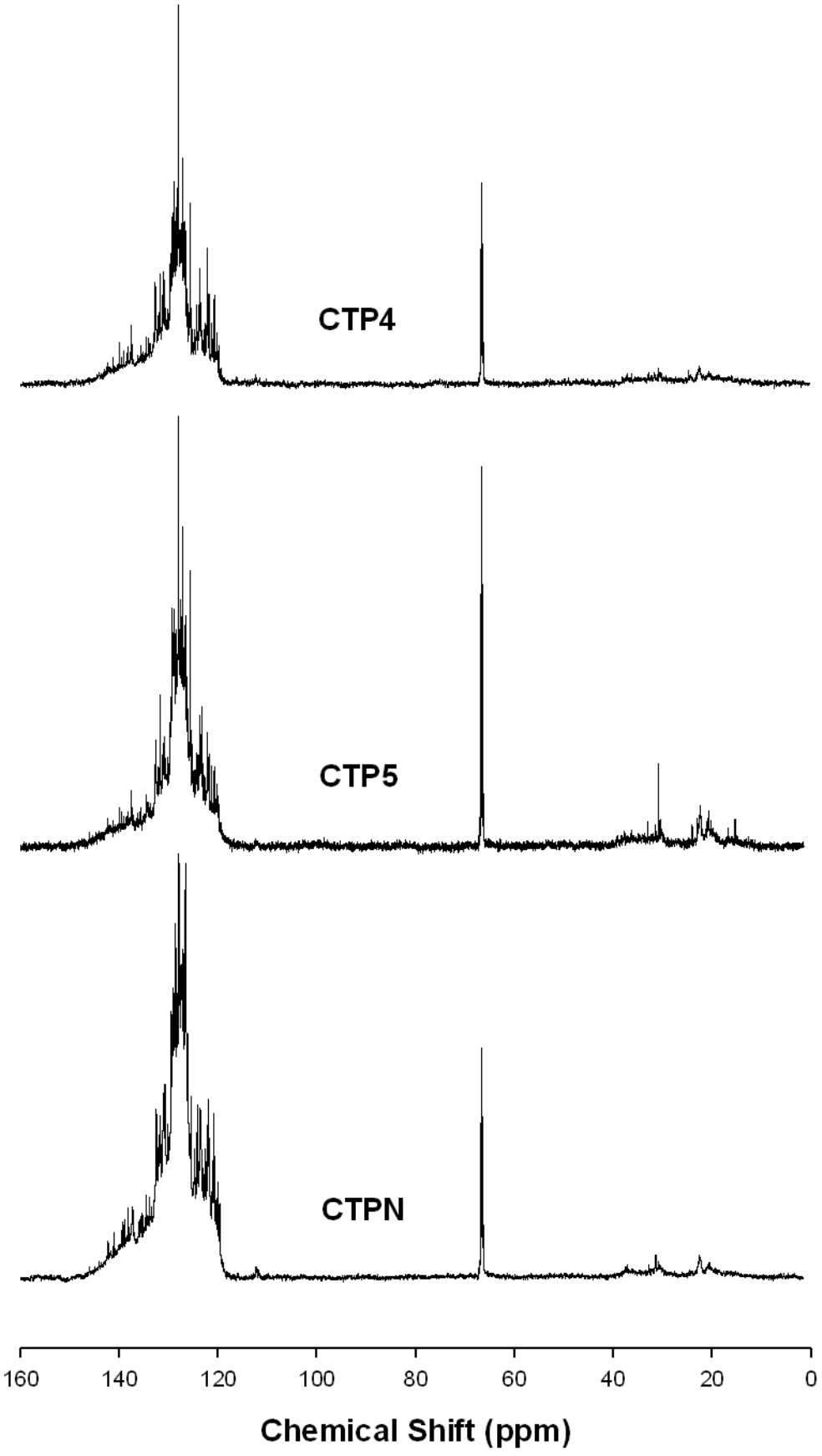

Figure A.2.2. ^{13}C NMR spectra of CTP4, CTP5 and CTPN.

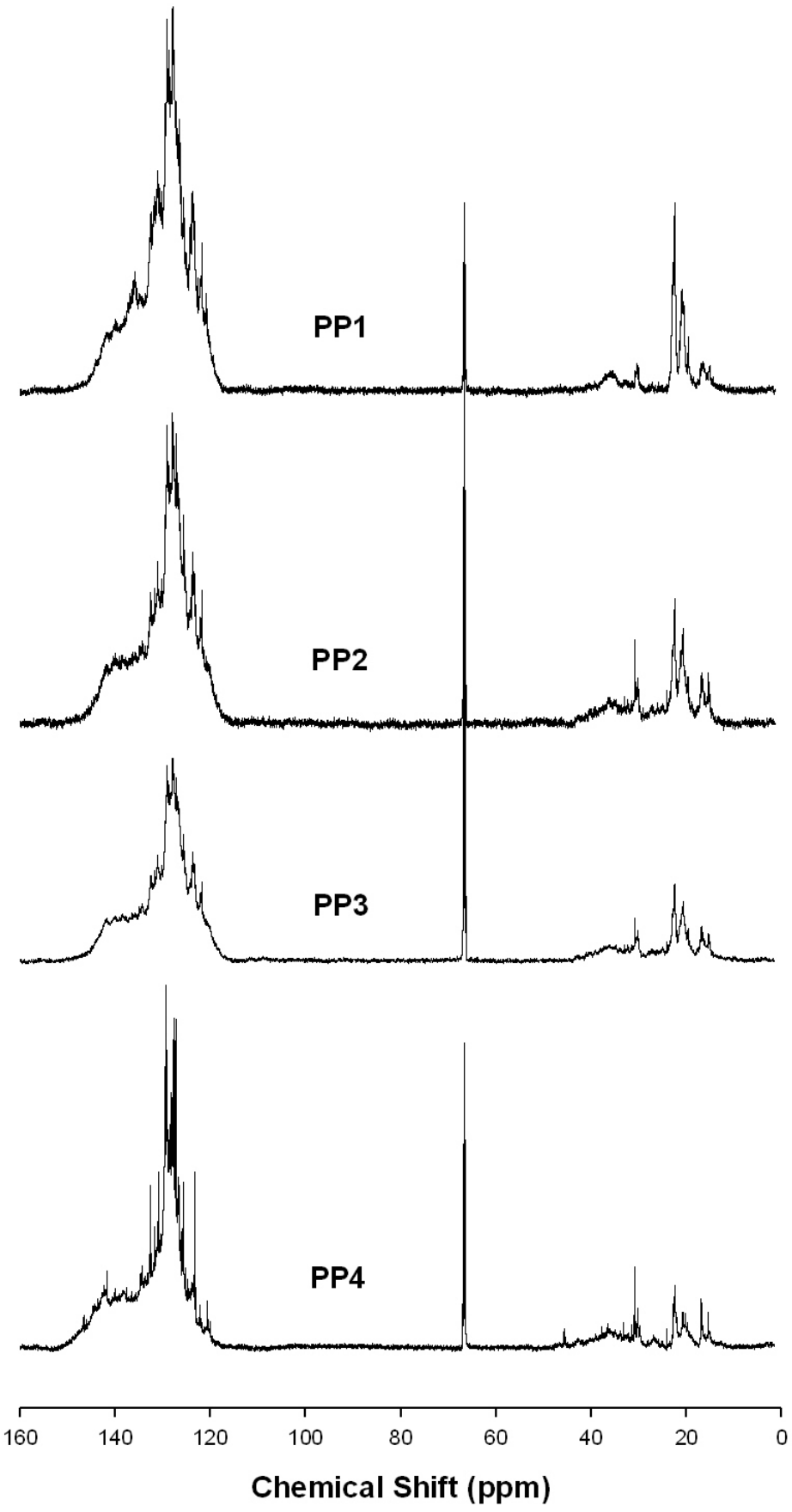

Figure A.2.3. ^{13}C NMR spectra of PP1, PP2, PP3 and PP4.

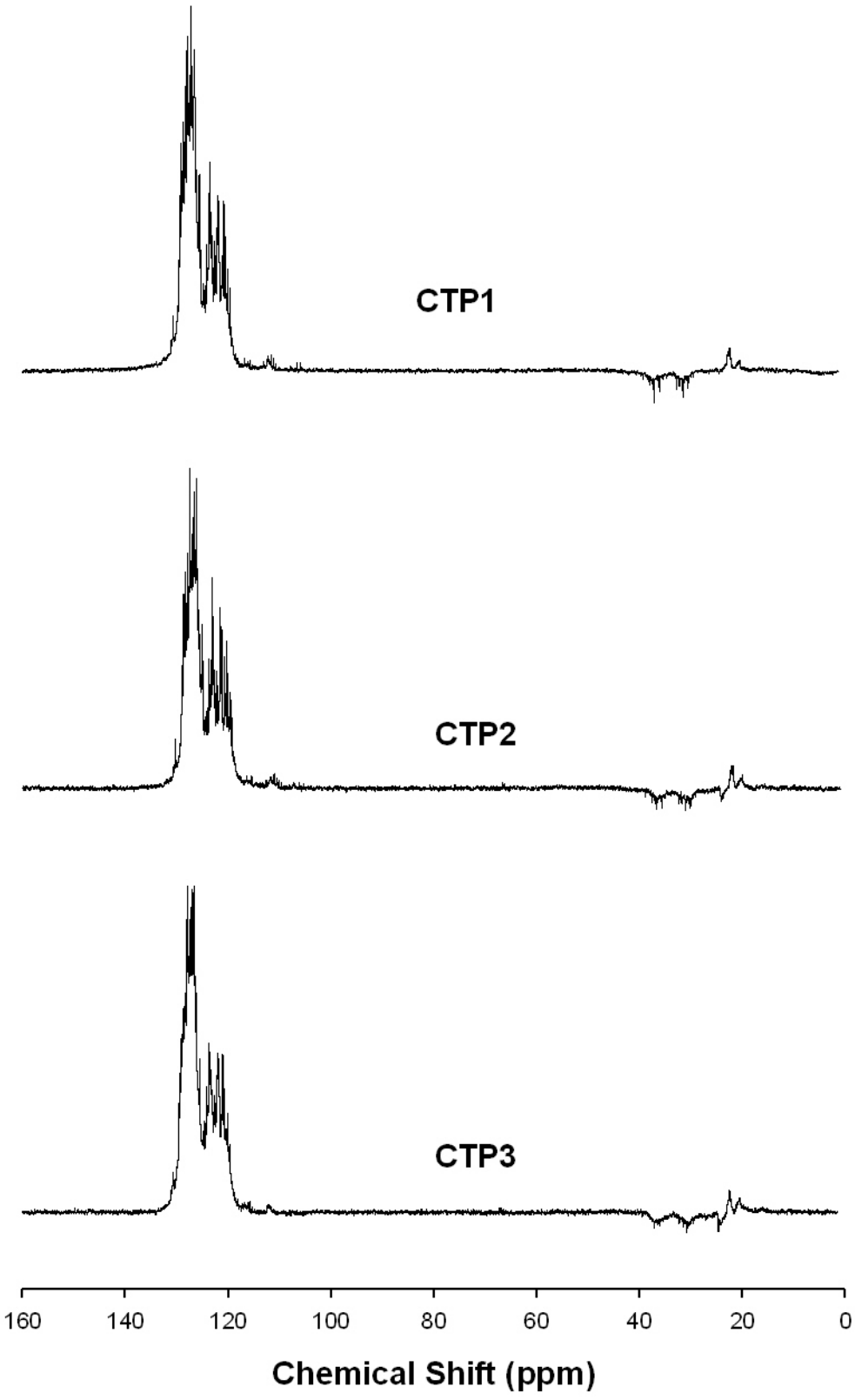

Figure A.3.1. ^{13}C NMR (DEPT) spectra of CTP1, CTP2 and CTP3.

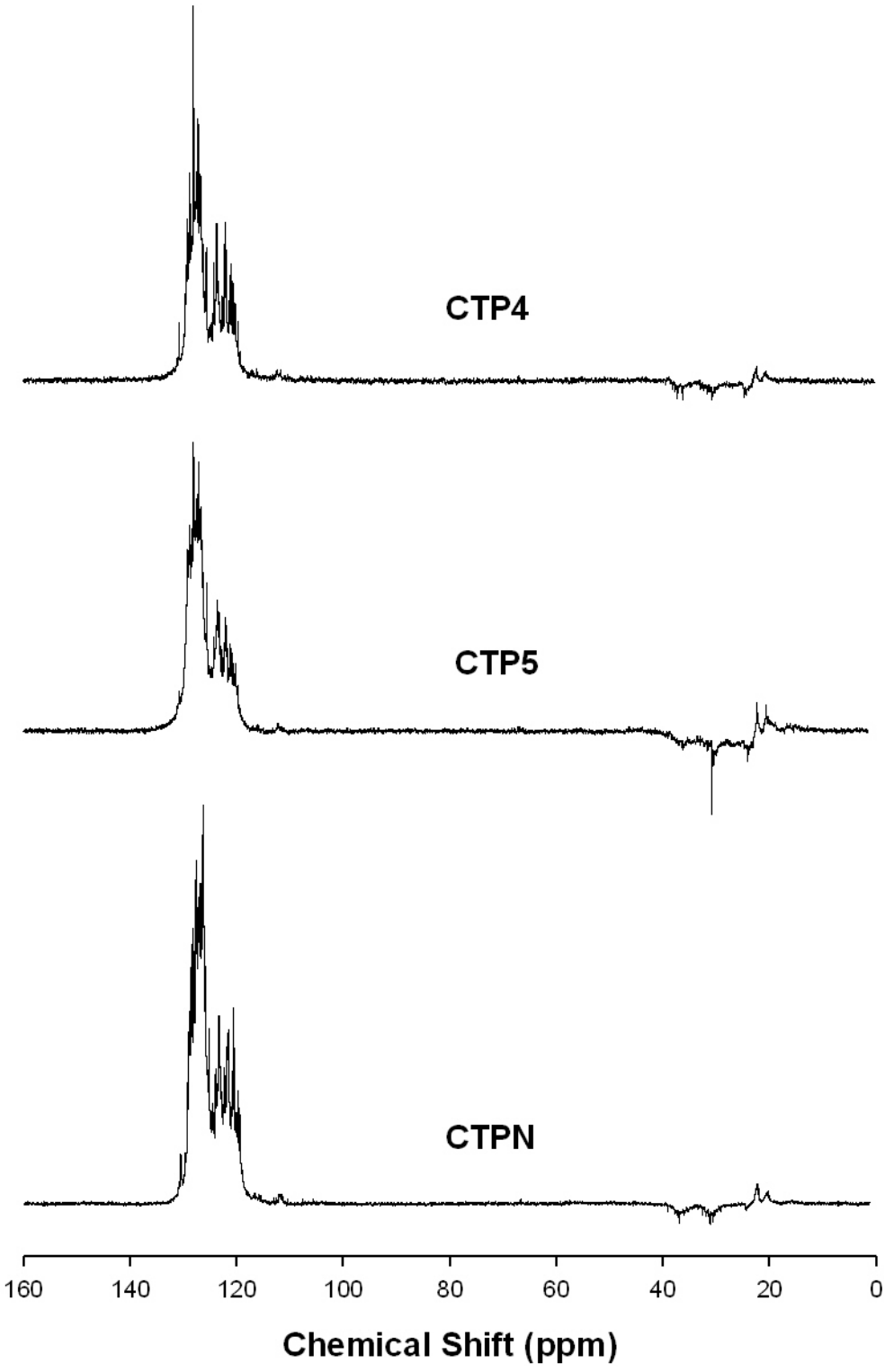

Figure A.3.2. ^{13}C NMR (DEPT) spectra of CTP4, CTP5 and CTPN.

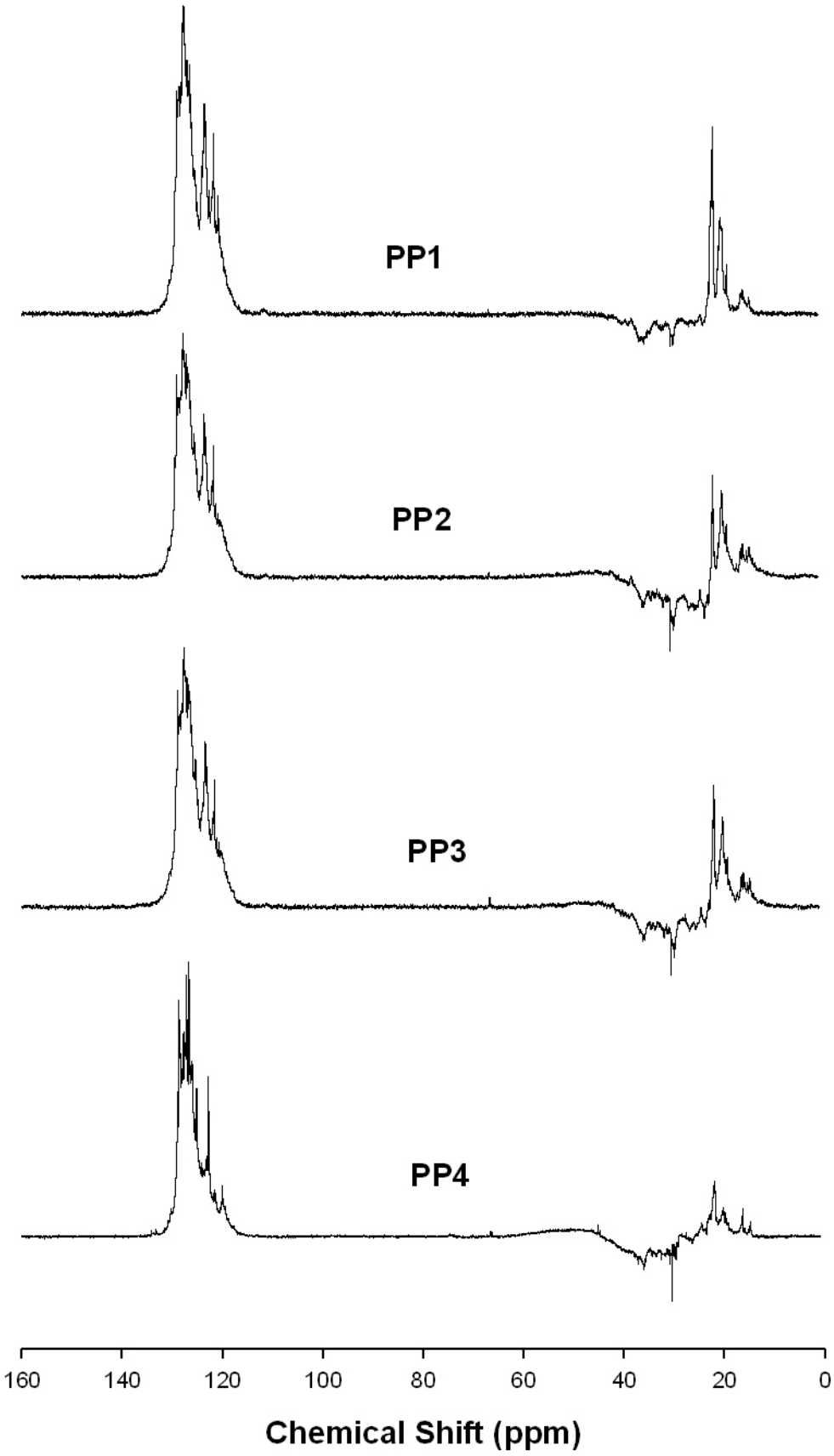

Figure A.3.3. ^{13}C NMR (DEPT) spectra of PP1, PP2, PP3 and PP4.